AD-A210 918

ed

ICATION OF THIS PAGE

(2)

REPORT DOCUMENTATION PAGE

Form Approved
OMB No 0704-0188
Exp. Date Jun 30, 1986

IRITY CLASSIFICATION ed	1b RESTRICTIVE MARKINGS
ASSIFICATION AUTHORITY	3 DISTRIBUTION / AVAILABILITY OF REPORT Approved for public release, distribution unlimited
TION / DOWNGRADING SCHEDULE	
ORGANIZATION REPORT NUMBER(S)	5 MONITORING ORGANIZATION REPORT NUMBER(S) R&D 4794-MS-01
RFORMING ORGANIZATION University of Bristol	6b OFFICE SYMBOL (If applicable)
7a NAME OF MONITORING ORGANIZATION European Research Office USARDSG-UK	
6c ADDRESS (City, State, and ZIP Code) Tyndall Avenue Bristol BS8 1TL, UK	7b ADDRESS (City, State, and ZIP Code) Box 65 FPO NY 09510-1500
8a NAME OF FUNDING / SPONSORING ORGANIZATION ARO-E, USARDSG-UK	8b OFFICE SYMBOL (If applicable)
9 PROCUREMENT INSTRUMENT IDENTIFICATION NUMBER DAJA45-85-C-0004	
8c ADDRESS (City, State, and ZIP Code) Box 65 FPO NY 09510-1500	10 SOURCE OF FUNDING NUMBERS PROGRAM ELEMENT NO: 61102A PROJECT NO: 1L161102BH57 TASK NO: 04 WORK UNIT ACCESSION NO:

11 TITLE (Include Security Classification)
(U) Hierarchical Structure in Polymeric solids and its influence on properties

12 PERSONAL AUTHOR(S)
Professor A. Keller

13a TYPE OF REPORT	13b TIME COVERED	14 DATE OF REPORT (Year, Month, Day)	15 PAGE COUNT
Final	FROM 12 84 TO 05 89		

16 SUPPLEMENTARY NOTATION

17 COSATI CODES			18 SUBJECT TERMS (Continue on reverse if necessary and identify by block number)
FIELD	GROUP	SUB-GROUP	
11 09			
20 03			

19 ABSTRACT (Continue on reverse if necessary and identify by block number) Within the broader subject of the title the work was centred on main chain liquid crystal forming polymers (LCP-s) such as have potential structural applications as advanced materials. A close ongoing UK-US collaboration has been established where the US workers (Prof. Percec, Cleveland) are synthetizing tailor made rigid group-flexible spacer polyethers for Physics based examination at Bristol. The varied lines of work and accomplishments are as follows.

As a synthesis of the diverse findings a broad thermodynamics based scheme was established providing unifying threads through hitherto disconnected phenomena in the LCP field with significant predictive power for ongoing works. Amongst others it encompasses the numerous situation where mesogens are not required for the formation of a liquid crystal (LC) state.

We have been establishing phase diagrams as a function of molecular weight, chemical constitution and copolymer composition. This serves to identify and predict the LC region as a function of the above variables with due distinction between thermodynamic and kinetic factors.

20 DISTRIBUTION / AVAILABILITY OF ABSTRACT	21 ABSTRACT SECURITY CLASSIFICATION
☒ UNCLASSIFIED/UNLIMITED ☒ SAME AS RPT ☒ DTIC USERS	Unclassified
22a NAME OF RESPONSIBLE INDIVIDUAL Dr. W. Simmons	22b TELEPHONE (Include Area Code) 01-409-4423
	22c OFFICE SYMBOL ANXSN-UK-RM

DD FORM 1473, 84 MAR — 83 APR edition may be used until exhausted. All other editions are obsolete.

SECURITY CLASSIFICATION OF THIS PAGE
Unclassified

20. Abstract cont'd.....

In aid of this, a new methodology was introduced: simultaneous X-ray diffraction and thermal analysis which was greatly facilitated by synchrotron generated X-rays. Further, the way has been opened for combining lyotropics and thermotropics in a unified phase diagram.

In the course of the above, the importance of non-equilibrium states was recognized, both in the LC and isotropic (L) states, as order deficiency in the former and excess order in the latter. Methods were established to characterise these non-equilibrium effects and to eliminate them for enabling a meaningful thermodynamic analysis of the systems. Closely tied to this issue was the discovery of memory effects, by which structural and thermodynamic features are being carried over from one phase to another. These greatly influence the final structure hierarchies and resulting properties, and need erasing for consistent sample preparation and scientific characterisation.

The most conspicuous consequence of memory effects is in the morphology on the optical microscopic scale of the structure hierarchy, here extensively explored. Amongst others quite unusually large scale structures were observed and created in a controlled manner together with the recognition of a new microscopic sub-hierarchy with many implications.

On the molecular level the systems in fibre form were examined by X-ray diffraction. Different kinds of layer structure and a novel "intermeshed" structure were identified. The underlying molecular packing modes were rationalized in terms of unequal cross-sectional areas of the rigid and flexible constituents within the same molecule involving the possibility of configurational disorder of the flexible unit within the 1,2, or 3 dimensional lattice order set by the rigid group. In the important case of layers such considerations provide examples of how to match order and disorder along layer interfaces with implications for polymeric layer morphologies in general, and on the modes of organization of copolymers in particular.

A separate line of work was on the orientational behaviour of rigid molecules, most of it on the fully rigid rod PBZT. A two-stage relaxational behaviour was identified in semi-dilute (entangled) solutions by birefringence analysis. Further, a new methodology was established for in-situ X-ray diffraction registration of orientation behaviour in the lyotropic state. Through this, it was made possible to extract direct information on molecular behaviour in addition to aggregate features in the orientation - relaxation behaviour, involving the full orientation distribution (not just averages). It was shown that the new method is applicable also to pure thermotropics, and a connection with polarising optical banded structures, ubiquitous, technically important, but so far unexplained has been established. The latter provides a link also with natural substances possessing hierarchical structure architecture with lessons for purposeful material design.

1. PREFACE

1.1 Relation of Work to the Original Objectives

The study undertaken was to be on liquid crystal forming polymers (LCP), to be obtained through collaboration with the Macromolecular Department, Cleveland. Under the comprehensive title of structure hierarchies two somewhat separate aspects were considered specifically. a) Study of structures such as arise when passing from one phase to another isotropic, liquid-crystal, crystal,in particular their hierarchical relation b) Study of orientation of LCP forming polymers in flow and its influence on phase behaviour and structures evolved. As will be apparent from this reporting these objectives were all adhered to, nevertheless in many instances their realization was along different paths compared to what was originally envisaged dictated by practicalities and due to new perspectives arising as the work proceeded. Specifically: Materials indeed were as obtained from and shared with Cleveland. However, they were not the widely studied main chain polyesters of technological origin, as originally envisaged, because these were found chemically insufficiently characterised, and from the physical point of view not sufficiently versatile (e.g. cannot be taken to the isotropic state without degradation) for the purposes intended. However, suitable, in fact uniquely favourable, materials were acquired through novel methods of synthesis by Professor V. Percec from the same Department in Cleveland with whom an ongoing collaboration has developed providing us with tailor made materials. Eventually our own physically oriented work feeds back into Professor Percec's synthesis. We regard the establishment of this Physics - Chemistry, UK-US interaction across scientific and national boundaries as one of the significant outcomes of the programme.

In terms of subject areas; a) the part of structure-morphology aspect of structure hierarchies was pursued as proposed, however, in the main along new unforeseen directions. The latter arose through

the recognition of both, new principles and practicalities. The principles involve wider perspectives of thermodynamics, by which it became apparent that the field original chosen is only one facet of a much wider canvas, which we then embraced in a more comprehensive manner. The practicality referred to includes the fact that successive phases "remember" their origin to a much greater extent than initially envisaged, both in terms of their thermodynamic parameters and structural features. Further, the direction of the work became also influenced by new experimental methods which are expected to be of wider applicability for materials science. In b) the orientation part of the original programme , the initially proposed wider utilisation of the elongational flow based methodology of our laboratory, proved somewhat premature for the specific purposes envisaged. The work therefore has remained within the boundaries of simple shear flow, but has developed in a new direction within it thanks to the creation of new instrumental capabilities with promising forward looking consequences.

1.2 Form of Report

The main text of this Report attempts to string together the multitudinous facets of the work under the ERO Grant. This will not be done in the historic sequence as the work evolved, but from our present perspective at the time of writing. It will be essentially confined to guiding principles and conclusions on the different aspects; for actual documentation it will refer to the publication material featuring as Appendices to which the main text should serve as a guide. The latter consist of reprints and scripts in the form submitted to journals (not yet appeared). The text of the report will be closely integrated with these Appendices. For other documentation reference will be made to the individual period reports. Only in some instances, where required by comprehensibility, will primary documentation (1 table, 4 diagrams) be reproduced in the main report text. Some major publications are being currently prepared. These are presently with our US collaborators (Prof. Percec) and can thus only be briefly referred to at this stage.

Finally, the ERO sponsored work has not been an isolated activity: it has fed on and interacted with the rest of the researches in the laboratory. In a coherent account compounding of some of this mutually interacting material has been inevitable; where this has happened, the non-ERO material will be clearly delineated.

In what follows the accomplishments under the grant will be presented under 9 main and numerous subheadings with 9 Appendices.

2. Unifying Thermodynamic Scheme

We start with a unifying scheme of mesophase formation which has evolved during the ERO grant period. This was largely thanks to the ERO sponsored work, but as the ideas developed it also encompassed other material from this laboratory and from elsewhere. Once the scheme was perceived it had a decisive influence on the development of the work, in fact presently it forms the guiding principle of the physics - chemistry cooperation between Bristol and Cleveland referred to above.

The scheme has had its first public exposured recently (Conference on "Integration of Fundamental Polymer Science and Technology", Rolduc, Holland Apr. 1989, and a seminar at US Air Force Laboratories, Dayton) when it met a most enthusiastic response. In fact, it was regarded as virtually self evident truth not perceived in the present context before. Appendix I contains its first write up in the form presently submitted to the journal "Macromolecules". A further instalment focussed on the Physics-Chemistry relation with explicit examples is under preparation (with Prof. Percec).

A concise guide to the 'Scheme' in Appendix I is as follows. The liquid-crystalline state is a special form of material in between the crystal and the liquid (melt or solution), and as such, (irrespective of more rigorous definitions featuring elsewhere), has distinct properties of salient importance for materials and their applications. Obtaining materials in this form and/or designing

materials capable of being in this state is therefore of utmost significance and topicality. Our "scheme" provides quite general, and we believe, universal guidelines towards such a quest. It takes the Free energy (G) temperature (T) diagram of a conventionally crystalline material as a starting point (Fig.1 in Appendix I) and shows how the free energies in the liquid (G_L) and the crystal (G_C) are to be altered to attain the liquid crystalline state. This arises by either raising G_L or G_C or both (Figs 2,3 App. I). By doing so we may 'uncover'a stable mesophase region in the phase diagram which otherwise may be only virtual (hence hidden). Raising of G_L corresponds to lowering of melt entropy. This can be achieved through chemical synthesis by 'stiffening' the molecules. The introduction of stiff groups into otherwise flexible chains encompasses much of the current effort in LCP synthesis concerned with mesogen-flexible spacer combinations, the extreme end of the flexibility-rigidity spectrum being the fully rigid rod of great present topicality (e.g. PBZT). Conversely, making rigid rod material more processable involves introduction of flexible spacers without, however going so far as to remove the LCP 'window' in the phase behaviour; the 'scheme' provide guidelines for such chemical tailoring.

Alternatively G_L can be raised and stable LCP state created by physical means, in particular by orientation, thus the LCP promoting effect of orienting flows. The latter is a potentially significant factor, say in processing Kevlar, but also in that of a fully flexible chain such as polyethylene (PE) worked on under other auspices in this laboratory. A recently discovered striking example of the latter showing the way how to make very high MW PE processable is being quoted in App. I (Figs 9,10). Thus while PE has not originally featured in the ERO programme it has in this way, amongst much else come within its orbit.

Raising G_C (Fig. 3 App. I) arises by creating imperfections in the crystal. In fact, imperfect materials are prone to form liquid crystals, particularly in polymers. The most common chemical way of introducing imperfections is by copolymerisation. The present 'scheme' therefore provides signposts towards the purposeful achievement of LCP-s along this route. This is currently being

followed by Professor Percec, in collaboration with ourselves, in his systematically planned synthesis of mesogen-spacer systems, where the spacers are of differing lengths. One example is Fig. 6 in Appendix I, others will feature in the forthcoming joint publication presently in the hands of Professor Percec. Crystal imperfections can also be introduced by physical methods (e.g. irradiation) and the imperfections themselves can be of a physical nature (e.g. kinks), examples for which are being quoted in Appendix I.

Amongst the important generalities which emerge through the scheme is the realization that the presence of a "mesogen" is not an absolute necessity for having an LCP; fully flexible chains may also be LCP-s under appropriate circumstances. Thus, they may possess an LCP 'window' in the phase diagram as such (e.g. some main-chain syloxanes and phosphazines), or can be made to acquire one by appropriate treatments (e.g. in PE by cross-linking (Fig. 8), or pressure (Fig. 7), or melt orientation (Fig. 10); the Fig numbers are referring to Appendix I). Even if flexible chain LCP-s have been reported before in connection with specific studies, we believe ours is the first attempt to integrate this subject matter with the rest of the LCP literature.

Finally, the 'scheme' also embodies the possibility of metastable LC phases, helping to clarify ambiguous and often confusing nomenclature adopted in the literature e.g. "monotropic", "enantiotropic". In this respect it also helps to distinguish between the effect of thermodynamic and kinetic factors in underlying LCP formation.

Summing up, the 'scheme' perceived and formulated during the work under ERO sponsorship provides a unifying perspective over many, what so far appeared to be disconnected aspects of the LCP field. This as judged from the response so far should have input into the creation of the LCP state by chemical and physical means and into the appreciation of effects associated with it.

3. THE MATERIALS (SEGMENTED LCP POLYETHERS)

The major part of the hierarchy - phase behaviour work relied on a family of new materials synthetized by Professor Percec at Cleveland. They are polyethers consisting of an alternating sequence of "rigid" diphenyl and flexible alkyl spacer groups linked by ether oxygen. They are all potentially main chain LCP forming.

They have the following general formula

1) Rigid group α-methyl stilbene

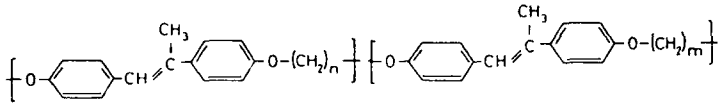

2) "Rigid" group diphenyl ethane

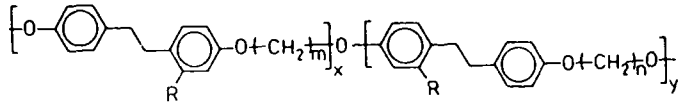

In both 1) and 2) n and m are variables.

The significance of having these compounds is as follows:

The ether linkage. Compared with the more familiar polyesters this linkage imparts thermal stability to the chain enabling the attainment of all phases, including the isotropic, and application of heat treatments without danger of chemical degradation. This is coupled with enhanced flexibility of the ether linkage which leads to accessible phase transition temperatures anyway.

Variation in spacer lengths. This enables the over-all chain flexibility to be varied in a systematic manner for a given "rigid" group. This corresponds to a chemical realization of varying G_L in the thermodynamic scheme of the preceding section (and Appendix 1).

Copolymerisation of different spacers ($n \neq m$). This greatly widens the scope of chemical tailoring and corresponding

manipulation of mesophase window. To be noted: for a given pair of n and m the ratio n:m affects the phase behaviour largely through raising of G_C in the thermodynamic scheme (Fig. 3 Appendix 2). Note also that the chemical synthesis involved with these polyethers (Professor Percec) ensures the randomness of the copolymerisation better than in most other systems.

Variation in "rigid" group. While the α-methyl stilbene (1, above) is mesogenic, i.e. forms LC-s also in its low MW form, the diphenyl (compound 2 above) is not mesogenic in itself but becomes so in the appropriate conformation within the polymer. This has interesting consequences for the systematic design of phase behaviour. Also it is one of the several illustrations that the 'rigid' group in itself need not necessarily be a mesogen.

4. PHASE DIAGRAMS

4.1 General

Determining phase regimes has been a primary task throughout, important for its own sake and for structure hierarchy research to follow. In particular, this was directed towards identifying the mesophasic temperature 'window' and defining it quantitatively. In thermotropic material this is meant to determine crystal melting (T_m) and temperature of isotropization (T_i) by DSC calorimetry in the first instance. The LC region is between T_m and T_i; above T_i is the isotropic melt achieveable with Professor Percec's polyethers. Fig.1 in Appendix II represents such a phase diagram with molecular weight (MW) as a variable for a given chemical constituent of compounds in class 1) in the preceding chapter (more about MW dependence below). This Fig. also shows the glass transition, T_g. T_g although not of thermodynamic origin is an important parameter. In principle it can be located in any phase, and where it happens to be it freezes in that particular phase preventing its transformation to any other phase below this temperature. We have mapped a large number of phase diagrams of LCP compounds in this way. Fig.6 in App. I represents one for a compound type 2 (previous chapter) as a function of copolymer composition.

DSC reveals transitions but in itself does not identify structure. The latter has been done either by optical microscopy or by X-ray diffraction, or by both, throughout this work. A particularly important accomplishment in the latter respect was the design and realization of a combined DSC and X-ray method (XDDSC) providing heat (and thus transitions) and X-ray diffraction patterns (thus structure) simultantously. A separate section[7] with an Appendix (VI) will be devoted to the XDDSC technique and to the establishment of its applicability further below.

4.2 Application of new DSC X-ray technique (XDDSC) to LCP research

At this point we shall illustrate the application of XDDSC to some salient issues arising in Prof. Percec's materials. The materials are of the category 2) of section 3. As stated in section 3 here the diphenyl groups are not mesogens as small molecules but are becoming so as a result of being built into polymer chains. This was originally inferred from DSC measurements alone by Professor Percec, an assertion of major potential consequence in chemical design of LCP-s. In view of its unconventional implications however, X-ray diffraction confirmation was required. This was achieved by ourselves thanks to the new XDDSC technique as documented by Appendix IV. In brief this Appendix provides verification of the nematic state in three cases for the above family of compounds described therein. It also deals with further transition providing a small but distinctive heat signal, tentatively termed 'smectic' by Professor Percec. Figs 8,10c App. IV. In contrast to the main claim of having verified a nematic phase; this latter assignment we were so far unable to verify by DSXD, leaving the corresponding transition unidentified, subject for further research.

The material in Appendix IV also provides examples of differences between heating and cooling runs demonstrating the influence of kinetic factors in the identification phase behaviour and the potential ambiguities arising therefrom. It also contains crystallogaphic information such will tie up with section 8.

4.3 The prospect of bridging Thermodynamic with Lyotropic systems

As some of Professor Percec's materials were not only fuseable but also soluble in tractable solvents they can form both thermotropic and lyotropic LCP-s. This for the first time ever promises the establishment of a combined lyotropic-thermotropic phase diagram. This is to bring about a long outstanding unification of the two fields , lyo and thermotropic LCP-s. These have been hitherto separate, because the lyotropics studied so far are infuseable and the thermotropics insoluble. The resulting combined phase diagram with concentration and temperature as variables should, by our predictions, have the schematic form in Fig.1. We made significant steps towards this (Period report April - Sept. 1986) but for definitive confirmation we are awaiting further materials from Professor Percec specifically designed for this purpose.

5. MORPHOLOGY

5.1 General Trends

In line with our declared purpose the morphology and its changes associated with phase transformation was followed, in the first instance through optical microscopy, representing the upper range in the structure hierarchy. Amongst our multitudinous findings some which provide general guidelines will be summarised.

Liquid crystal (LC)→crystal(C). For normal low MW LC-s both phases are readily identifiable by their polarising optical image. When cooling from the isotropic melt first the LC then the C texture appears from which, amongst others, the corresponding transitions can be identified. We now find that this is not generally the case for polymers. As the molecular weight (MW) increases the LC texture can become "frozen in"; the resulting crystalline state will, on the microscopic scale of the structure hierarchy, appear like an LC (Period Report Sept. 1985-March 1986) the more so the higher MW.

The LC texture itself is a function of MW, high MW giving finer textures. In fact, as well known, for MW-s of a typical polymer the texture (so called 'worm' texture) is too small for polarising microscopic analysis impeding advances similar to those made over a century on low MW LC-s. It was therefore a major surprise when the highest MW-s in Professor Percec's materials produced surprisingly large scale textures. These are both interesting in themselves and are opening up hitherto closed avenues to LCP research (Period Report Sept. 85 - March 86). Much more recently the origin of these large scale structures was identified and their reproducibility (for a period in doubt) assured. As we consider this of special importance the next section will be devoted to it.

5.2 Nature and Origin of Large Scale Texture

The present stage of this subject is contained by App.V
A brief guide, here in the main text, is as follows. Surprisingly the large scale textures were found to be a consequence of preceding ordering in the isotropic state. They can be systematically produced by first shearing - preferably multidirectionally - the isotropic melt. Even after all visible order is relaxed the large scale textures (Fig. 3 in App. V) appear in cooling to the LC state. In the absence of preceding shear only the familiar 'worm' structure is obtained (Fig. 1 App.V). As this only happens for the highest MW it must mean that the longest chains must have retained the memory, a kind of skeleton of preexisting long range order in the isotropic state, produced by the preceding shear which then is 'developed' into a large scale structure by the newly forming nematic state on subsequent cooling. The significance of this effect is manifold. First, it reflects the possibility of long range organisations of what has hitherto been believed to be a truly random isotropic state: clearly therefore in an LC forming polymer this finding challenges the concept of full randomness. Secondly, it calls for a rescrutinization of past literature on texture of LCP-s as expounded in Appendix V. Thirdly, the large scale structures, such as in Fig. 3 Appendix V, represent unsuspected further level of structure hierarchy beyond those of fine grains. In fact as observed, these large structures are constituted of such fine grains (Fig. 6 Appendix V). Fourthly, this whole structure hierarchy will

need to be taken into account in the interpretation of properties of the final LC (or crystals on further cooling), and finally, and possibly most importantly, of the rheological-flow properties of melt and LC states. Work on the latter, as prompted by the above recognition is in progress.

6. NON EQUILIBRIUM STATES - MEMORY EFFECTS

6.1 General

This subject is laid out in Appendices II and III. The present text is to aid their appreciation.

Our extensive experience has shown that neither the isotropisation temperature (T_i) nor the heat of isotropization (ΔH_i), as measured from DSC thermograms, is a uniquely defined function for a given compound. Repeated experimental runs gave different values, which of course greatly affects the construction of phase diagrams. This was eventually traced down to the possibility of a range of non-equilibrium states. These in turn are influenced by memory effects, namely that the previous history of the sample can affect the thermodynamic parameters as measured. This means, in the first instance, that parameters just as measured in any arbitrary DSC run, are not likely to be the correct ones for the equilibrium structure, and secondly that special measured have to be taken to obtain the correct values. These recognitions are having profound effect on the whole LC field in general, and phase behaviour-structure morphology work in particular. They mean that in any given phase the sample usually does not attain its final state of equilibrium: there is a non-equilibrium disorder in the crystalline and LC states and residual order in the isotropic state, variable with sample preparations. This departure from equilibrium needs first to be identified for structure characterisation and eliminated for determining true phase diagrams. While this situation may not be unfamiliar for the crystalline state in conventional polymers, where the issue of 'degree of crystallinity' has long been a material parameter, its recognition in the LC and isotropic states with the present material was totally unexpected.

Such non-equilibrium and memory effects also had profound manifestation in the morphology (Appendix II), in fact the large scale structures in the preceding section was one of them (Appendix V).

6.2 Non-equilibrium order deficiency - memory in the LC state

The original recognition is described in Appendix II, and as a further stage in Appendix III. As a brief guide, the T_i and ΔH_i values, as normally obtained by just any experimental run, were found to be too low and were dependent on the holding time in the liquid crystal nematic state. Increasing holding time was increasing values for both quantities (Fig.2 in Appendix III). Correspondingly and strikingly, this was also reflected by the polarising optical morphology: the initial texture was fine grained, but coarsened on increasing holding time (Fig. 3 Appendix II). (It is to be noted that in spite of the prominence of this coarsening the truly large scale structures as in Appendix V are not obtained in this way: for that the treatment in the isotropic state, shearing in particular as described there is required). The discontinuities at the grain boundaries should contribute to, or even be, the source of *non-equilibrium imperfections*. This raises the possibility of interpreting deficiencies in thermodynamic quantities in terms of morphology on the optical microscopic level of the structure hierarchy.

Following the recognition of the non-equilibrium effects extrapolation treatments were developed (Fig. 4 in Appendix II) by which the equilibrium $(T_i)^{\infty}$ and $(\Delta H_i)^{\infty}$ could be obtained. These are the values which are then used for the phase diagrams and for thermodynamic characterisation and comparison of samples, and this is the procedure adopted since, as a result of our work, by Professor Percec in his work in designing new families of LCP-s.

6.3 Non-equilibrium order deficiency - memory in the isotropic state; its effect on T_i and ΔH_i

This totally unexpected factor, the influence of the isotropic state on the subject matter under discussion is contained by Appendix III. In brief summary,it was recognized that the time of

residence in the isotropic state can have major influence on T_i and ΔH_i (hence perfection of the nematic state) formed on subsequent cooling, Figs 2,3, App. III. This means that contrary to all previous conceptions, even the isotropic state need not be uniquely defined but contains the memory of the preceding nematic state. When cooled again into the nematic phase regime, this "isotropic memory", presumably due to the underlying persistent residual structure features will influence the perfection of the newly arising LC phase. Thus the non-equilibrium perfection (or imperfection) of the LC state has a double dependence on sample history: dependence on holding time in the preceding isotropic state and on the holding time in the LC state itself. Thus for obtaining well defined samples in the isotropic state, or LC, or even crystal states on subsequent cooling the "isotropic" memory needs first erasing. This recognitions and procedures of achieving it are documented in Appendix III.

6.4 Summary and significance of non equilibrium states and associated memory effects

In any of the phases (crystal, liquid crystal and isotropic) the material is usually in a non-equilibrium state with order deficiency in the first two and excess order in the last one.

Definition of these states is an important aspect of material characterisation.

Elimination of non-equilibrium effects is a prerequisite for meaningful thermodynamic phase mapping with consequence for planning purposeful synthesis based on thermodynamic predictions. Both of these are being taken note of by current works by ourselves and Professor Percec on which comprehensive publications are in preparation.

The 'memory' of one phase, and its state of perfection, can be carried over to other phases even through more than one phase transition.

Memory and non-equilibrium effects are more pronounced for higher molecular weights, but become reduced with increasing chain flexibility hence for compounds with longer aliphatic segments (Appendix III).

All the above factors influence the texture and its hierarchy, the creation of unusually large scale structures of special interest (Appendix V) representing a striking extreme.

The newly recognized variability of optical microscopic structure and new hierarchical elements of this structure (Appendices II,V) should have important consequence for properties and rheological behaviour to be explored.

7. SIMULTANEOUS THERMAL ANALYSIS AND X-RAY DIFFRACTION (XDDSC)

The desirability of recording thermograms and X-ray diffraction patterns simultaneously has been raised in the preceding section. It was stated there that such a method was developed by ourselves under the ERO grant. This was done originally to identify the structural nature of phase transitions in some of our LCP-s, in cases where this is not obvious a priori, and where the transitions are so subtle that separately conducted DSC and X-ray experiments cannot be relied on with certainty. Such results on LCP-s were presented in section 4.2 and Appendix IV.

The development of the new instrument and the assessment of its capability is forming a separate chapter described by Appendix VI in the form submitted for publication.

As a brief guide, the main instrument is a Mettler DSC designed for an optical microscope stage. The instrumental development was to adapt it so as to make it transparent for X-rays while ensuring adequate heat conduction, and also allowing for a sufficiently wide exit angle for the diffraction pattern. The key innovation was to use Boron Nitride as DSC sample holder material which has made it far superior to anything that has been tried previously, making it, so we believe, a universal facility not only for polymers but also

for materials science in general. High X-ray intensity is clearly a requirement. In our case it was a synchrotron X-ray source, clearly optimum for the purpose. We had the good fortune to have access to this facility.

Of the many tests we did three are quoted in Appendix VI providing examples over a range of applications in materials science.

i) A small molecular LC, such as of interest for device applications (for formula see Appendix VI). This material displays a series of crystal and smectic LC phases which our new XDDSC could identify and/or confirm. (Fig. 3 App. VI).

ii) Oligomers of the presently topical high performance polymer PEEK. Here subtle rearrangements could be identified and followed on changing temperature such as reflect chain-end register and interlayer packing. (Fig.4 App. VI).

iii) Reversible orthorhombic -hexagonal transitions in constrained (epoxy embedded) ultra high strength polyethylene (PE) tapes. This is a topic featuring in section 2 (Appendix I). It is the first time that a mesomorphic phase transition could be followed reversibly in PE made possible by our XDDSC facility.

8. MOLECULAR PACKING - CRYSTALLOGRAPHY

8.1 General

This part of the programme is directed towards the small scale end of the structure hierarchy, the mutual arrangement of molecules, the method of study being X-ray diffraction. It straddles the area between the perfect 3 dimensional positional order of crystalline fibre and the purely parallel directional correlation without any lateral order of the oriented nematic state. Our concern here is the mutual packing arrangement of segmented chains of the kind synthetized by Professor Percec, the sytems under consideration being at the interface of liquid crystalline and true crystalline

states. This line of work highlights a largely bypassed area: the mutual packing requirements of rigid group - flexible spacer units in LCP forming chains, and possibilities of conformational disorder within the flexible spacer units. The work was carried on both type 1) and 2) compounds (section 3) with essentially identical result. In this account documentation is chosen from the HMS polymer (of formula type 1). Most of the basic material contained by a publication is appended as Appendix VII. Some essential material is still unpublished except for period reports. Because of their salient importance such further items relating to interlayer separation and copolymers, as represented by a Table and 2 figures are included in the main text.

8.2 Rigid group - flexible spacer packing modes

This is laid out in Appendix VII to which a brief guide is as follows. Potentially rigid aromatic groups and flexible spacers have alternating unequal cross-sectional areas along a given chain (e.g. Fig. 3 in Appendix VII) which makes optimum packing for each constituent impossible. We explored the response of the system to this situation by preparing oriented fibres and examining them by X-ray diffraction in the course of which highly informative X-ray diffraction patterns could be obtained (Fig. 1 Appendix VII). The flexible spacer length was one of the principal variables (n and/or m in homopolymer of formula 1) section 3).

For a given n the packing mode was found to be incisively affected by temperature, leading to two basic kinds of packing modes derivable from the diffraction patterns.

a) Layer packing. Here the rigid groups stack side-by-side (Form III in Fig. 3 of Appendix VII) giving rise to alternating layers of rigid groups and flexible spacers.

b) Intermeshed structures. In this newly discovered totally unexpected mode of packing the bulky aromatic groups form a kind of "chess board" arrangment as in Form II in fig. 3 of Appendix VII.

Packing conditions between a) and b) seem to be delicately balanced, and even for the same compound are affected by temperature. At lowest temperature a very poorly ordered layer structure forms (Form I, presumed to be similar to Figure III but with less register between chains and layers). On increasing temperature this transforms into the intermeshed structure of Form II which, on further increase of temperature, changes into the more ordered layer structure of Form III. The symmetry conditions are noteworthy. Only Form II is truly 3 dimensional consisiting of a fully 3 dimensional array of blocks (mesogens) and holes (spacer). This 3 dimensional structure is seemingly determined by interblock contacts. The envisaged layer strucure of Form I is closer to being 1 dimensional while in the stabler Form III the order within the mesogen layer corresponds to the most perfectly developed crystallographic order on the local mesogen scale but not to the most perfect 3 dimensional order over distances encompassing the rigid group - spacer alternation, which in turn is realized by Form II. Clearly the system is trying to balance between the conflicting packing requirements imposed by the mismatch in cross-sectional areas of two of its chain constituents.

8.3 Accommodating flexible spacers

When either of the two packing requirements of the aromatic groups are satisfied there is excess space for the flexible chain portion of lower cross sectional area allowing some conformational disorder in the latter.

Conditions are most restricted for the "intermeshed" Form II where the volume for the spacer is fixed. Nevertheless as described in Appendix VII as n is varied, more than one spacer length, e.g. either n = 5 or n = 7, can be accommodated within the same 3 dimensional structure which in turn is determined by "interblock" contact alone.

In the layer structure the thickness of the flexible spacer is variable allowing for further possibilities. These are described in Appendix VII but here we invoke the additional Table 1 for concise representation.

Here the sketches in the second row represent the principal situations. They show a flexible chain interlayer with attachments to the rigid unit layers bounding it from above and below. There are three situations as emerging from our works.

A) The spacers are fully stretched out, the case of short spacers. The measured thickness of the combined rigid unit-flexible spacer layer corresponds to the sum of the lengths of rigid unit and flexible chain portion, the former having been assessed by conformational calculations and models (Fig.1 Appendix VII). The straight spacer form has optimum chain conformational energy but, as constrained by attachment to the rigid group, is least favourable for space filling, hence leads to low density.

B) As the length of flexible chain portion increases space filling requirements override the chain conformational one. Randomisation of spacer segments leads to improved space utilization while introducing energetically less favourable bond conformations. Most notably, the interlayer spacing itself remains virtually unaffected when going e.g. from n=5 to 9. The excess length of the flexible spacer portion for n larger than 5 is being accommodated by excess space within the otherwise identical layer volume between the strata of rigid units.

C) For still longer flexible chain portions a new factor intervenes: the spacer-rigid unit interface becomes inclined (as opposed to being perpendicular with respect to the overall chain direction, a fact deducable from X-ray diffraction. Further, in this inclined form the flexible chains proved to be fully extended as drawn in C) of the Table. Because in this inclined arrangement the lateral interchain distances are reduced, clearly it is the resulting improved spacer packing which is the driving force. The latter implies that some interchain interaction is setting in for arrangement C. This indeed has been verified calorimeterically as an additional heat of fusion when going from n=9 to 11 as shown by Fig. 2 in present main text. The constancy of ΔH_f in Fig. 2 over n=5 to n=9 is consistent with rigid unit packing, which is identical for the full n range, alone contributing to the ordering process below

n=11. The excess $^{\Delta}H_f$ for n=11 is well below that for crystallization of alkane chains and thus corresponds to a mesophase. Accordingly, we have the most interesting situation of a "micro mesophase" localised to a portion of a molecule within a conformationally disordered "macro mesophasic" crystal.

A further important category is the case of copolymers with n≠m in compounds 1) and 2) of section 3, i.e. chains constituted by two or more unequal spacer types. We find that for spacers where n and m differ by only a few carbon atoms a combination of the situation in A) and B) in the Table pertains. I.E. the shorter spacers are fully extended determining the layer thickness, with the longer ones accommodated in a random fashion a situation described explicity in Appendix VII and illustrated schematically by Fig. 3 in this main text for ready appreciation. (In Fig. 3 featuring as Fig.10 in period report Oct. 1985-March 1986) the mesogens are drawn as heavy straight lines, and inclined, which was appropriate for the particular system in that early report).

8.4 Summary of crystallographic work

In summary, our crystallographic work under ERO grant has identified the factors controlling mesogen (or in general, rigid group) packing in segmented LCP forming polymers and its influence on layer formation at the submolecular level of the structure hierarchy. Further, it highlighted the delicate balance between the differing packing requirements of unequal constituents in rigid unit - flexible spacer systems, leading to different structure geometries, including a totally new non-layer type fully 3 dimensional yet, on a micro level still partially disordered structure ('intermeshed'). Further, in the case of layer structures, the space filling mismatch between chain constituents leads to different identifiable and rationally analysable types of layer disorder in the flexible chain sub-layer including fully extended, yet amorphous, randomly disordered and locally mesomorphic strata. It also provides information of how unequal randomly distributed chain segments in copolymers can be accommodated within one and the same overall layer structure. All these results are embodying general structure principles and thus should have implications beyond the

LCP field; in particular for the envisaging of alternating order-disorder in layered structures of whatever source, a core issue in polymer morphology, and in envisaging structural organisation in copolymers.

9. ORIENTATION

9.1 Background

Orientation and orientability is one of the most important aspects of long chain polymers, for its unique scientific interest, its interest for processing, for its influence on final structure, including the various levels of the structure hierarchy, and finally for its influence on resulting properties. In addition to these generalities, in LCP-s there is the further specific issue of influence of orientation on the liquid crystal transitions, and vice versa, of how such transitions react back on the orienting influence (flow behaviour, rheological parameters). As stated in section 1 we found the commercial polyesters unsuitable for the intended basic study (unrealizable isotropic state, chemical changes at elevated temperatures, opacity for in situ melt observations), and we decided to turn to Professor Percec's polyethers. Here the phase-behaviour structure hierarchy work had to be mapped first, the main body of the present report, and also larger amounts of material had to be acquired. This has been accomplished and the work is currently in hand, of which one item will be quoted (section 9.5 below).

Against the above background the main body of the orientation work was on the lyotropic fully rigid rod molecule poly(1,4-phenylene - 2,6 benzbisthiazole) PBZT, an advanced high performance material. This material is only processable in solution where, at sufficient concentration, it is in the LCP (lyotropic) state. We have studied it before, and it is with this previously gained background that we took it up again. The orientation behaviour of this material is of fundamental significance, as it is possibly the best model for rigid rod molecule behaviour, and of technological importance, because creation of orientation and its retention (minimisation of relaxation) is the most important aspect to its processing.

For reporting purposes the work is presented in three parts. The first is an optical (birefringence) investigation of disorientation from the highly oriented state, a follow up of preceding works in this laboratory, which had been carried out earlier on US Air Force grant (European Office). The second and third parts represent a newly initiated programme relying on a technical innovation by which creation and decay of orientation can be followed in situ by X-ray diffraction.

9.2. Disorientation of rigid rods (PBZT), followed by birefringence

This investigation is laid out in the first part of Appendix VIII, the essentials being conveyed by Fig. 5 in that Appendix. In essence, we followed the decay of birefringence from near perfect orientation after cessation of the shear producing it, the system being in an 'entangled' state, that is of concentration high enough for the rods to interact, but not so high as to form LC-s. The principal result was the identification of three consecutive stages of the relaxation i) A first, very fast one, up to a stage of disorientation where neighbouring rods start abutting in their rotational Brownian motion ii) A final slow process which can be distinctly identified by a rate determining step corresponding to 'entangled' rods getting out of each other's way, and iii) a less well defined intermediate process in between.

9.3. Technique for in situ X-ray recording of orientation

We consider the establishment of this technique as an important step in the field reinforced by the positive response to it by all those concerned (including US Airforce Dayton, Dow Chemicals in the US, University of Cambridge UK) who acquired advanced knowledge of it. It is described by the two somewhat overlapping Appendices VIII, IX with more experimental detail in Appendix IX, and has been reported and photographically illustrated in Periodic report Apr.-Sept. 1988. The instrument operates in simple shear with controlled, variable shear rate and temperature. The most essential point is transparency to X-rays achieved by windows made of Boron Nitride, and fast recording time made possible by our access to a

synchrotron X-ray source. Another important practical feature is exclusion of moisture and oxygen during operation to enable the handling of such sensitive dopes as PBZT.

9.4. Capabilities of technique and first results

The first stages of the promising ongoing work are contained by the publication material in Appendices VIII, IX. Here the main points are as follows.

i) X-ray diffraction signal from the PBZT rod molecule itself. This corresponds to the one-dimensional periodicity of the chemical repeat along the chain. The angular distribution of the corresponding reflexion provides the most direct information possible about the orientation distribution of the rods, which can thus be studied directly as a function of specified orienting influence. This orientation registration is independent of phase state and intermolecular interactions. Also, the relaxation from the oriented state can be followed. Appendices VIII, IX provide experimental illustrations in terms of actual diffraction patterns and their photometered traces.

ii) When in the lyotropic state, there is an X-ray diffraction signal arising from the inter-rod packing. This provides evidence, in the first place, of the phase state at a given concentration, temperature and under the influence the particular rate of shear (with the possibility to identify orientation-induced phase changes), and secondly of the orientation distribution in terms of the nematic inter- molecular spacing.

iii) There is also a notable orientation of the solvent, polyphosphoric acid, as apparent from four-fold intensificiation of the corresponding diffraction halo. (Fig. 6a App. VIII). This feature is remarkable, and suggests interaction between solvent and polymer a novel issue requiring exploration.

8.5 Initial observation on thermotropic LCP-s; Banded structures; natural polymers

As indicated in section 1 we are now in the process of extending the PBZT work to Professor Percec's materials in their thermotropic state. This stage was reached thanks to previous mapping of phase behaviour, latest larger supply of materials from Professor Percec, and our new instrumental developments. As a result, we can now follow orientation and its decay in situ under controlled conditions, optically, by calorimetry (DSC) and by X-ray diffraction.

At this stage only one point, which is additional to those in the preceding sections will be made: the frequent observations of banded structures, as revealed by the polarising microscope (Fig. 4). This is a general yet still unexplained phenomenon throughout the whole LCP field (also Kevlar, PBZT and Vectra). It corresponds to a zig-zag type arrangement of alternating orientation along the orientation direction. It is known to arise on relaxation from the fully oriented state, sometimes unavoidably on spinning fibres or tapes, and when present, limits the ultimate mechanical modulus. We are now in the position where we can approach this problem as part of our systematic orientation in relaxation work. We have acquired through our preceding works, the instrumentation and the ideas by which we should have a good start.

As a final remark, banded structures such as in Fig.4, feature prominently in natural substances. The author was codiscoverer of this effect in collagen jointly with Cleveland colleagues (Diamant, Keller, Baer, Litt and Arridge Proc. Roy. Soc. A, 180, 293, (1972) and many later publications). This was the work which established the original Cleveland-Bristol association and led to the formulation of the wider programme on Structure Hierarchies at both places, and played an important part in the formulation of the explicit programme here reported. Thus, a large circuit, in the course of which much else was uncovered, has led us back to one of the source problems involving nature. These examples in natural materials are important by themselves, and chiefly, provide lessons

in purposeful material design, the reason for their inclusion in a materials programme (e.g. in collagen tendon properties arising from the banded structures are to lessen the injurious effect of impact). Our Cleveland colleagues (Professors Baer, Hiltner) have been more intensively concerned with this aspect of the programme, also under US Army (Durham USA) auspices during the last few years than ourselves, even if it has featured in our own original proposal parallel with our Cleveland colleagues. Nevertheless, as will be apparent, thanks to the other works we have done, we are now in a much better position to return to these issues on structure hierarchy in natural polymers, and this time as part of a comprehensive approach embracing phenomena in natural and synthetic systems within the same conceptual framework.

Table and Figure Captions

Table 1 — Interlayer spacings and flexible chain segment packing as a function of flexible alkyl spacer length and uniformity.

Fig. 1 — Expected phase diagram of a liquid crystal (LC) and true crystal forming (C_f)polymer which is both fusable and soluble in a low molecular weight solvent in all proportions. Notations: Iso ≡ isotropic solution and melt; LC ≡ liquid crystal; C_f ≡ true crystal (polymer); C^s_f ≡ crystal of solvent; T_i ≡ isotropization temperature (liquid crystal melting) in the thermotropic state; T_m ≡ crystal melting temperature in the thermotropic state

T_g ≡ glass transition of pure (amorphous) polymer

T^s_g ≡ glass transition of solvent, E ≡ crystal eutectic point.

Fig. 2 — Molar heat of fuson ("layered" crystal form nematic transition) for a series of well annealed PHMS-n homopolymers with increasing number of carbon atoms in the spacer (n). The constant ΔH_f for n = 5,7 and 9 indicates that spacers do not contribute to the crystallization enthalpy. The anomalously high ΔH_f for PHMS-11, on the other hand, suggests that the $(CH_2)_n$ spacers do interact forming a mesophase.

Fig. 3 — Schematic representation of flexible chain segment packing in a layered structure of a copolymer (n=5, m=7) with two different segment lengths. Here the shortest segment type is fully extended determining the interlayer spacing, with the longer spacer curling up so as to fill space available. The rigid group is represented by heavy lines forming regular layers. They are inclined for the specific case so as to account for the appropriate X-ray diffraction pattern.

Fig. 4 — Polarising optical banded structures as developing during relaxation from the sheared state in a thermotropic polyester. Shear direction vertical. Material PHMS-C5/7, M_n=32100. Polarizing optical micrograph.

TABLE 1.

Three options for minimizing spacer free energy realized in layer structures of PHMS

er length -groups)	SPACER EXTENDED, NON-CRYSTALLINE:	SPACER CONTRACTED, NON-CRYSTALLINE:	SPACER EXTENDED AND TILTED, CRYSTALLINE:
	+ low intramolecular (conformational) energy - lowest density	+ higher density + higher conformational entropy - higher intramolecular energy	+ highest density - best mesogen packing possibly sacrificed and/or Ar-O-CH bond angle strained
	A. 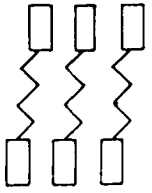	B. 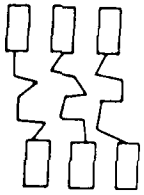	C. 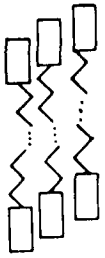
5	o		
6,7		o	
7		o	
9		o	
11			o

(+ an - signs indicate favourable and unfavourable points for the overall free energy which the system will optimise for each spacer length).

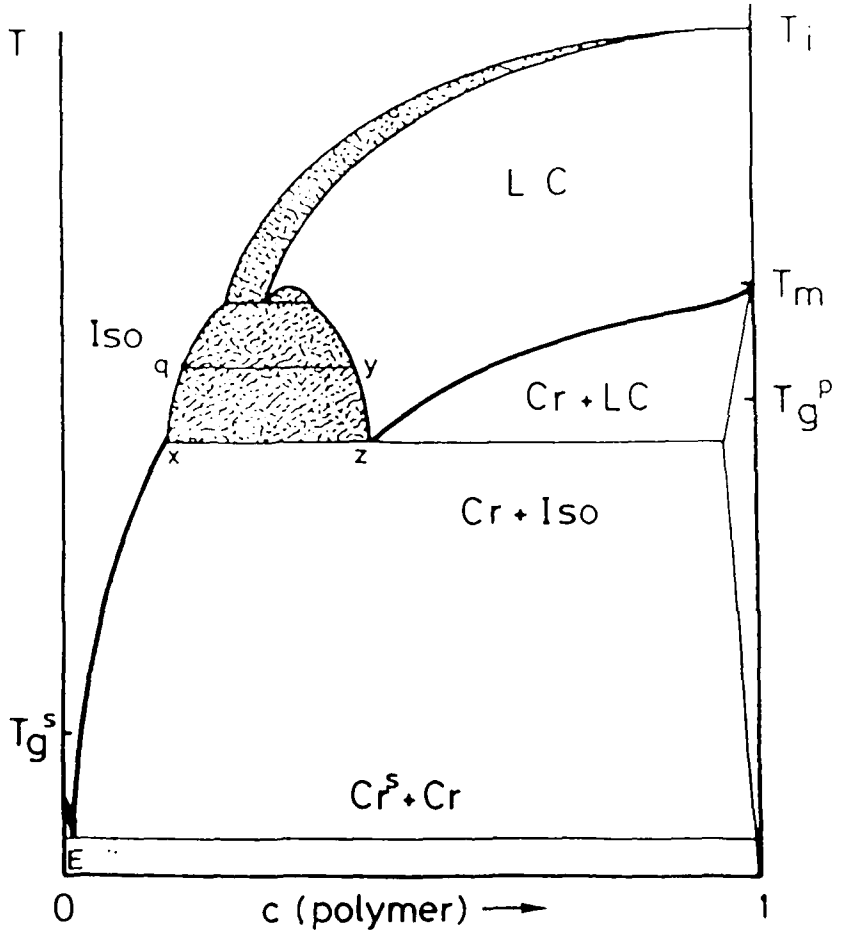

FIG 1

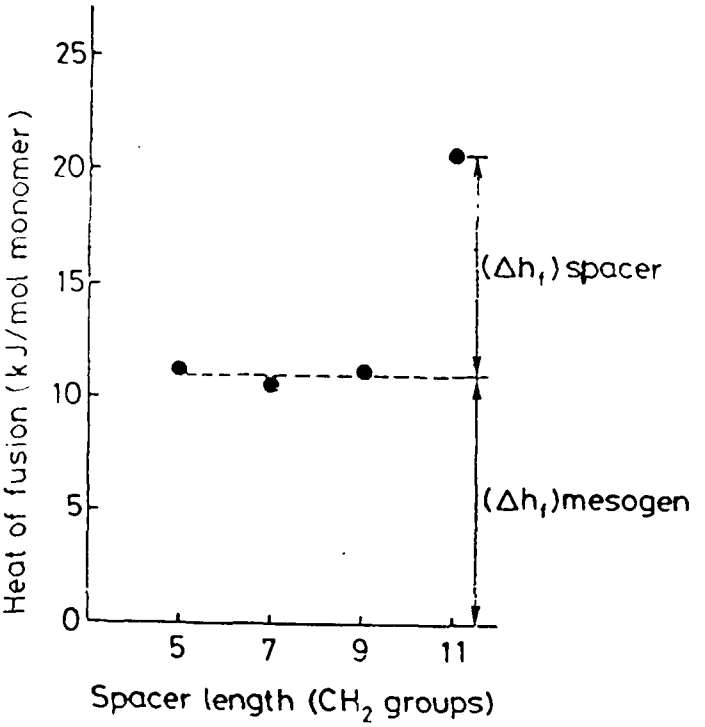
25
20
15
10
5
0
Heat of fusion (kJ/mol monomer)
(Δh_f) spacer
(Δh_f) mesogen
5
7
9
11
Spacer length (CH_2 groups)

FIG 2

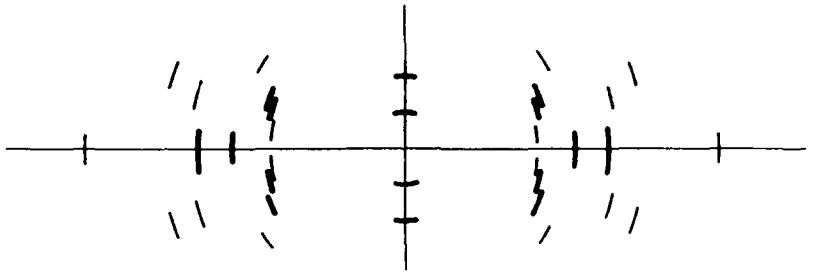

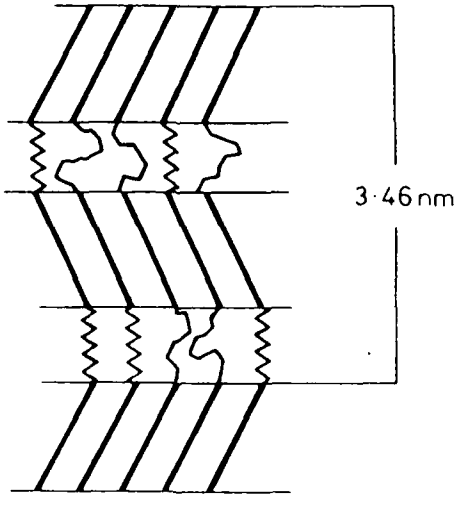

FIG 3

FIG 4

PUBLICATION LIST

"Effects of thermal treatment on the temperature and heat of isotropization in a nematic polyether"
Mol. Cryst. Liq. Cryst., 1988, Vol. 155, pp. 487-494

"Crystal and Pseudocrystals phases in main chain mesogenic homo- and copolymers with flexible spacers"
Mol. Cryst. Liq. Cryst. 1988 155, 313-325

"Liquid crystal polymers: a unifying thermodynamics based scheme" Macromolecules, in the press.

"Non-equilibrium excess order in the isotropic state of main chain liquid crystal forming polymers" Polymer, in the press.

"Simultaneous X-ray/DSC study of mesomorphism in polymers with a semiflexible mesogen", Macromolecules, in the press.

"Evidence for disclinations in the isotropic state of liquid crystal forming polymers", Mol. Cryst. Liq. Cryst. in the press.

"Simultaneous X-ray diffraction and differential scanning calorimetry (XDDSC) in the study of molecular and liquid crystals" Molec. Cryst. Liq. Cryst. in the press.

"Orientability of rigid rodlike molecules in solution and controlled preparation of model systems" in Rigid Rod Polymers, Materials Research Publication, Ed. W. Adams, in the press.

"Synchrotron X-ray analysis of disorientation in nematic solution of PBZT", Polymer Communication, in the press.

LIST OF APPENDICES

KEL/GU (1.4)

APPENDIX I

Macromolecules, in the press.

LIQUID CRYSTAL POLYMERS; A UNIFYING THERMODYNAMICS BASED SCHEME

A. Keller and G. Ungar

H.H. Wills Physics Laboratory, University of Bristol,
Tyndall Avenue, BRISTOL BS8 1TL.

ABSTRACT

It is shown that conditions for realizing mesomorphic states in polymers are readily expressed in terms of the relative thermodynamic stabilities of the crystalline, liquid crystalline and liquid phases. The simple scheme here presented has the merit of providing: i) a unifying perspective over a wide range of mesophase behaviour which otherwise may be considered in isolation as disconnected occurrences, ii) a signpost for purposeful attainment (or enhancement) of the mesomorphic state also in the case of systems which are not normally considered liquid crystal forming. Examples are quoted from a range of materials, most comprehensively from polyethylene, bringing together diverse past and some rather striking new observations illustrating the validity and usefulness of the scheme.

PURPOSE OF NOTE

In recent years the mesomorphic state has come increasingly to the forefront of polymer science, particularly since the purposeful synthesis and study of polymeric liquid crystals. Most frequently it is associated with the presence of mesogenic groups, (such as on their own would form small molecular liquid crystals) built in, or attached to, the macromolecular chain where the mesomorphic state is usually attributed to the stiffness imparted by these groups. In other instances of mesophase forming stiff molecules the chains are too irregular to crystallize in which case the suppression of crystallization is considered as the factor which promotes the mesophase. However, there are chains, including quite regular ones, which can give rise to the liquid crystalline state without any constituent capable of forming liquid crystals as separate small molecules. Such are e.g. the polymers based on the flexibly jointed diphenyl compound diphenyl ethane [1], the totally flexible main chain polysiloxanes with side groups beyond the length of methyl [2], main chain polyphosphazenes [3] and even the fully flexible and chemically simplest long chain compound polyethylene under circumstances to be discussed in specific detail below. Many examples of mesophases in polymers of the latter type have been listed in the review by Wunderlich et al. [4]. The purpose of the present communication is to lay out a simple thermodynamic scheme which embraces all the above categories. It will be purely diagrammatic and qualitative, along familiar lines, yet we hope that in the context presented it will provide a coherent thread linking together the various manifestations of mesophases, thus contributing towards the understanding of their interrelation and providing guidance for their purposeful design. Illustrative examples will be quoted from available experimental material such as are not readily found all together in the literature at least in the present context. Such will embrace cases with chemical constitution and/or physical parameters as variables. They will include some examples of chains with varying ratios of rigid and flexible constituents but mostly polyethylene in its diverse forms and circumstances.

THE SCHEME

Equilibrium States

For the considerations to follow it will suffice to consider the basic thermodynamic relationship

$$dG = Vdp - SdT \quad \ldots \quad \ldots \quad \ldots \quad 1$$

where G is the free enthalpy, S the entropy, V the volume, p the pressure and T the temperature. For the scheme in question take first the melting of a true crystal at constant pressure (dp=0). As seen from Fig. 1, and as follows from eq. 1, the free energies of both crystal (G_C) and isotropic liquid (G_L) decrease with increasing temperature where the decrease in G_L is the steeper, due to $S_L > S_C$. Where G_L crosses G_C the crystal melts, which of course is at $T_{C-L} = T_m$, the melting point of the crystal. In this case, as drawn in Fig. 1, the free enthalpy of any hypothetical mesophase (if such can exist at all), G_M, cannot fall below both G_C and G_L, hence correspond to a stable state at any temperature. While G_M decreases faster with T than G_C it will only cross G_C at a point which is above G_L, i.e. where the isotropic liquid is already the stablest phase. Thus the mesophase is virtual and remains unrealizable as a stable phase.

In order to create a stable mesophase a section of the G_M v. T curve will need to be brought beneath both G_C and G_L (thus to a state of greatest stability). This can be achieved either a) by raising G_L (Fig. 2) or b) by raising G_C (Fig. 3), or by a combination of both a) and b). As seen in Figs 2 and 3 the mesophase will be "uncovered" in a temperature range bounded by T_{C-M} and $T_{M-L} \equiv T_i$ corresponding to temperatures of crystal melting and isotropization respectively. (The lowering of G_M would have the same effect; but changes in G_M are expected to be small compared to those in G_L and G_C and will be disregarded in what follows). In general, raising of G_L (case a)) arises from the lowering of the melt entropy, while raising of G_C (case b) from the reduction

in the perfection of the crystal as to be shown in specific examples later.

Footnote 1

Note that in case of a) the crystal melting point, T_m, is raised, while in b) it is lowered, a situation clearly brought out by the experimental examples to be quoted.

Footnote completed

We can generalise further by considering the influence of change in pressure, i.e. the Vdp term in eq. 1. Usually the specific volume is larger for the liquid than for the crystal with the mesophase expected to lie in between; hence $(\delta G_C/\delta p)_T<(\delta G_M/\delta p)<(\delta G_L/\delta_p)_T$. In principle it could therefore happen that at some p G_M falls below G_C and thus a mesophase may become 'uncovered'. It has been found that in most experimental systems (e.g. ref. 6) the effect of increased hydrostatic pressure is to promote the mesophase ("barophyllic" behaviour).

Footnote 2

However, there is no fundamental reason that would make this a general rule. This is clearly illustrated by the example of the sequence of alkanes→polyethylene (see below, (Fig.8)), where "barophobic" behaviour of short n-alkanes changes continuously with increasing chain length towards the "barophyllic" behaviour of polyethylene [6].

Footnote completed

The above scheme, as it stands is for single component systems leading to thermotropic mesophases. It can readily be extended, with appropriate elaborations, not to be pursued here, to two-component systems which would then also embrace the lyotropic state of matter.

Metastable states

Figs 1-3 refer to states of thermodynamic equilibrium. However, systems may not respond immediately when passing from one stable regime to another within the phase diagram, hence metastable phases can often arise.

In what follows we shall digress into the possibility of metastable states, as they are frequent in polymeric liquid crystals, and in particular, as they generate an ambiguous nomenclature which we are anxious to clarify. The most commonly encountered metastability is that arising on crystallization. As familiar, crystallization only sets in at certain supercooling. In polymers in particular, crystallization temperature $T_{L\rightarrow C}$ can be appreciably below the equilibrium melting point $T_{C\rightarrow L} \equiv T_m$. On the other hand, the formation of a mesophase generally requires less supercooling. Now, if the temperature of the transition from the isotropic liquid to a normally unstable mesophase lies somewhere between $T_{C\rightarrow L}$ and $T_{L\rightarrow C}$, such a "virtual" mesophase may materialise on cooling. As the temperature is lowered still further, crystallization will occur. At this stage two extreme situations may be envisaged, as depicted in Figures 4 and 5. On crystallization the free enthalpy either drops from G_C' to G_C, i.e. the value for the perfect crystal (Fig. 4, where the dotted line indicates a possible pathway), or else there is no discontinuous change in G, i.e. a highly imperfect crystal is formed with its free enthalpy remaining at G_C' (Fig. 5). The realistic path would be somewherer in between these two extremes, i.e. some decrease in G is expected, which may not quite reach the level of G_C.

We shall first consider the extreme situations of Figs. 4 and 5. When the perfect crysal of Fig. 4 is reheated, it melts directly into the isotropic liquid at $T_{C\rightarrow L}$; thus such a system displays the mesophase only on cooling, and is called 'monotropic'. On the other hand, the imperfect crystal of Figure 5 first changes back into the mesophase at $T_{C'-M}$ and then into the isotropic liquid at T_{M-L} on reheating; thus the mesophase occurs both on cooling and heating and is called 'enantiotropic'. The latter case clearly illustrates that an enantiotropic mesophase does not necessarily mean stability of the mesophase, as sometimes implied, although a stable mesophase, naturally, must be enantiotropic. As mentioned before, real systems are in between those described by Figs. 4 and 5. Some decrease below G_C' will occur upon crystallization, the magnitude of the drop depending, amongst others, on

crystallization kinetics. Accordingly, neglecting possible perfectioning on subsequent heating, mono-and enantiotropic behaviour are distinguished by the magnitude of the drop in G on crystallisation: if G stays above a critical value (G^c_C) the system is monotropic, if it falls below it is enaniotropic, the definition of G^c_C being apparent from Fig.4. It is easily seen how crystal perfectioning on annealing can lead to a "conversion" of a monotropic into an enantiotropic mesophase, an effect frequently observed in both polymeric and small molecule liquid crystals.

While it was assumed above that only G_C is affected by thermal history, in the case of main chain polymeric liquid crystals pronounced time dependent variability in G_M has recently also been observed [7]. It was shown that the lack of equilibrium perfection in the nematic phase can lead to substantial depression of the isotropization temperature $T_{M-L} \equiv -T_i$. Thus non-equilibrium *mesomorphic* states can also, in principle, affect the phase sequence (enantiotropic, monotropic) in the case of polymeric liquid crystals.

It is worth noting further that, under certain conditions, polymers will also display superheating effects, in which case the mesophase may only appear on heating; this can be regarded as "monotropic" behaviour in the reversed sense. An example of this in connection with polyethylene will be quoted further below.

As seen from the above, kinetics will always play part in any LCP phase diagram as determinable in practice. Its influence on our present considerations will depend on its magnitude. If it is small enough, so as not to alter the sequence of appearance (or disappearance) of the different phases with changing temperature, the equilibrium situations in Figs 1-3 will be taken to apply with the kinetics as an overlay, affecting only the exact numerical values of the actual divides. If, however, the phase sequence itself is affected, and in fact new phases are created due to metastability, then the whole phase behaviour will become kinetically determined and considerations in Figs 4,5 will pertain.

Finally a further kinetic factor, the glass transition (T_g), needs invoking, particularly pertinent to LCP-s. On cooling the system becomes immobilised at T_g (more precisely also dependent on the rate of cooling), hence phase transformations will be arrested or altogether prevented. The inverse will apply when a previously immobilised system is heated above T_g when the system will again be able to follow its course towards the equilibrium state. In practice, this will lead to inaccessibility of certain portions of the phase diagram, or conversely, lead to the freezing in of the liquid or of the liquid crystal state enabling their attainments at temperatures where by thermodynamic criteria they would be unobtainable otherwise (isotropic or LC glass respectively [4]. Even if T_g is not a thermodynamic quantity the indication of its location in the phase diagram can therefore serve a useful purpose.

Having placed metastability, glass transition and related kinetic issues on the map we shall resume our argument as referring to thermodynamic equilibrium alone.

EXAMPLES - GENERAL

Mesogenic polymers

The scheme embodied by Fig. 1-3 encompasses most known situations. Thus high (or raised) G_L (Fig. 2) corresponds to low melt entropy which is consistent with the familiar tendency of stiff chains (worm-like or rigid rods) to give rise to mesophases. From this in turn follows the mesophase promoting role of mesogenic groups, the most often quoted single factor responsible for polymeric liquid crystals (LCP) and principal subject area of present day LCP research. In fact, the whole presently active subject area of chemical stiffening of chains, so as to give rise to liquid crystals, all relies in the first instance on appropriate shifting of G_L in the context of Fig. 2.

The extreme limit of stiffness is the fully rigid rod such as results from the polymerisation of all phenyl or

other condensed ring containing monomers of which poly(phenylene benzbisthiazole) (PBZT) of currently increasing topicality is a salient example [9]. In such cases of fully rigid rods G_L (or even G_M) becomes so high that T_i (or even T_m) may lie beyond the chemical stability limit of the molecule, in other words the material becomes infuseable (and also practically insoluble). As well known this fact has given rise to the widespread activity of chemically loosening the liquid crystal forming rigid rods so as to make them more readily fuseable and/or soluble (i.e. processable) without, however, losing the mesophase 'window' in the phase diagram*.

*Footnote

For processing purposes fluidity alone is required. This is achieved once T_m is reached. Hence, in practice the attainment of T_i for the technologically important rigid rod type molecules (e.g. Kevlar, PBZT, Vectra - see below) is not usually pursued.

Footnote completed

In present practice the loosening of rigid rod polymers is being pursued by copolymerising rigid phenyl containing mesogenic groups with flexible alkane or ethylene oxide spacers in varying predesigned ratios (e.g. refs. [10,11]). Here the number of CH_2 (or CH_2 CH_2 O) groups within the spacer in the different preparations determines the overall flexibility/rigidity, longer spacers leading to more flexible molecules and vice versa. The corresponding T_i will be higher with shorter spacers (e.g. ref.7,8) due to decreasing entropy of the isotropic liquid.

The above type of molecular tailoring of mesophases may well appear self evident from the chemical point of view. Even so, its incorporation in an underlying thermodynamic scheme should be helpful for a purposeful planning of chemical design and perceiving wider interconnections. For this purpose phase diagrams with chemical (e.g. spacer) composition as variable should be particularly appropriate, specially when the limiting conditions for the existence of mesophases are approached. Explicit reference to such phase diagrams

will be made in the next section (and beyond in ref.16), in that case in connection with the influencing of crystal perfection with which this issue becomes combined.

Returning to Figs. 1-3 the position of G_L, hence the existence or creation of mesophases, can also be influenced by physical means. Thus orienting chains, which would otherwise be randomly arranged, in the isotropic phase and also stretching them (in the case of chain flexibility) will reduce the configurational entropy,hence raise G_L, with consequent facilitation of liquid crystal formation. This LC promoting effect of orientation is familiar amongst rigid or partially stiff liquid crystal polymers, as manifest e.g. by the drop of viscosity when passing through orifices, a situation arising on processing (see e.g. ref. 12 on Kevlar). It is perhaps less familiar that fully flexible chains, which on their own are not liquid crystal forming (i.e. correspond to Fig. 1), can be transformed into a mesophase by orientation and/or constraints according to the scheme in Fig. 2, to be invoked explicitly for polyethylene below.

Crystal imperfections

High (or raised) G_C (Fig. 3) means crystals which are either imperfect due to defects or, while otherwise regular, contain loosely packed molecules. The latter, i.e. loose packing, may be due to bulky side groups. The liquid crystal forming ability of the otherwise regular and fully flexible long side group containing siloxanes [2] could be relatable to this cause. In addition (or alternately) bulky side groups could, due to steric congestion, stiffen a chain which then will raise G_L contributing to (or causing) LCP formation. The possibility of chemical irregularities of course are manifold in polymers. Irregularly placed branches or side groups, whether deliberate or accidental, are common features, again to be more explicitly referred to in connection with polyethylene. The LC forming tendency will be particularly pronounced when the influence of relatively bulky side groups and irregularity combine, as in the case of hydroxypropyl cellulose (e.g. ref. 13). Here the inherent stiffness

of the chain is biassing the system in the same direction in any case by raising G_L, while the presence and irregular disposition of the sidegroups suppress crystallization by raising G_C.

Introduction of comonomer units, even without necessarily involving branches will similarly reduce crystal perfection, hence raise G_C, thus promoting formation of the mesophase. Again, this will combine with the mesophase promoting tendency of stiff units within the chain, when such are present in any case, as e.g. in the technologically topical copolymers of hydroxybenzoic and naphthoic acids[14].

Mesogen - flexible spacer systems are particularly amenable for controlled adjustments in phase behaviour through variation in copolymer constitution. As stated previously, introduction of flexible spacers can render otherwise rigid rod polymers fuseable. If say, two different flexible spacer lengths are used the resulting copolymers will have enhanced mesomorphic tendencies through raising of G_C, thus lowering T_m, the result being a widened T_i-T_m interval in the phase diagram. Varying the copolymer composition ratio for say a given pair of flexible spacers then provides a subtle control over T_i-T_m, hence the width of the mesomorphic zone. This situation can be readily realized and systematically explored with polyethers of alternating diphenyl type mesogens and alkyl spacers linked by ether oxygen. These compounds, synthetized and explored by Percec and collaborators [1,15,16], possess sufficient thermal stability to permit the traversing of the various phase transitions without the danger of chemical changes, such as beset the more familiar, but otherwise analogous family of polyesters.

Of these studies here we shall illustrate one case involving chains with formulae such as

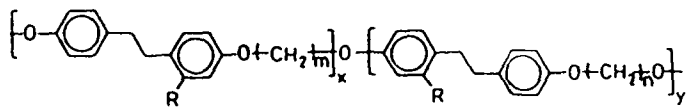

This is a copolymer where the "mesogen" itself is a semi-flexible moiety of diphenyl ethane, which is not LCP forming as a homopolymer, with $(CH_2)_7$ as a sole spacer, but is turned into LCP on copolymerization with $(CH_2)_9$ as the alkyl portion of the comonomer unit. The result is shown by Fig. 6. We see that a stable mesophase ($T_i > T_m$) results beyond a $(CH_2)_9$ composition of 0.2 with $T_i - T_m$ being largest at around 1:1 $(CH_2)_7/(CH_2)_9$ ratio.

Choosing the more rigid α-methyl stilbene, which is a familiar mesogen, instead of diphenyl ethane, in the above family of polyetheres enhances the LCP forming tendency throughout. Here T_i lies always above T_m, hence the mesophase is the stable one over the full comonomer composition range again with $T_i - T_m$ being maximum at around the 1:1 ratio (16).

The cases quoted thus provide examples for passing into the mesophase and for the controlled widening of this mesophase through chemical tailoring and this in a systematic manner in accordance with basic thermodynamic principles.

Amongst imperfections we may count further the random placement of isomeric variants of otherwise identical chemical moities along the chain. The mesogenic character, of α-methyl stilbene , a common mesogen (10,11) is in fact partly due to this reason. Here, the presence of the methyl group introduces nonplanarity into the otherwise planar stilbene moiety (17). Thus two enantiomers are possible, the polymer itself having no stereoregularity. The result is that G_x is raised and the melting [illegible] is suppressed; hence

4,4'-substituted α-methyl stilbenes, but not stilbenes, are nematogenic even as small molecules. When incorporated in a chain a further type of isomerism, namely head to head or head to tail (with relation to the methyl group in the mesogen) is added, the random sequence of which undoubtedly reinforces the LC forming tendency through raising the imperfection content of the crystal. All the above, relating to the methyl stilbene polymer, relies on the raising of G_C as in Fig. 3. This clearly combines with the chain stiffening effect of the stilbene group raising G_L by Fig. 2, the subject of the preceding section. The above case therefore provides an example of the mutually reinforcing interplay of the two thermodynamic factors highlighted by Figs. 2 and 3 respectively.

The above merely serves to place chemical tailoring on the map within the broader framework of our scheme. This line, with the added variable of molecular weight, will be pursued further in a forthcoming publication specifically devoted to it [18].

EXAMPLE : POLYETHYLENE

Crystal imperfections

In what follows we shall proceed with examples on polyethylene which illustrate the main aspects of the present scheme, and at the same time are noteworthy in their own right.

Polyethylene conforms to the situation of Fig. 1, i.e. under normal conditions it does not display a mesophase, only the familiar othorhombic crystal form (o). Nevertheless, there exists a virtual mesophase which can be 'uncovered'; the ways in which this can be achieved is the subject of what follows.

First about the mesophase itself. This corresponds to a hexagonal packing of the straightened polyethylene chain, i.e. to the packing of rods of circular cross-section which

in turn arises through cylindrical averaging of the polyethylene chain around its axis. This virtual hexagonal phase (h) in polyethylene is in direct continuity with the stable hexagonal crystal phase in n-alkanes as laid out by one of us elsewhere [6].

Of the various ways of 'uncovering' this virtual mesophase we consider first the route by Fig. 3, that is raising G_c. One example is provided by ethylene-propylene copolymers[19]. Here for high enough copolymer content, (for ca 70 CH_3 branches per 1000 main chain carbon atoms) the X-ray patterns reveal the hexagonal (h) as opposed to the familiar orthorhombic (o) packing of chains even at room temperature. Here the randomly distributed (CH_3) branches disturb the regular packing of the chains thus leading to the situation as in Fig. 3.

Another example is the influence of irradiation on linear PE with γ-rays or electrons[19] with doses large enough (more than 300 Mrads) to start influencing the a spacing of the orthorhombic lattice, but not yet sufficient to appreciably reduce, or even less destroy, crystallinity (the latter happens well beyond 1000 Mrads). When such an irradiated sample is heated the o phase changes first into an h phase before melting (Fig. 7). Thus the irradiation has created a mesomorphic region in accordance with Fig. 3, the temperature interval $T_i - T_m$ increasing with irradiation dose received (Fig. 7). As familiar by now, irradiation cross-links the polyethylene chains, preferentially in the amorphous regions [21,22], yet as the dose becomes large (approaching and exceeding 1000 Mrad) cross-links are being increasingly created also in the crystal. The latter will produce lattice defects which will increase G_c and thus, by Fig. 3, will lead to a stable mesophase in the appropriate temperature region with lowered T_m. It is worth noting that the introduction of cross-links also affects G_L: by reducing the configurational entropy of the melt it will raise G_L, hence lead towards a situation as in Fig. 2. (There is evidence for it through an initial increase - as opposed to the subsequent overall decrease - in the o melting point at doses which are too low,

5-20 Mrad, to have other consequences for the phase diagram [19-20].) Thus we have a situation where an increase in both G_C and G_L (Figs 3 and 2 respectively) contribute to the uncovering of the mesophase.

As laid out earlier hydrostatic pressure could promote the mesophase. Polyethylene provides a good example. As explored by Bassett et al [5] a hexagonal phase with mesophase characteristics (no longitudinal register between chains, high chain mobility enabling ready sliding of chains) appears above 3 kbar pressure - even with the (chemical) defect-free linear PE, at suitably elevated temperature (Fig. 8). Now, if the chain contains chemical defects, such as cross-links produced by irradiation, the triple point will shift towards lower pressures with increasing cross-link content until the hexagonal phase will become stable even at atmospheric pressure[20]. The latter is in fact the situation in the preceding paragraph represented by Fig. 7, thus highlighting the continuity between the effects of crosslinking and pressure: both increase G_L by reducing the entropy of the liquid.

Fig. 8 also displays the connection between the stable hexagonal phase in short n-alkanes and the hexagonal mesophase in polyethylene as a function of chain length in the p-T diagram. A full discussion is given by one of us elsewhere [6]. At this place our emphasis is on the continuity, despite the fact that the pressure coefficient of the width of the temperature interval is of opposite sign in these two families of material. This continuity is apparent also by a structural feature, namely the concentration of conformational "kink" defects, C_K. As described in ref.6 C_K can be directly registered spectroscopically and inferred from X-ray diffraction, and is found to be a continuous function of temperature (T) and chain length ℓ. The mesophase ('rotator' and/or 'hexagonal' phase) appears in different systems under different conditions, and the corresponding C_K (ℓ,T) values lie on a master surface given by an appropriate set of ℓ,T coordinates. The gradual changeover from 'barophobic' to 'barophilic' behaviour of the mesophase with increasing ℓ

and T is attributed to the steeply increasing configurational entropy associated with the introduction of 'kinks', while maintaining a comparatively low volume [6].

Orientation

While still with PE, we pass on to situations conforming to Fig. 2, i.e. to the uncovering of the mesophase through raising of G_L. For a flexible chain like PE the latter is realized by stretching out of the chains and keeping them stretched [23] or otherwise constrained [24] while in the melt (or solution), thus preventing the full conformational entropy to be recovered. Since in ultraoriented (and thus ultra strong and stiff) PE fibres the molecules are virtually fully stretched out they lend themselves well to the creation of such a situation. Such fibres when held at fixed length, are heatable beyond their usual orthorhombic crystal melting point, when within an appreciable temperature interval and, for a limited time, the hexagonal form is apparent. Here the DSC scans display two melting peaks corresponding to o→h and h→L tranformation as verifiable by X-ray diffraction. In such a situation (realized by holding fibres clamped at their ends [23], or constrained through embedding in a resin [24] the mesophase is necessarily transient as the chain orientation will relax in time; such a situation therefore will not correspond to a final equilibrium.

An equilibrium situation, however, can be approached by light cross linking of the fibres, where the cross-links are too few in number to significantly influence the thermodynamic stability of the solid phase (say 10 Mrad dose as compared to several hundred Mrad quoted in Fig. 7), but nevertheless are sufficient in number to create a loosely connected infinite network. Such a network can be stretched out into a highly oriented system, either in the melt as an elastomer, or in the partially crystalline state through usual fibre drawing. There are several reports, past [25,26] and more recent relating to high modulus fibres [27,28,29], of such lightly cross-linked oriented systems converting to, or forming in the hexagonal phase above the crystallization or melting temperature of the usual orthorhombic crystal form.

Here, when held at constant length the stress, and with it the hexagonal form, can be maintained over a considerable length of time, if not indefinitely, and can also be reconstituted after repeated cooling and heating into the orthorhombic and liquid regimes. While full reversibility, hence the equilibrium nature of the L↔h and h↔o transitions has not been purposefully followed up in existing reports, this possibility, hence the attainability of an equilibrium situation according to Fig. 2 is clearly suggested inviting renewed explicit investigations to this effect.

Finally, we quote a most recent finding which seems to fall into the above scheme and is of potential practical consequence [30,31]. Very high molecular weight (MW) PE-melts behave in a highly elastic manner: they do not stretch (or flow) or extrude smoothly, but fracture and spurt respectively instead. Latest work here, however, identified a narrowly and sharply defined temperature window (under existing experimental conditions between 150-152°C) where such material extrudes smoothly with surprisingly low flow resistance ('viscosity'). Going below 150°C the viscosity rises sharply until on further lowering of temperature the system blocks, while above 152°C it extrudes in spurts at increased mean extrusion pressure. Fig. 9 shows a pressure v. temperature curve at a constant exit velocity (piston speed in rheometer) for a polymer of $\bar{M}_w$ = 410000, displaying the sharp minimum between 150-152°C. This is to be compared with the 'normal' extrusion behaviour displayed by a polymer with M_w = 280000 (Fig. 10) i.e. no minimum in pressure, only a steady decrease with temperature, under otherwise identical conditions.

To our mind the existence of the above temperature window must be associated with the presence of a distinct new phase which has all the hallmarks of a liquid crystal mesophase, hence for polyethylene the hexagonal phase. Accordingly, the lower temperature end of the window would correspond to a o↔h transformation, while the upper end (sharply defined within 0.2°C) to h↔L transformation. The ensuing spurt corresponds to the usual behaviour of such high molecular weight melts at conventional processing temperatures,

where such materials are in practical terms unprocessable. In the above situation the reason for mesophase formation would lie in the transient alignment of the chains while passing through the conical portion (with decreasing cross section) of the extrusion barrel on its way to the die exit. Here the flow field will be elongational, which is known to be the requirement for stretching out chains (e.g. ref.32). It is known from work on solutions, and from preceding theoretic predictions (see e.g. ref. 32) that such elongational flow induced chain stretching is critical both in strain rate $\dot{\varepsilon}$, with a critical value $\dot{\varepsilon}_c$ the coil→stretch transition, and in molecular weight (MW), $\dot{\varepsilon}_c$ being a sharply decreasing function of MW. The critical dependence of the effect on MW for a given $\dot{\varepsilon}$ (defined by the polymer exit- hence piston velocity in the rheometer) is apparent from the comparison of Fig. 10 with Fig.9. There is a similar effect, i.e. the appearance of a pressure minimum in the pressure-temperature curves recorded at constant piston velocity, when surpassing certain piston speeds (hence $\dot{\varepsilon}$) demonstrating the existence of a critical $\dot{\varepsilon}$ for a given grade of polyethylene [31]. Clearly, the situation exemplified by Fig. 9 falls within the scheme in Fig. 2 with the added factor that the chain orientation, and consequent mesophase formation, is transient. It is confined to the duration of the appropriate passage time, and even then it pertains only to the appropriate portion of the flow field. The flow-enhancing effect of the mesophase with respect to the melt is attributed to self-straightening and disentangling of polymer chains promoted by the L→h phase transition. Thus the number of chain entanglements, which is so high in a ultra-high molecular weight polymer as to prohibit flow of the melt, is appropriately reduced in the mesophase. On the other hand, the translatory chain diffusion remains high compared to that in the ordered orthorhombic crystals accounting for the low flow resistance.

Admittedly, the existence of the postulated transient mesophase would still require structural confirmation. Even so, the taking of a sharp drop in viscosity as indicator of mesophase formation has well estabilised precedents in the liquid crystal field. Such is e.g. the well documented effect in Kevlar referred to above [12] which in many respects

has similarities to the presently discussed PE, except that Kevlar is 'mesogenic' and can exist as stable liquid crystal under ambient conditions, while the mesophase in the flexible PE is 'virtual'. The latter 'virtual' phase only becomes 'real' transiently, which suffices to dramatically affect the entire flow behaviour of the material, the effect through which it is being detected.

CONCLUSION

It has been shown how the diverse manifestations of the mesomorphic state in polymers can be encompassed by a simple unifying scheme based on the relative thermodynamic stability including metastability, of the crystalline, liquid crystalline and liquid phases. The scheme embraces not only traditional LCP-s with mesogenic groups but also flexible polymers such as may not be considered liquid crystal forming a priori, but which nevertheless can be obtained as such by 'uncovering' virtual mesophase regimes within their phase diagrams. As shown, the latter can arise in suitable chemical variants within a given family of compounds, can be purposefully accomplished by subsequently induced chemical modifications and also by appropriate choice of physical parameters and constraints, sometimes with quite unsuspected results, (e.g. the transient mesophase and consequent narrow processing temperature window in high MW Polyethylene). Since few other polymers have been studied as comprehensively as Polyethylene - the polymer of most of our examples - it may well be that many more polymers, not considered to be mesogenic at present will be found to exhibit mesomorphic behaviour under appropriate conditions. The present note, amongst others, should hopefully provide signposts for the purposeful creation of mesophases and to their "uncovering" - in cases where they may be "hidden" - on the basis of simple thermodynamic considerations.

ACKNOWLEDGEMENT

We are much indebted to Professor V. Percec, Cleveland, for close working contacts (including supply of materials) which provided some of the examples quoted and, in general, contributed to the evolvement of the views expressed in this paper.

Sponsorship by US Army European Office, London, enabling the establishment of the scheme here presented, is gratefully acknowledged.

REFERENCES

1. Percec V. and Yourd R., Macromolecules 1989, 22, 524.

2. Godovsky Y.K. and Papkov V.S. Makromol. Chem., Macromol. Symp.,1986 4, 71.

3. Schneider N.S., Desper C.R. and Beres J.J. in Liquid Crystalline Order in Polymers, Ed. Blumstein A. Academic Press, New York, 1978, p. 299.

4. Wunderlich, B., Grebovicz,J., Advances in Polymer Science, 1984, 60-61, 1.

5. Bassett D.C., in 'Developments in Crystalline Polymers - 1' Ed. Bassett D.C., Appl. Sci. Publ.1982 p.115.

6. Ungar G., Macromolecules, 1986, 19, 1317-1324.

7. Feijoo J.L.,Ungar G.,Owen A.J., Keller A., and Percec V., Mol. Cryst.-Liq. Cryst.,1988, 155, 487-494.

8. Feijoo J.L., Ungar G., Keller A., and Percec V., Polymer, submitted.

9. Odell J.A., Keller A., Atkins E.D.T., and Miles M.J., J. Materials Sci., 1981, 16, 3306.

10. Percec V., Schaffer T.D., and Nava H., J. Polymer Sci., Polym. Lett. Ed.,1984, 22, 637.

11. Ober, C.K., Jin, J.-I and Lenz, R.W. Adv. Polymer Sci.,1984, 59, 103.

12. Cifferi A.,and Valenti B.,in 'Ultra-High Modulus Polymers' Edts. Cifferi A., and Ward I.M. Appl. Sci. Pub.1979, p.203.

13. Atkins E.D.T., Fulton W.S. and Miles M.J., TAPPI Conference Papers: 5. International Dissolving Pulps Symposium Vienna,1980, p. 208.

14. Blackwell J., Biswas H., Cheng M., Cageao R., Mol. Crystl. Liq. Cryst. 1988, 155, 299.

15. Percec V., Yourd R., Macromolecules in the press.

16. Percec V., Yourd R., Ungar G., Feijoo J.L. and Keller A. to be published.

17. Young W.R., Aviram A., and Cox R.J., J. Am. Chem. Soc.,1972, 94, 3976.

18. Percec V., Keller A., and Ungar G., to be submitted.

19. Ungar G.,and Keller A., Polymer, 1980, 21, 1273.

20. Vaughan A.S., Ungar G., Bassett D.C., and Keller A., Polymer, 1985, 26, 726.

21. Keller A., in 'Developments in Crystalline Polymers - 1' Edt. Bassett D.C., Appl. Sci. Publ. 1982, p.37.

22. Keller A., and Ungar G., Radiat. Phys. Chem., 1983, 22, 155.

23. Pennings A.J.,and Zwijnenburg A., J. Polym. Sci., Polym. Phys. Ed.,1979, 17, 1011.

24. Lemstra P.J., van Aerle N.A.J.M., Polymer,1988, J. 20, 131.

25. Clough S.B., Polym. Lett.,1970, 8, 519.

26. Clough S.B., J. Macromol. Sci., B4, 1970, 199.

27. Hikmet R.M., Lemstra P.J., Keller A., Colloid & Polymer Sci. 1987, 265, 185.

28. Hikmet R.M., Keller A., and Lemstra P.J., to be published.

29. Hikmet R.M., Ph.D. Thesis, Bristol 1987.

30. Waddon A., and Keller A., J. Polymer Sci. Letters Ed. submitted.

31. Waddon A. and Keller A. to be published.

32. Keller A. and Odell J.A., Colloid & Polymer Sci.,- 1985, 263, 181.

Figure Captions

Fig. 1 Schematic plot of free enthalpies vs. temperature for a system that does not show a mesophase. G_C G_M and G_L are, respectively, the free enthalpies of the crystalline, mesomorphic (virtual) and isotropic liquid states. $T_{C-L} = T_m$ is the crystalline melting point. Here, as in subsequent Figs.2-5, the heaviest lines correspond to the stablest state at a given temperature.

Fig. 2 Schematic plot of free enthalpies vs. temperature for the system in Fig. 1 but with G_L raised (to G_L')so as to "uncover" the mesophase. T_{C-M} and T_{M-L} are the crystal-mesophase transition and the isotropization transition temperatures.

Fig. 3 Schematic plot of free enthalpies vs. temperature for the system in Fig. 1 but with G_C raised (to G_C' so as to "uncover" the mesophase.

Fig. 4 Schematic free enthalpy diagram illustrating the origin of a monotropic liquid crystal (see text). Here, as in Fig.5, the arrows represent cooling and heating pathways.

Fig. 5 Schematic free enthalpy diagram for an enantiotropic liquid crystal, where the mesophase is metastable (see text).

Fig. 6 Crystal-isotropic (C-I), crystal-nematic (C-N) and nematic-isotropic (N-I) transition temperatures as a function of mole fraction of $-(CH_2)_{10}-$ spacer pertaining to the series of MBPE-8,10 copolyethers, containing methylbiphenyl ethane mesogen and randomly distributed $-(CH_2)_8-$ and $-(CH_2)_{10}-$ spacers (adapted from ref. 15).

Fig. 7 Transition temperatures T_{C-M}, T_{M-L} and T_{C-L} at three pressures of irradiated polyethylene as a function of radiation dose. Here the mesophase is the hexagonal phase (from [20]).

Fig. 8 Pressure-temperature diagrams of n-alkanes and polyethylene. Shaded areas indicate regions of stability of the mesophase ("hexagonal" or "rotator"). The figures indicate the number of carbon atoms in the chain (from [6]).

Fig. 9 Extrusion pressure plotted against extrusion temperature for extrusion of a polyethylene of $\bar{M}_w$ = 4×10^5 during heating at approximately 0.3 to $0.4\ ^{\circ}C\ min^{-1}$. Approximate piston velocity 5×10^{-2} cm min^{-1}. 1mm diameter die. The vertical, double headed arrow(s) represent pressure oscillations in the region of spurt [30]. (Waddon and Keller[30].

Fig. 10. Extrusion pressure plotted against extrusion temperature for extrusion of a polyethylene of $\bar{M}_w$ = 2.2×10^5 during heating at approximately 0.2 to $0.6\ ^{\circ}C\ min^{-1}$. Approximate piston velocity 3.3×10^{-2} cm min^{-1}. 1mm diameter die. (Waddon and Keller [30]).

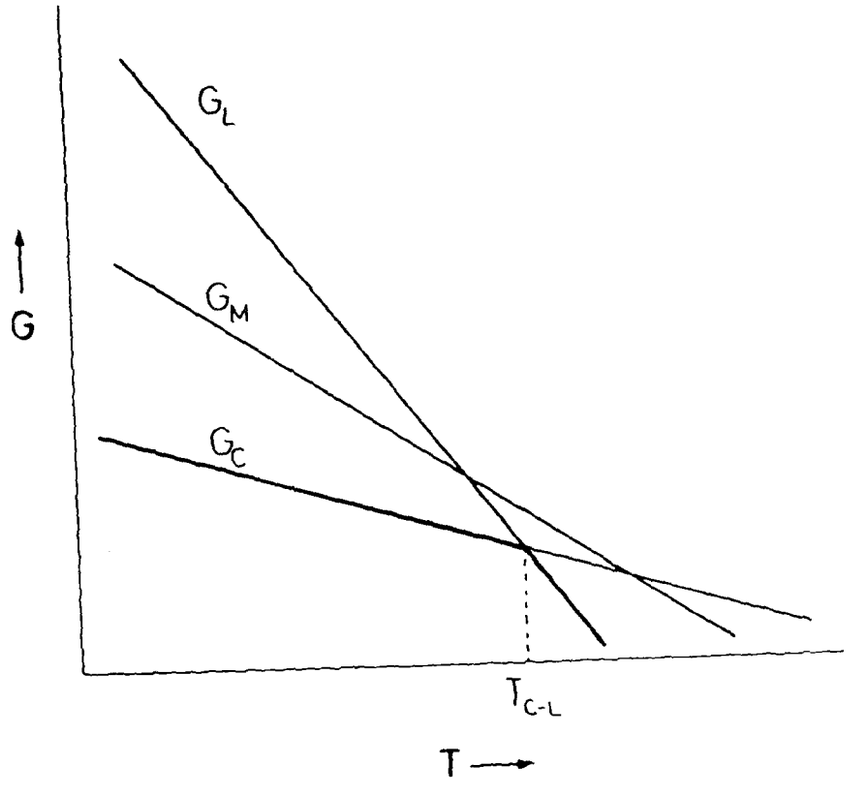

Fig 1

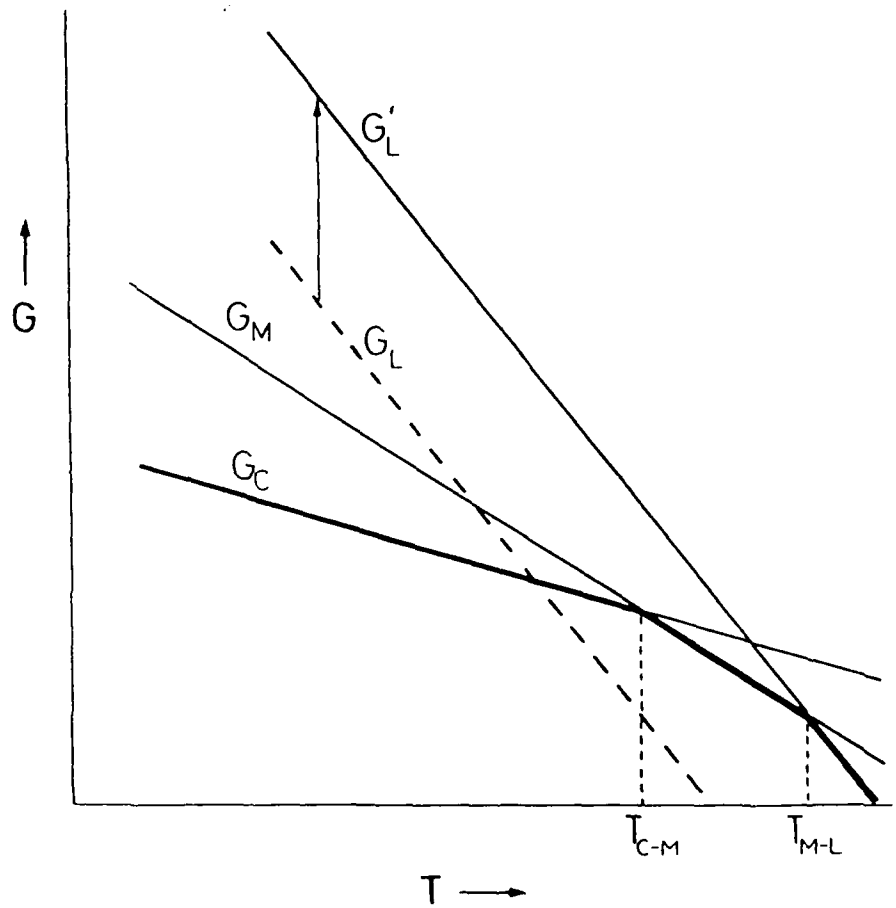

Fig. 2

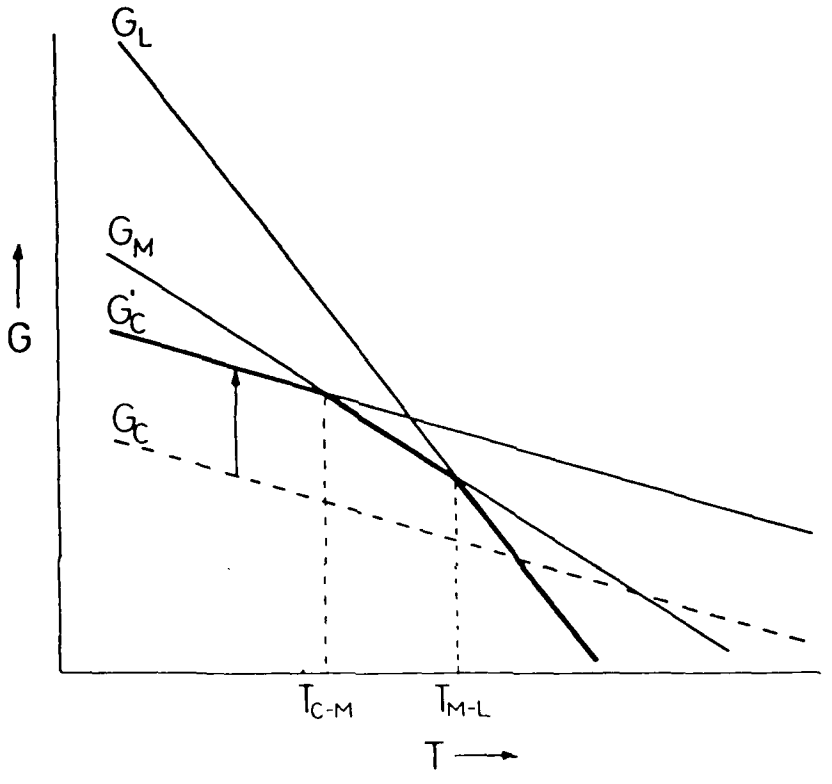

Fig 3

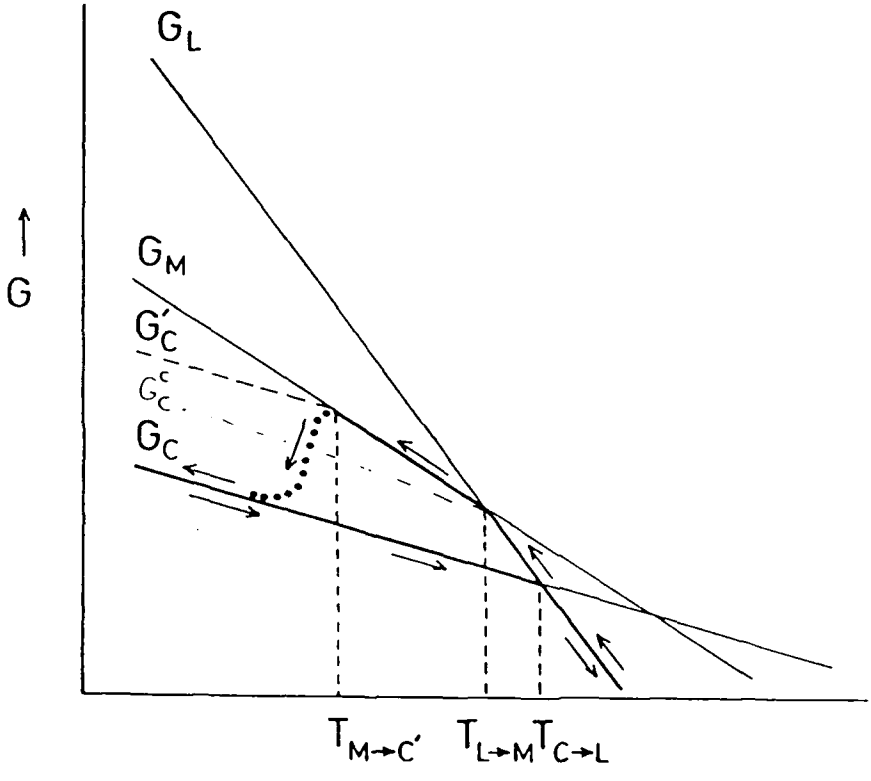

Fig. 4

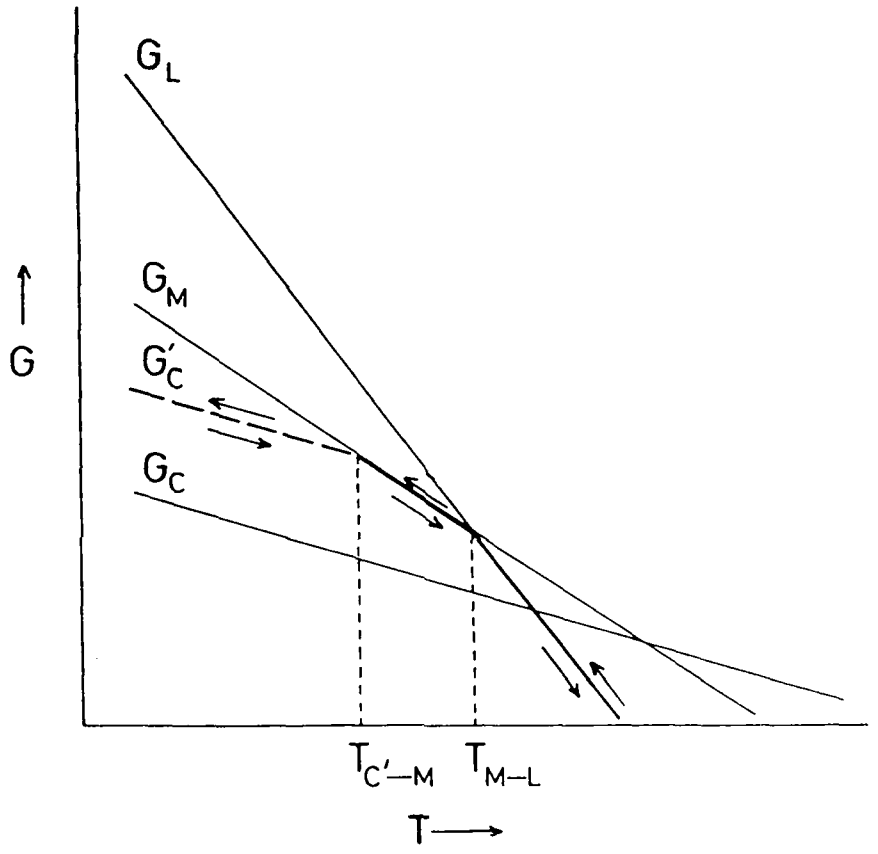

Fig 5

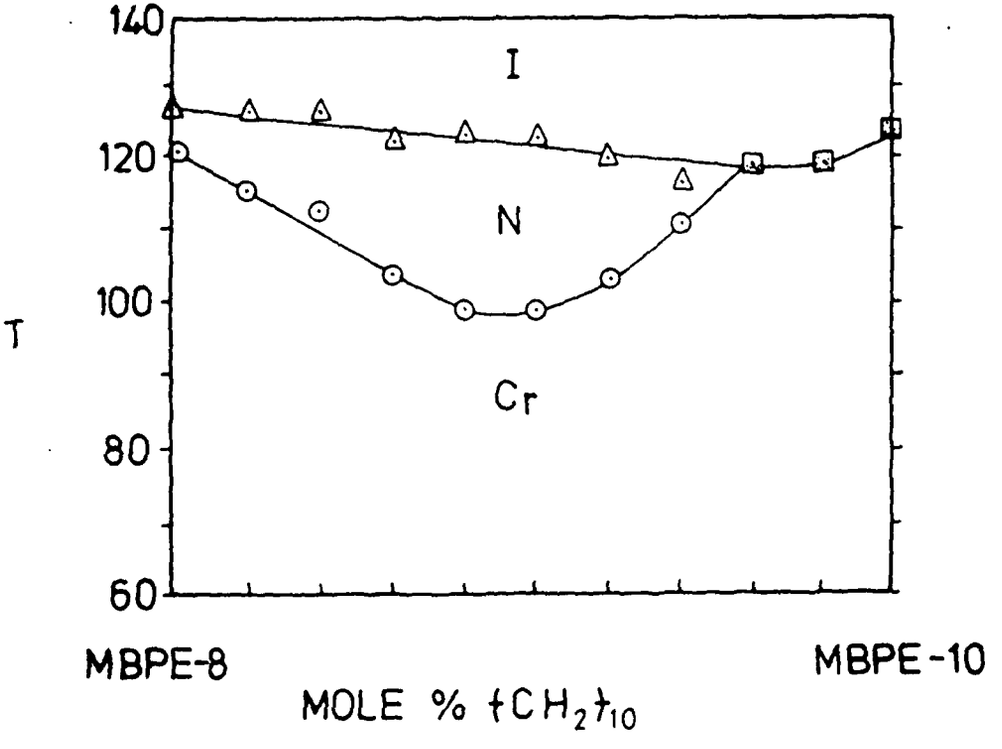

Fig. 1

A.I.

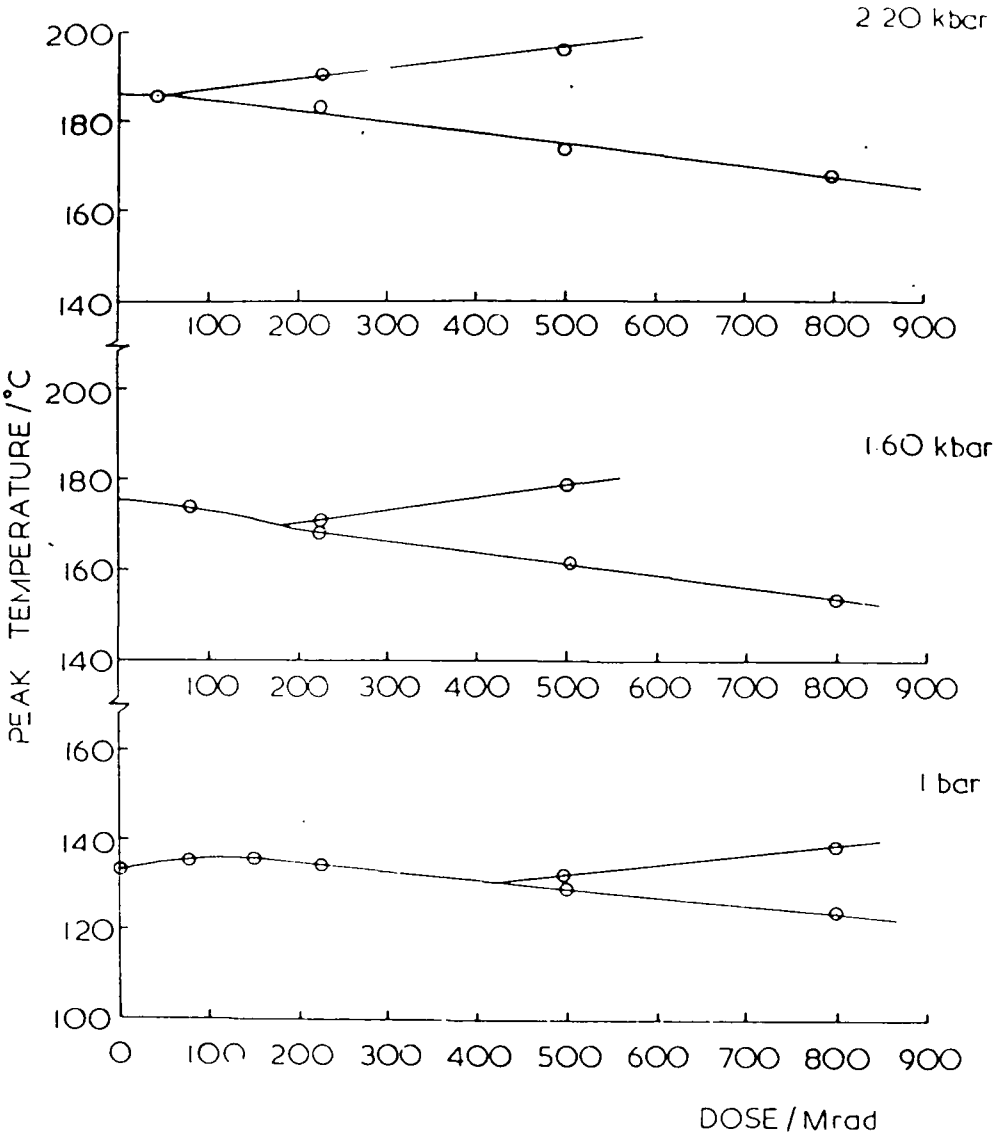
2·20 kbar
1·60 kbar
1 bar
PEAK TEMPERATURE / °C
DOSE / Mrad
200
180
160
140
120
100
0
100
200
300
400
500
600
700
800
900

Fig. 7

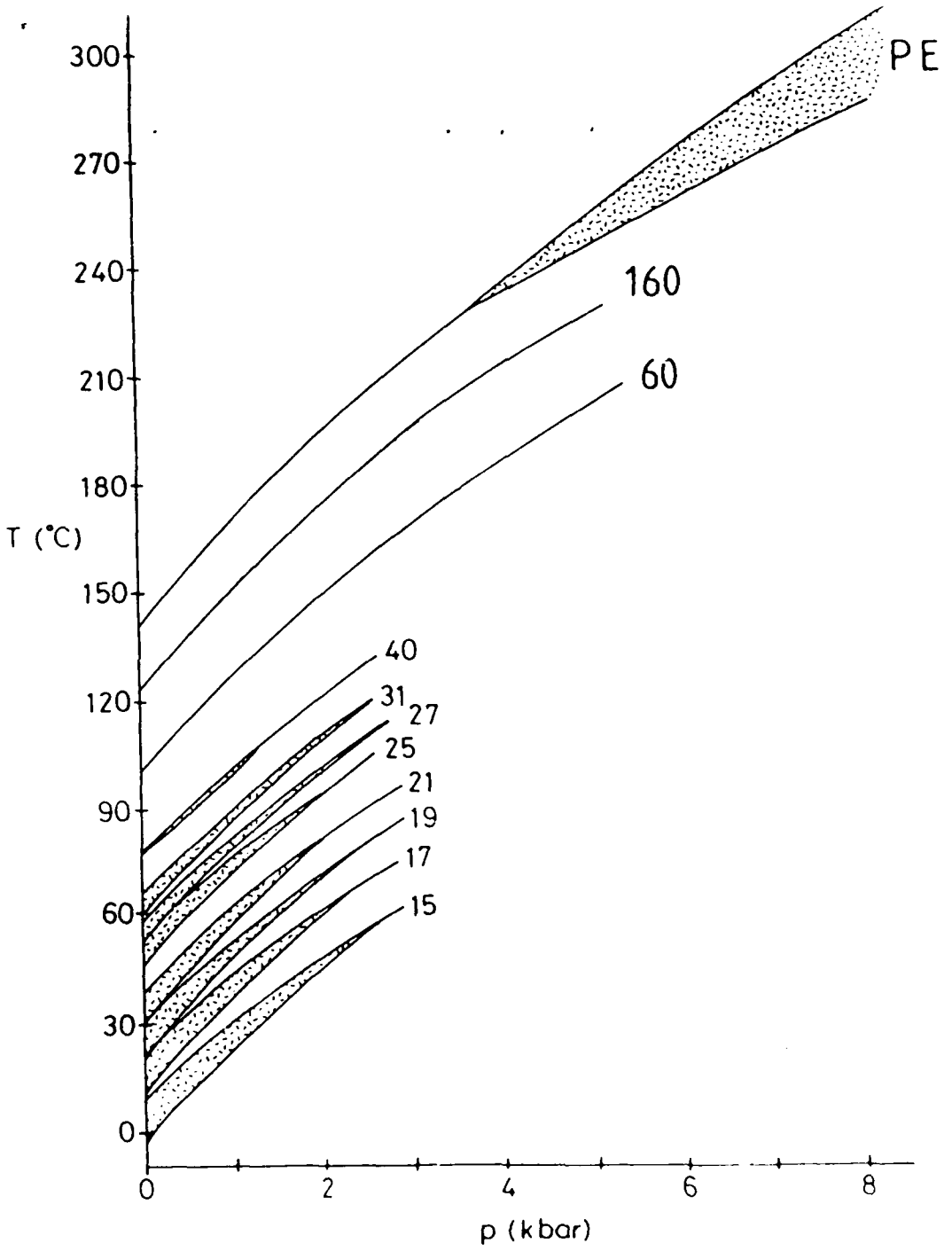
PE
160
60
40
31
27
25
21
19
17
15
T (°C)
300
270
240
210
180
150
120
90
60
30
0
0
2
4
6
8
p (kbar)

Fig 8

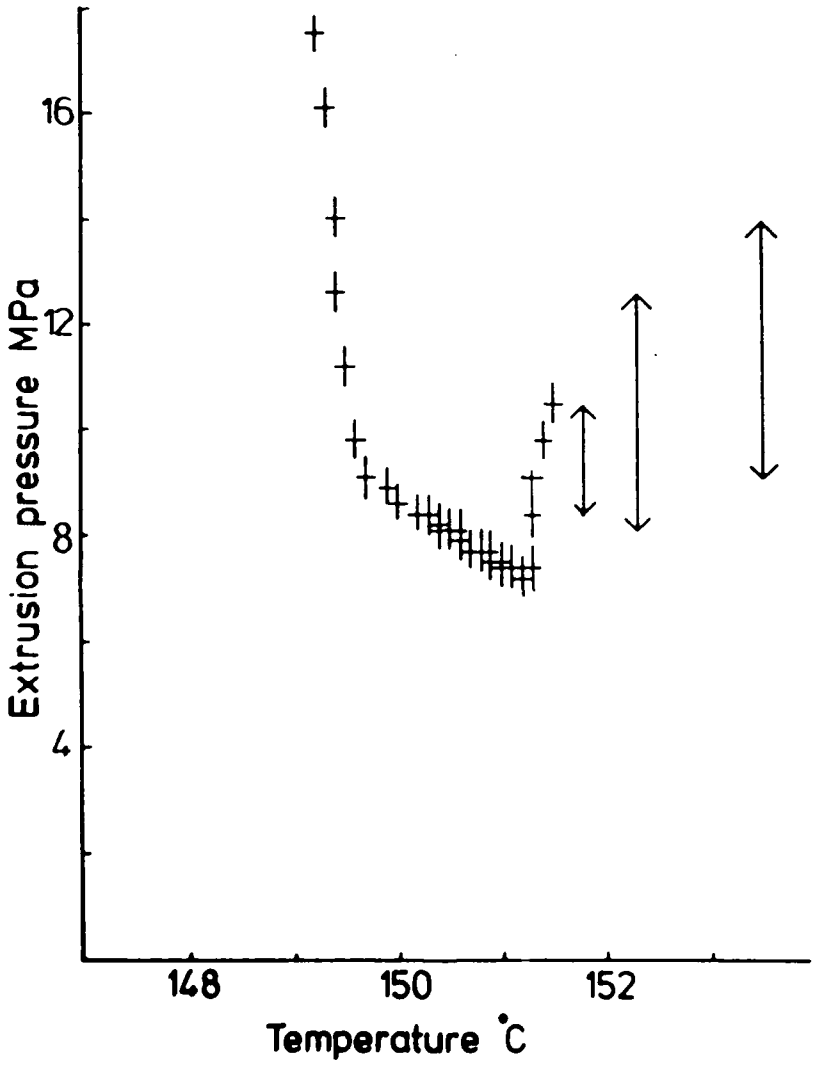

Fig. 9

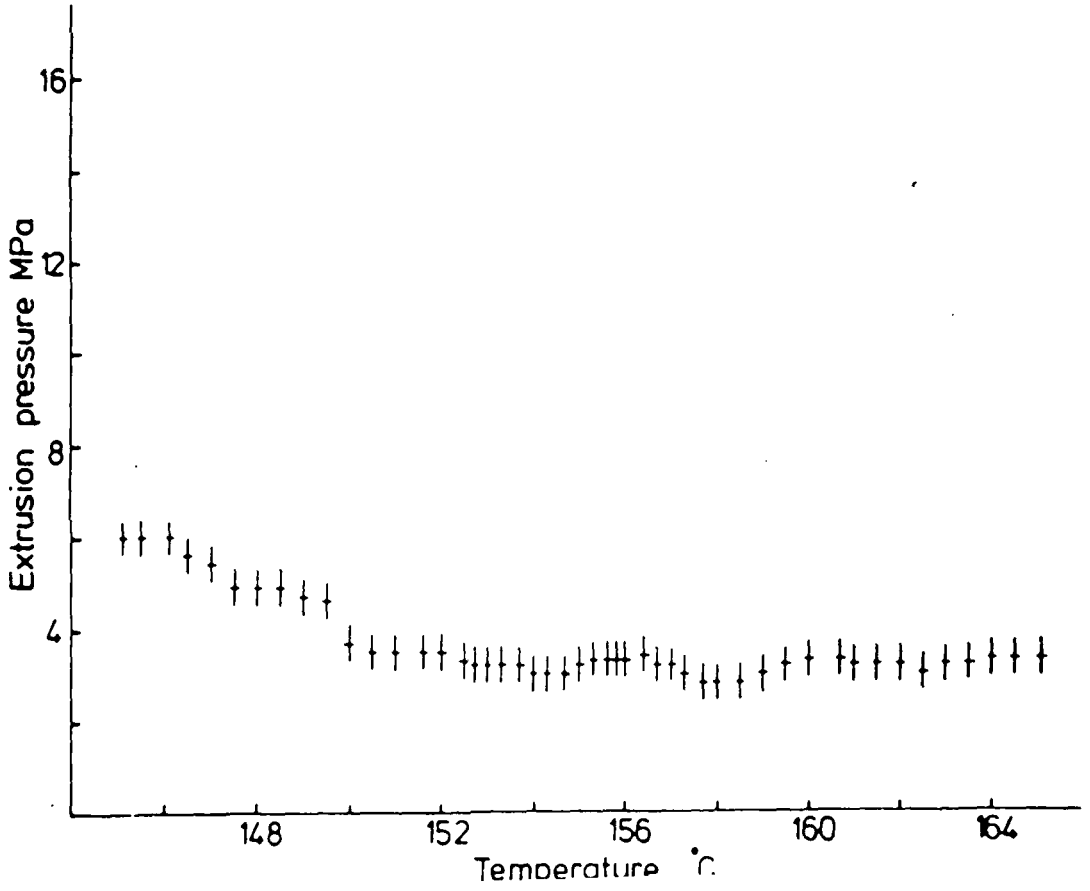
Extrusion pressure MPa
16
12
8
4
148
152
156
160
164
Temperature °C

Fig 10

A. II

APPENDIX II

Mol. Cryst. Liq. Cryst., 1988, Vol. 155, pp. 487-494
Photocopying permitted by license only

Printed in the United States of America

EFFECTS OF THERMAL TREATMENT ON THE TEMPERATURE AND HEAT OF ISOTROPIZATION IN A NEMATIC POLYETHER.

J.L. FEIJOO, G. UNGAR, A.J. OWEN, A.KELLER
H.H. Wills Physics Laboratory, University of Bristol, Tyndall Avenue, Bristol BS8 1TL. U.K.
V. PERCEC
Case Western Reserve University, Cleveland, Ohio, U.S.A.

Abstract A new family of liquid crystal forming compounds, polyethers constituted of a mesogen (α-methylstilbene) and flexible aliphatic spacers provides a ready realization of isotropic-liquid crystal-true crystal regimes in one and the same material in a convenient temperature range without degradation problems. Within the thermotropic range the isotropization temperature was found to be variable, affected by preceding thermal treatment: heat treatment shifts the transition to higher temperatures with correspondingly higher heat of isotropization. The effect was found to correlate with coarsening of visible texture.

INTRODUCTION

The findings here presented form part of a wider programme on main chain mesogenic polymers first introduced by Roviello and Sirigu [1] and since more recently by Percec and collaborators [2].

In these materials mesogenic and flexible spacer units are joined through ether linkages, which, from the point of view of the present works, has the advantage over the more extensively studied and used polyesters of greater chain flexibility and higher thermal stability. The combined effect of these two properties enables the isotropic state to be readily attained at convenient

A. II

temperatures without the risk of thermal degradation. In addition, the materials are soluble to varying extents through which they can be obtained in the lyotropic state with the concommitant possibility of mapping the full lyotropic - thermotropic phase diagram [3].

In the work here reported we are confining ourselves to the thermotropic range and shall use the opportunity offered by these materials to explore the nematic - isotropic transition in some depth. In the course of it we find that the isotropization temperature (T_i) cannot be uniquely identified by just any temperature scan because, as in the case of crystal melting in crystalline polymers, it is affected by the thermal history of the sample. The latter has visible manifestations in the microstructure observed in the form of coarsening of the disinclination networks. These findings open up future possibilities of quantitative correlations with disinclination content and of determining the disinclination free enthalpy.

EXPERIMENTAL

Materials and Methods

The materials used in this study were main chain random copolyethers of 4,4'-Dihydroxy-α-methylstilbene (HMS) and 1:1 molar mixtures of 1,5-dibromopentane and 1,7-dibromoheptane. These were synthesised by phase transfer catalyzed polyetherification [2]. The random copolymers studied were with 1:1 mole ratios of 5 and 7 $-CH_2-$ units, and they have the general formula:

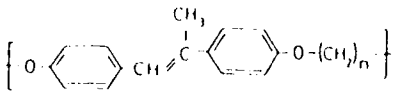

PHMS-5/7 (50:50)

A Perkin-Elmer DSC-2 calorimeter was used to measure the thermal properties of random copolymer samples as a function of temperature. Various heat treatments (annealings) were also carried out in the calorimeter when the need for these arose. The heating rates used were 10^{o}K/min. The D.S.C. instrument was calibrated according to recommended procedures.

Solvent-cast films were prepared on microscope cover glasses and used as test specimens for optical microscopy. Isothermal heat treatment of the films was performed by placing the specimens in the .D.S.C. sample holders. Selected samples were examined under the polarising microscope.

RESULTS AND DISCUSSION

Figure 1 displays three transition temperatures, glass transition (T_g), crystal melting (T_m^{max}) and isotropization (T_i) as a function of molecular weight ($\bar{M}_n$). Here T_m^{max} represents the maximum melting temperature of the most stable crystal form obtainable by heat annealing at small supercoolings. As anticipated all three transitions first increase and then level off with $\bar{M}_n$. T_i, the principal subject of our investigation, initially increases sharply with $\bar{M}_n$ until $\bar{M}_n \sim 12000$. From thereon, while broadly levelling off, the data points are multivalued. It did turn out that this variability is affected by heat treatment both below and above the crystal melting point T_m prior to isotropization. In view of the fact that the as-measured T_i is generally thought to be an equilibrium quantity this behaviour is unexpected and was examined further.

A II 4

Fig. 2 shows DSC thermograms corresponding to the isotropization transition as a function of heat treatment time for $\bar{M}_n$ = 17700, in this case below T_m^{max}. As seen,

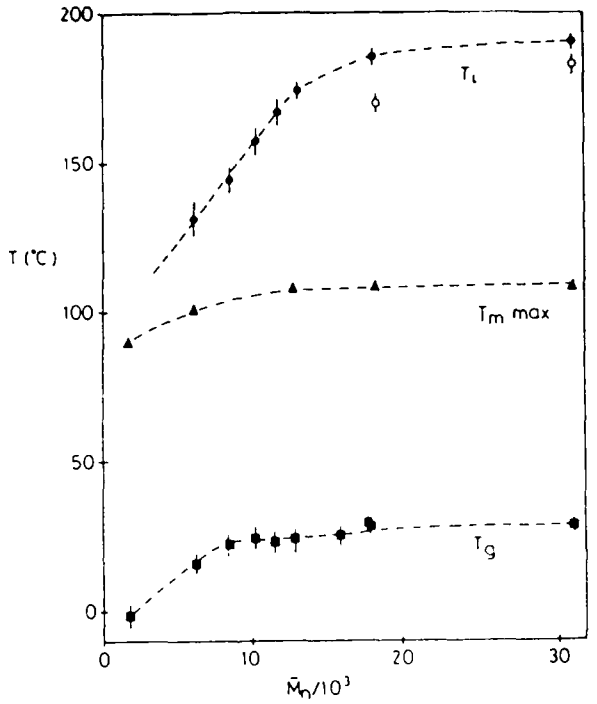

FIGURE 1. Transition temperatures of PHHS - 5/7 (50:50) copolymer as a function of molecular weight as determined by DSC: T_g = glass transition temperature; T_m^{max} = maximum melting point of the most stable crystal form, achieved by annealing at low supercooling; T_i = nematic-isotropic transition temperature (ϕ= some as-prepared samples which were transformed into the corresponding samples ● on heat treatment).

both the transition temperature T_i and the heat of isotropization (ΔH_i), as assessed from the endotherm peak area, are increasing with annealing time. It follows therefore that T_i and ΔH_i, simply as measured, may not

correspond to equilibrium values beyond a certain molecular weight, M_n^c, and it is necessary to anneal the sample for the equilibrium to be approached.

Beyond M_n^c, the molecular weight dependence would then reflect the lowered mobility of the chains, and in particular, that of the mesogenic units.

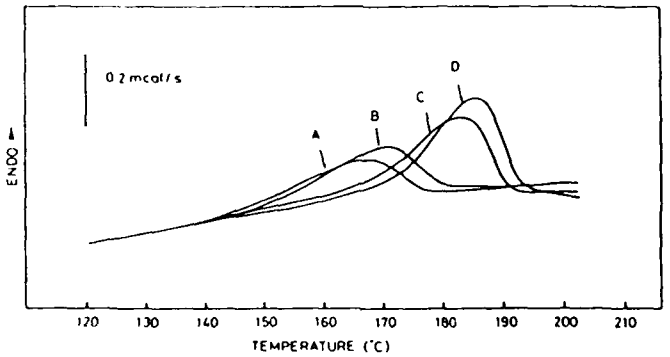

FIGURE 2 DSC thermograms of PHMS-5/7 (50:50), $\bar{M}_n$ = 17700, samples annealed at 100°C: A(2.0h),B(6.4h), C(13.5h) and D(16.6h).

Fig. 3 displays the polarising optical images for the same samples as in Fig. 2. The dark lines, are most likely to be disinclinations circumscribing, what appears as "domains". The size of the "domains" increases with annealing time, the texture coarsening and the number of disinclinations reducing accordingly. The latter in itself would entail a reduction of net enthalpy and free enthalpy of the nematic phase thus, at least in a qualitative sense, correlating with the trend in the thermograms of Fig. 2.

The above findings allow a sample which is in an imperfect nonequilibrium state to be characterized using the measured heat and temperature of isotropization, ΔH_i and T_i, in relation to the corresponding equilibrium

values ΔH_i^∞ and T_i^∞.

We assume an exponential approach of ΔH_i to ΔH_i^∞ and find the latter parameter by linearizing ℓ_n ($\Delta H_i^\infty - \Delta H_i$ (t)) versus annealing time t (fig. 4). This then provides ΔH_i^∞ = 12.5 J/g for the heat of isotropization in the equilibrium state. With this value we can then characterise a sample by considering $\Delta H_i(t)/\Delta H_i^\infty$ a quantity which, risking some objections to the term, may,

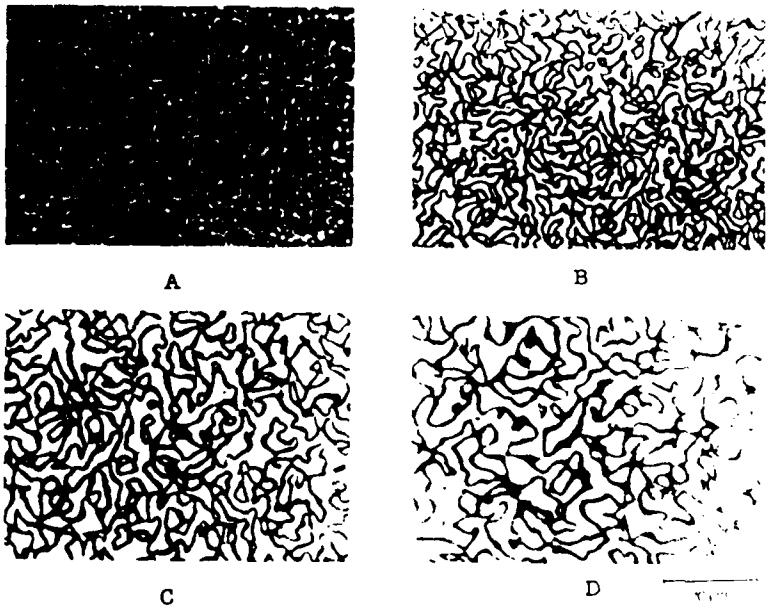

FIGURE 3. Sequence of optical micrographs for PHMS 5/7 (50:50), $\bar{M}_n$ = 17700, taken at different time intervals during annealing at 100°C. A(Unannealed), B(6.4h), C(13.5h) and D(16.6h).

in analogy with crystalline polymers, be termed degree of liquid crystallinity.

Values of $(\Delta H_i(t)/\Delta H_i^{\infty}).100$ together with the actual ΔH_i values as a function of annealing time are plotted in Fig. 5. As seen the $(\Delta H_i(t)/\Delta H_i^{\infty})100$ values range from 39% to 72% representing the perfection of liquid crystallinity as a percentage of its equilibrium value.

The reason that in the experimental series presented here the heat treatment was conducted below T_m^{max} is that some oxidation of the polymer was detected during prolonged annealings in air above T_m^{max}. Currently, vacuum

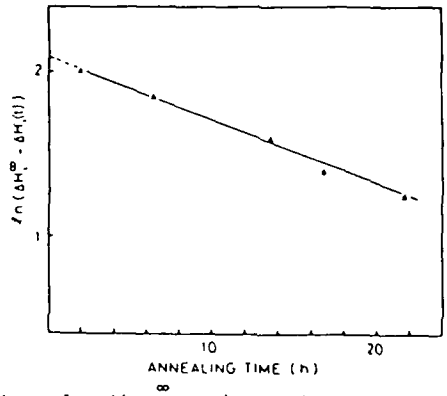

FIGURE 4. $\ell_n (\Delta H_i^{\infty} - \Delta H_i(t))$ vs annealing time as derived from the thermograms of PHMS - 5/7 (50:50) ($\bar{M}_n$ = 17700), with ΔH_i^{∞} = 12.5 J/g.

annealings are being performed above T_m^{max}, i.e. while in the nematic state. In the latter case shorter annealing times are required to obtain the same ΔH_i value than for heating below T_m.

The preliminary results here presented contain, in our view, an essential recognition: namely that in high molecular weight material there can exist non-equilibrium states of liquid crystallinity, where departures from the equilibrium states can be quantified calorimetrically and also correlated (even if so far only qualitatively) with

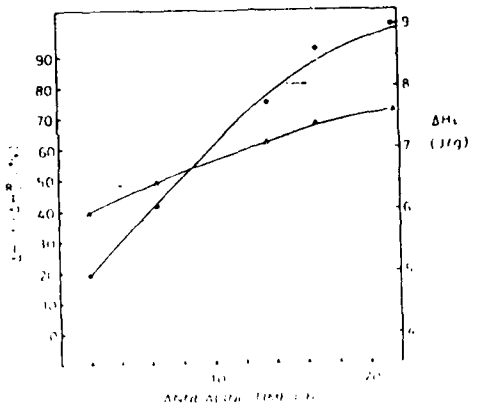

FIGURE 5 ΔH_i and $\Delta H_i(t)/\Delta H_i^{\infty}$ vs annealing time as derived from the thermograms of PHMS-5/7 (50:50) samples (M_n = 17700).

the scale of the disinclination texture as observed visually under the polarising microscope. Above all, this recognition is essential for the correct identification of isotropization temperatures (T_i). The observed effect also presents an opportunity for experimental determination of the free enthalpy of disinclinations. The work on this issue is currently in progress.

REFERENCES

1. A. Roviello and A. Sirigu, J. Polym. Sci. Polym. Lett. Ed., 13, 455 (1975).
2. T. Shaffer and V. Percec, Makromol. Chem. Rapid Commun. 6, 97 (1985).
3. A. Keller, G. Ungar and J.L. Feijoo work in progress.

ACKNOWLEDGMENTS

The authors gratefully acknowledge the support by the U.S. Army European Office (London) making this work possible.

APPENDIX III

Polymer (in the press)

NON-EQUILIBRIUM EXCESS ORDER IN THE ISOTROPIC STATE OF MAIN CHAIN LIQUID CRYSTAL FORMING POLYMERS

J.L. Feijoo, G. Ungar, A. Keller
H.H. Wills Physics Laboratory, Tyndall Avenue,
Bristol BS8 1TL.

and V. Percec
Department of Macromolecular Science, Case Western Reserve University, Cleveland, Ohio 44106-2699

ABSTRACT

A new non-equilibrium phenomenon has been recognized in main chain liquid crystal polymers. Persistence of non-equilibrium residual short range nematic-like order can be detected in the isotropic phase up to several minutes after the nematic to isotropic transition had occurred. The effect was observed by differential scanning calorimetry and is closely related to the pronounced non-equilibrium effects in the nematic state. As we reported previously, annealing in the nematic phase, on the time scale of hours, is required to bring the temperature and enthalpy of isotropisation up to its equilibrium value. Now we find that even in the isotropic state annealing is required in order to achieve thermodynamic equilibrium; only upon holding above T_i is the residual excess nematic-type order fully removed, and thus all memory of previous annealings in the nematic state erased. The non-equilibrium effects are particularly pronounced for higher molecular weight polymers. In the case of the α-methylstilbene polyether with alkylene spacers, $\bar{M}_n$=31,100 the time constant of the exponential approach to equilibrium is found to be 2.1 minutes at $T = T_i+10^{\circ}C$.

INTRODUCTION

In the case of phase transformations in polymeric systems, such as melting or crystal-crystal transitions, studying the variations in transition temperature and enthalpy has often been useful in learning about nonequilibrium states. Thus the values of lamellar crystal thickness, energy of chain folds and of other crystal defects could be derived from the variation in melting point. In contrast, little experimental information is available at present about the nematic to isotropic (N-I) transition, particularly in thermotropic main chain polymers. One reason (i) is the common belief that both the nematic and isotropic phases are fluid states very close to thermodynamic equilibrium; accordingly there would be no significant deviation of T_i from the equilibrium value. The second reason (ii) is the high temperatures of the N-I transition (T_i) in the commonly studied rigid rod polymers, with T_i often exceeding the decomposition temperature. Even when flexible spacers are introduced into the chain T_i often remains comparatively high if mesogens and spacers are connected by ester linkages. Finally (iii) thermal reactivity of the ester group, usually present in the latter polymers, leads to uncontrolled changes in molecular weight in the T_i region, even if no actual decomposition occurs.

Problems (ii) and (iii) can be largely overcome by resorting to polymers with ether rather than ester linkages in the main chain [1]: polyethers have a higher thermal stability and, generally, lower transition temperatures, than polyesters. We have thus performed calorimetric and optical studies of the nematic phase and the N-I transition in polyethers containing rigid α-methylstilbene mesogens linked via flexible alkyl spacers (PHMS). As reported previously [2], the heat and temperature of isotropisation, ΔH_i and T_i, were found to be remarkably affected by the preceding thermal treatment: annealing in the nematic state shifts the transition to higher temperatures and produces a significant increase in ΔH_i. These effects correlate with a coarsening of the visible texture. The above thermal evidence of highly non-equilibrium nematic states in polymers is in sharp

contrast to the common notion of the nematic phase as an equilibrium fluid at all times, a perception carried through from the field of low molar mass liquid crystals. Some new data on the effect of annealing in the nematic phase of PHMS polymers will be presented in the latter part of this article. It will be shown, e.g. that nematic ordering upon annealing can lead to a doubling of the isotropisation enthalpy.

However, the main thrust of the present paper is on demonstrating the following new phenomenon which has now been recognised: the memory of such ordering, achieved by annealings in the nematic state, is not erased instantly on reaching the isotropic state; it takes several, possibly ten, minutes of annealing well above T_i to revert the system back to the equilibrium disordered state. Thus, while heat treatment is required for the equilibrium nematic order to develop, annealing in the isotropic state is similarly required for the residual non-equilibrium order to be erased and for the short range molecular correlation to be reduced to its equilibrium isotropic value.

EXPERIMENTAL AND RESULTS

The material used in this study is a random copolyether containing α-methylstilbene mesogen units separated by flexible $-O(CH_2)_9O-$ or $-O(CH_2)_{11}O-$ units in a 1:1 ratio (abbreviated: PHMS-9,11). Molecular weights were: $\bar{M}_n$ = 31,000, M_w = 65,500. The crystal - nematic transition, T_m, of this polymer is at 103°C, and the nematic - isotropic, T_i^∞, at 172°C. All heat treatments were performed under high vacuum to prevent degradation. In order to study the kinetics of disordering in the isotropic phase, a well ordered nematic reference state had to be used as the starting point. It was found that such a state is best achieved by melting a solution-crystallized mat. The overall procedure was as follows: approx. 10mg of the mat was weighted and placed in an aluminium DSC pan, without the cover. The pan was inserted in a flat bottom thin wall copper test tube fitted with a ground glass top for convenient connection to the vacuum line. While under

high vacuum, the test tube was first heated briefly in the nematic state for degassing, and then immersed in a thermostated oil bath set at 10 degrees C above the isotropisation temperature, i.e. at 190°C, for a defined holding time t_h)*.
The design of the tube ensured good thermal contact between the sample and surrounding bath. After the heat treatment the tube was rapidly cooled to room temperature.

*Footnote:
For clarity heat treatment times are hereafter termed "holding time" (t_h) and "annealing time" (t_a), depending on whether the temperature was within the isotropic or nematic range, respectively.
Footnote ends.

In the first set of experiments (a), where the effect of t_h on the N-I transition was studied, no further heat treatment was applied before the thermal analysis run. The sample pans were taken out of vacuum, covered and scanned at 10°C/min heating rate in a Perkin Elmer DSC-7 calorimeter. The resulting N-I transition endotherms are shown in Fig. 1 for different holding times in the isotropic state, t_h. As seen, both the position (T_i) and the area of the peak (ΔH_i) greatly decrease with increasing holding time. The decrease in isotropisation temperature, T_i, and enthalpy, ΔH_i, with t_h is plotted in Figures 2 and 3 respectively. The extent of excess order in the as-created nontreated isotropic phase is remarkable: e.g. after $t_h \approx 2$ minutes of thermal treatment ΔH_i is reduced to 57% of the initial value.

In the second set of experiments (b) we followed the recovery of T_i and ΔH_i upon annealing in the nematic state subsequent to the thermal treatment in the isotropic phase. Thus the tube with the sample pan, while still under vacuum, was immersed in the oil bath which was now set to 120°C, i.e. a temperature within the nematic range. The annealing time, t_a, was varied from 0 to 15 hours. As before, a fresh specimen was used for each cycle of thermal treatments. After annealing in the nematic state, DSC thermograms were recorded as in (a). The recovery of T_i and ΔH_i with t_a for samples previously held in the isotropic state for

t_h=2 minutes, is shown in Figures 4 and 5. Compared with the disordering process in the isotropic phase, the rate of achieving equilibrium (re-ordering) in the nematic state is very slow. It should be noted that, up to t_h = 5 minutes holding time in the isotropic phase, the initial highest T_i amd ΔH_i i.e. the values corresponding to t_h = 0, were fully recoverable by prolonged annealing in the nematic phase. For longer t_h's irreversible reduction in ΔH_i occurred, which was attributed to degradation. Thus only experiments with t_h <5 minutes are considered in this work.

The respective dependencies of ΔH_i and T_i on treatment time, shown in Figures 3-5, were fitted to exponential functions of the form:

$$\Delta H_i(t) = \Delta H_i^{\infty} + (\Delta H_i^{O} - \Delta H_i^{\infty}) \exp(-t/\tau) \qquad (1a)$$

$$T_i(t) = T_i^{\infty} + (T_i^{O} - T_i^{\infty}) \exp(-t/\tau) \qquad (1b)$$

Here the superscripts o and ∞ refer to ΔH_i and T_i values for t=0 and t=∞, respectively. The resulting best fit parameters are listed in Table 1. The time constants τ for the disordering process in the isotropic state at 190°C was 2 minutes, while that for the re-ordering process in the nematic state at 120°C was 4 hours, the ratio of the two being 10^{-2}.

DISCUSSION

It is only thanks to the slow ordering process in the nematic phase [2] that the differences in the preceding isotropic state are reflected in the N-I endotherm on subsequent heating (see Fig. 1). If thermodynamic equilibrium in the nematic phase was quick to establish, as has been generally assumed until recently, the memory of any differences in the precursor isotropic state would have been erased in the nematic phase in the course of the DSC heating scan. Thus, due to its sluggishness, the nematic phase is preserved in its as-formed state, hence the N-I endotherm recorded on subsequent heating indirectly mirrors the state of local order in the precursor isotropic liquid.

The effect of thermal treatment in the isotropic state on the subsequent N-I transition, shown in Figs. 1-3, is a new, previously unrecognised phenomenon. It shows two particularly interesting features: (a) the nematic phase can be influenced by the state of the isotropic precursor to an unexpectely high extent (e.g. ΔH_i varies by a factor of more than 2, see Fig. 3), and (b) the rate with which nematic memory is erased in the isotropic state is unexpectedly low. The implications for measurements of thermodynamic parameters (temperature, heat, entropy) of the N-I transition in main chain polymers are self-evident. It is clear from the current results that great care must be exerted in properly annealing the nematic polymer before a DSC scan, and slow heating, preferably with extrapolation to zero heating rate, is recommended.

The form in which memory of the preceding nematic order is stored in the isotropic state is a matter for speculation. Similarly, we can only guess as to the mechanism by which such memory is passed back on to the reformed nematic phase during the subsequent I-N transition. However, that much is certain that, in contrast to low molecular liquid crystals, the equilibrium nematic order and isotropic disorder in main-chain polymers are attained very slowly. Even on the short-range scale, detectable calorimetrically, the approach to equilibrium is surprisingly slow indeed.

Concerning the isotropization transition, while any long range orientational order is clearly lost, it would appear that a significant degree of local order is preserved after the transition and it decays to its equilibrium level only upon subsequent thermal treatment. It is possible then that localized regions of such residual short range order serve as nuclei for nematic domain formation on subsequent cooling. As such "seeds" would largely preserve their original mutually parallel orientation, the resultant adjacent nematic domains may have their directors aligned parallel or almost parallel to each other, and may possibly coalesce. On the other hand, if the residual seeds in the isotropic phase are allowed to disappear, the director axes in the adjacent nematic domains formed on subsequent N-I transition would be randomly oriented and uncorrelated. Thus a higher density of defects (disclinations) may be expected in the latter case, resulting in lower T_i and ΔH_i.

An additional factor to consider is chain contormation. While longer extended chain portions normally exist in an equilibrium nematic, and a more coiled conformation prevails in the isotropic state [3,4], the required conformational change may be too slow for the equilibrium path to be followed during the N-I or I-N transitions. Both the orientational and conformational non-equilibria may qualitatively account for the observed memory effects and the variations in T_i and ΔH_i, and we cannot comment presently on which of the two effects might be dominant.

CONCLUSION

Immediately following the N-I transition, the isotropic phase of a thermotropic main-chain polymer is in a non-equilibrium state of considerable excess short range order. The equilibrium disorder is achieved only on subsequent heat treatment which, in the present case, is on the time scale of several minutes. Upon the subsequent I-N transition a largely non-equilibrium nematic is formed, with excess frozen-in disorder. The latter anneals out at a rate 100 times lower than the rate of equilibration of the isotropic phase, i.e., in a matter of hours. In contrast to

these unsuspected findings precautions are called for in performing measurements and interpreting thermal data on the N-I transition in main chain polymers.

ACKNOWLEDGEMENT

Sponsorship by US Army European Office, London, is gratefully acknowledged. One of the authors (J.L.F.) wishes to acknowledge financial support from Britannica Society (1 year scholarship), the British Council (Venezuela) and Simón Bolívar University.

REFERENCES

1. V. Percec, Mol. Cryst. Liq. Cryst.1988,155, 1

2. J.L. Feijoo, G. Ungar, A.J. Owen, A. Keller and V. Percec, Mol. Cryst. Liq. Cryst. 1988, 155, 487.

3. W. Renz and M. Warner, Phys. Rev. Lett. 1986, 56,1286.

4. J.F. D'Allest, P. Sixou, A. Blumstein, R.B. Blumstein, J. Teixeira and L. Noirez, Mol. Cryst. Liq. Cryst. 1988, 155, 581.

TABLE 1: BEST FIT PARAMETERS FOR THE DEPENDENCE OF HEAT AND TEMPERATURE OF ISOTROPISATION ON THERMAL TREATMENT TIME (Eqs. 1a, b)

Thermal treatment at:		T = 190°C (isotropic)	T = 120°C (nematic)
T_i	T_i^{∞}	-	172.0°C
	τ	-	4.0 hours
ΔH_i	ΔH_i^{∞}	4.95 Jg^{-1} (4.9 kJ mol^{-1})	13.9 Jg^{-1} (5.1 kJ mol^{-1})
	τ	2.13 minutes	4.1 hours

FIGURE CAPTIONS

Fig. 1 DSC heating thermograms spanning the T_i range for a sample of PHMS-9,11 (Mn=31,100, M_w=65,500 comonomer ratio 1:1). Prior to the scan the specimens, initially in a well ordered nematic state, were held in the isotropic phase (190°C) for t_h = 0 minutes (curve A), 1 (B), 2 (C), 3 (D) and 5 minutes (E).

Fig. 2 Peak N-I transition temperature (T_i) vs. holding time t_h in the isotropic state (190°C) for PHMS - 9,11.

Fig. 3 ΔH_i and $\Delta H_i/\Delta H_i^\infty$ vs. holding time t_h in the isotropic state (190°C) for PHMS-9,11.

Fig. 4 Peak N-I transition temperature (T_i) vs. annealing time t_a in the nematic state (120°. The samples had been held in the isotropic state for t_h = 2 minutes preceding the annealings at 120°C.

Fig. 5 ΔH_i and $\Delta H_i/\Delta H_i^\infty$ for PHMS-9,11 vs. annealing time t_a in the nematic state (120°C, cf. Fig. 4).

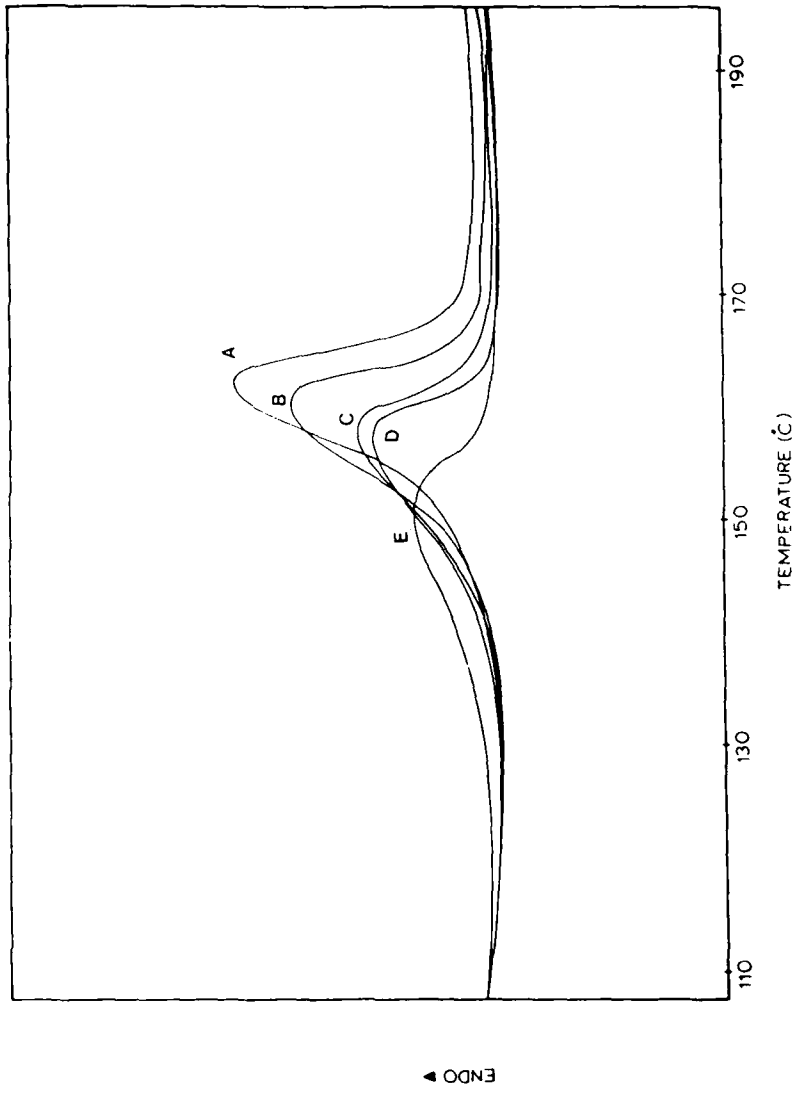

FIG 1

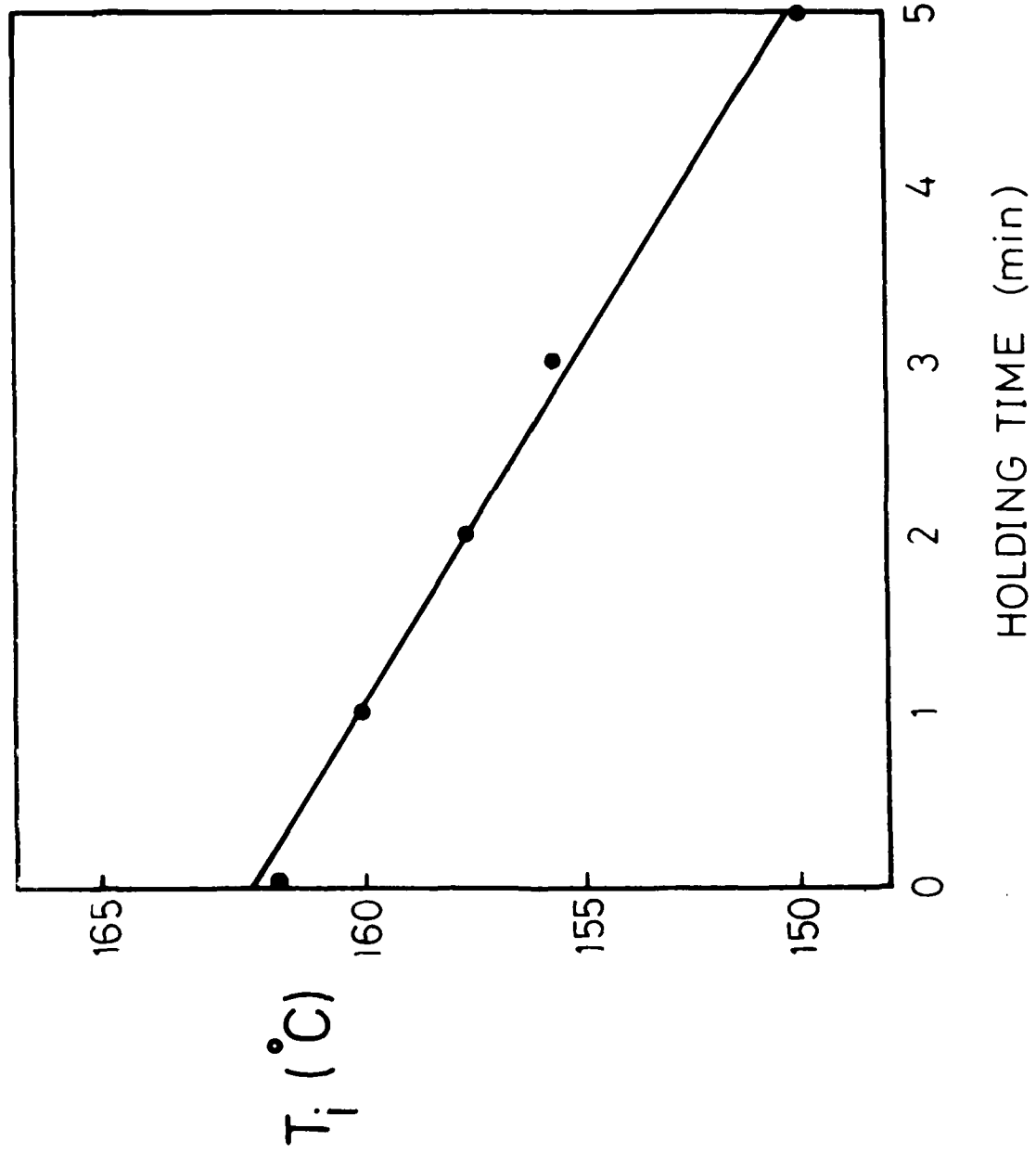

FIG 2

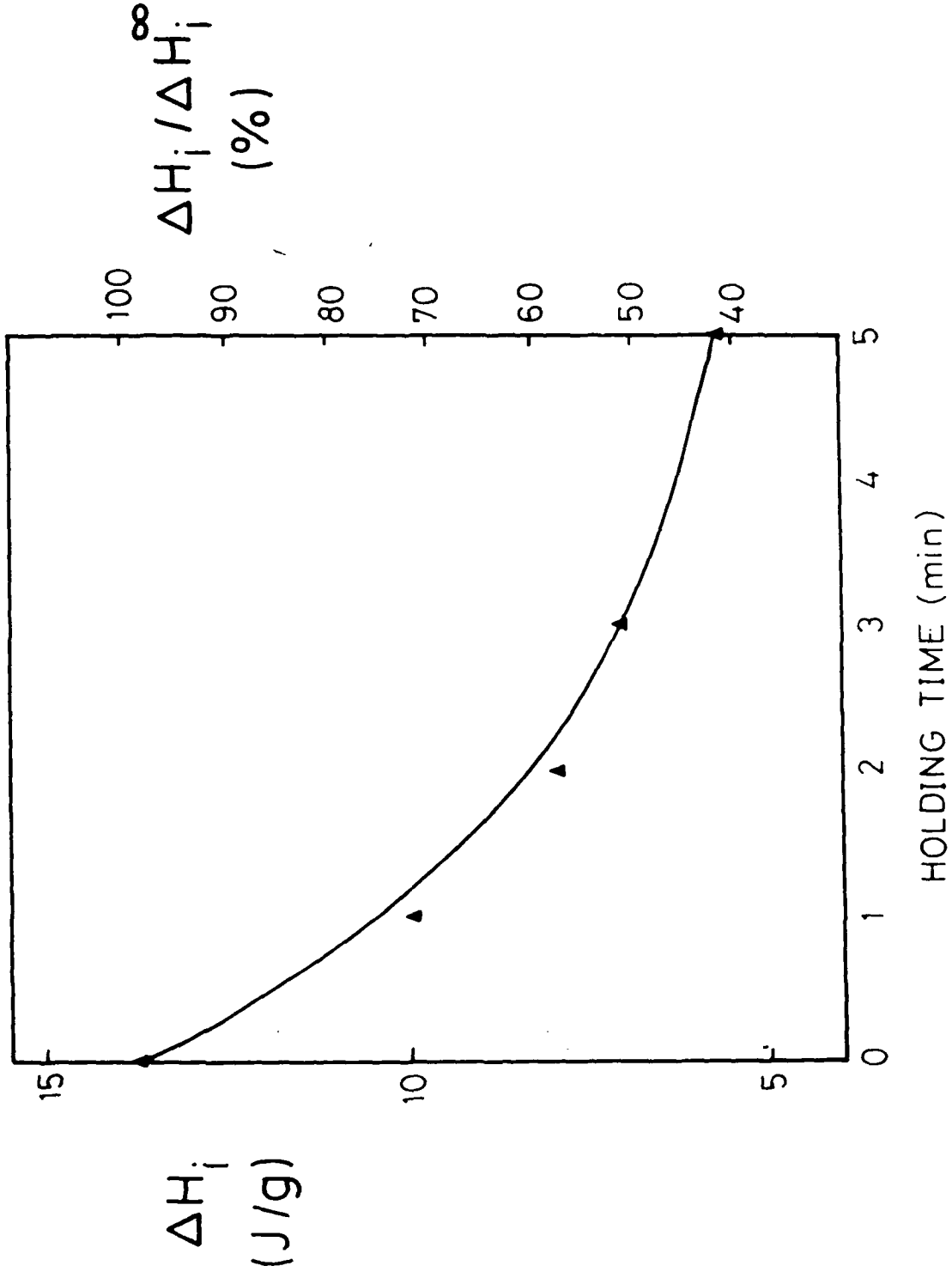
$\Delta H_i / \Delta H_i^0$ (%)
100
90
80
70
60
50
40
15
10
5
ΔH_i (J/g)
0
1
2
3
4
5
HOLDING TIME (min)

FIG 3

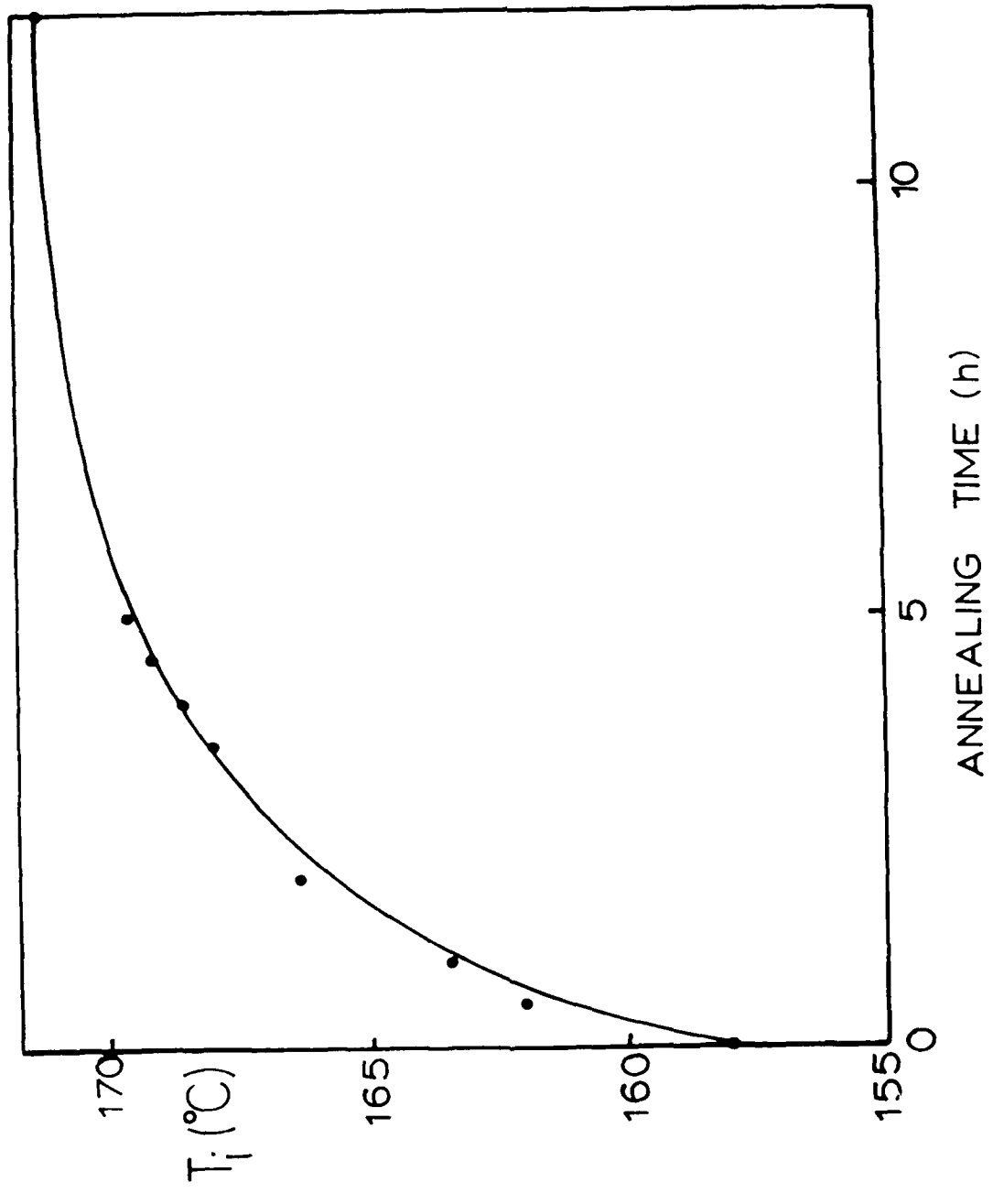

FIG 4

A.III

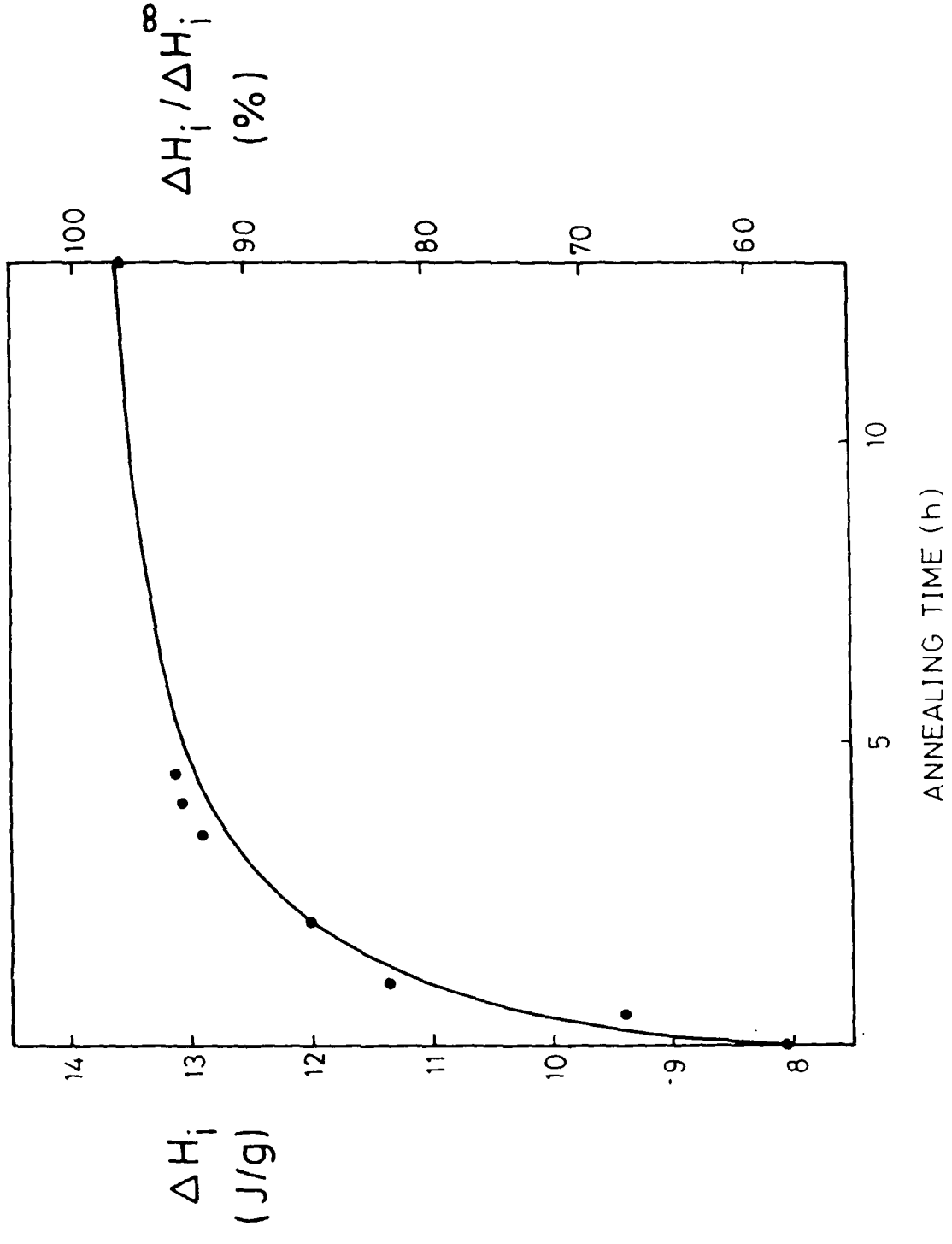
$\Delta H_i / \Delta H_i^8$ (%)
100
90
80
70
60
ΔH_i (J/g)
14
13
12
11
10
9
8
5
10
ANNEALING TIME (h)

FIG 5

APPENDIX IV

Macromolecules, in the press

SIMULTANEOUS X-RAY / DSC STUDY OF MESOMORPHISM IN POLYMERS WITH A SEMIFLEXIBLE MESOGEN

G. Ungar, J.L. Feijoo, A. Keller

H.H. Wills Physics Laboratory, Tyndall Avenue, Bristol BS8 1TL

R. Yourd and V. Percec

Department of Macromolecular Science, Case Western Reserve University, Cleveland, Ohio 44106-2699

ABSTRACT

In order to investigate the limits of macromolecular chain flexibility tolerated by the nematic state, a new group of polyethers has recently been synthesised, where not only the spacer, but also the mesogen provide a degree of flexiblity. This is achieved by introducing a rotationally mobile ethylene group linking the two phenyl rings in the 1-(4-hydroxyphenyl)-2-(2-methyl-4-hydroxyphenyl)ethane (MBPE). These "mesogens" are separated by flexible $-O(CH_2)_nO-$ spacers, where n is either a single value (homopolymers) or has two different values (copolymers). Original studies by DSC and optical microscopy suggested that the polymers exhibit liquid crystal phases, presumed nematic and possibly also smectic. Presently we show results of X-ray diffraction studies of MBPE polymers using the simultaneous X-ray diffraction and DSC technique (XDDSC). The results conclusively prove the existence of the nematic phase in most homopolymers and all copolymers. Depending on the polymer the phase is either mono- or enantiotropic. While in a few cases the phase is thermodynamically stable, in most cases it is metastable. The weak first order transition below the I-N transition temperature is shown not to be the nematic-smectic transition as previously suspected, but rather a nematic-nematic transition, yet to be investigated in detail. Current X-ray evidence shows further that the nematic phase in polymers with even spacers is considerably more ordered than that in polymers with odd spacers.

INTRODUCTION

The beneficial effect of liquid crystallinity in processing of polymers with superior mechanical properties is now well established. However, in order to facilitate processing of main chain nematogenic polymers, the introduction of flexible spacers into the chain has been experimented with extensively. In order to investigate still further the limits of flexibility tolerated by the nematic state a new group of polyethers has recently been synthesised [1-4], where not only the spacer, but also the mesogen provide a degree of flexibility. This is achieved by introducing a rotationally mobile ethylene group linking the two phenyl rings in the 1-(4-hydroxyphenyl)-2-(2-methyl-4-hydroxyphenyl)ethane (MBPE). Both homo- and copolymers were prepared, the latter containing spacers of two [1-3] or three [4] different lengths in a random sequence.

Original studies by DSC and optical microscopy suggested that the polymers exhibit liquid crystal phases, presumed nematic and possibly also smectic. Presently we show results of X-ray diffraction studies of MBPE polymers using the simultaneous X-ray diffraction and DSC technique (XDDSC) [5]. The results conclusively prove the existence of the nematic phase in most homopolymers and all copolymers. Depending on the polymer the phase is either mono- or enantiotropic. While in a few cases the phase is thermodynamically stable, in most cases it is metastable. In addition, it will be shown that the nematic phase in polymers with even spacers is considerably more ordered than that in polymers with odd spacers.

MATERIALS AND METHODS

MBPE homo- and copolyethers of the chemical formula:

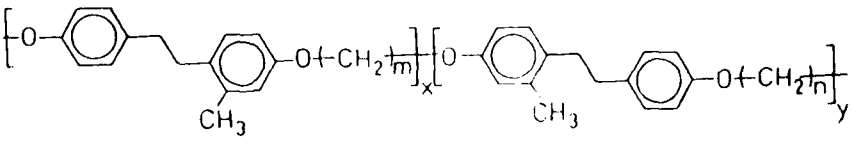

were synthesized as described in ref. [3]. Here m=n denote copolymers and m=n homopolymers.

Thermotropic behaviour was initially investigated by polarizing optical microscopy and by DSC (Perkin Elmer DSC-7). Fibre X-ray diffraction patterns showed rich polymorphism in the crystalline state, as will be described separately [6]. The main technique used in the present work is simultaneous X-ray diffraction and differential scanning calorimetry (XDDSC) [5]. In this method time resolved powder diffractograms are collected during linear heating or cooling of the specimen, while at the same time the differential heat flow in or out of the specimen is recorded. Thus diffractograms can unambiguously be related to the features (peaks) in the thermogram, and transient metastable phases, as well as those existing in a narrow temperature range, can be easily identified. The powerful X-ray beam was provided by the synchrotron source at Daresbury. The technique has originally been introduced by Russel and Koberstein [7], and the details of our improved version are given elsewhere [5].

RESULTS AND DISCUSSION

MBPE-9 homopolymer

DSC heating and cooling thermograms of a typical MBPE homopolymer, MBPE-9, are shown in Figures 1 a-c. There is only one endotherm on heating, attributed to crystal melting directly into the isotropic phase. On cooling, however, two exotherms appear if the cooling rate is low (Fig. 1b). The phase between the two exotherms has been presumed monotropic nematic [1,2]. On faster cooling the crystallization exotherm (the lower exotherm of Fig. 1b) is further supercooled to expose yet another small exotherm at 60 °C (Fig. 1c). This has been tentatively attributed to the nematic-smectic transition [1,2].

Typical polarizing optical texture produced upon the first

exothermic transition during cooling a MBPE polymer from the isotropic state is shown in Figure 2, MBPE-9 being the example. Based on such textures it has been proposed previously [1] that the first anisotropic phase produced on cooling is nematic, although clear Schlieren-type nematic textures could not be created by annealing since crystallization would intervene. For the same reason the conjecture that the lower temperature phase, below the small sharp exotherm, is monotropic smectic, could not be tested properly either. No apparent change in texture takes place upon this transition, and annealing again leads to crystallization. Conventional X-ray diffraction experiments were also limited by the transient nature of the presumed liquid crystal phases and, to some extent, by their narrow temperature interval. Thus we resorted to the XDDSC technique, which appeared ideally suited to resolving problems of this kind.

For reference, in Fig. 3 we first show the room temperature X-ray diffractogram of the MBPE-9 homopolymer, which had been annealed at 85°C. The material is clearly crystalline. For completeness, in Fig. 4 the diffraction pattern is shown of a melt drawn and annealed fibre of the same material. Crystal structures will be discussed elsewhere [6].

The results of a cooling XDDSC scan of MBPE-9 homopolymer are shown in Fig. 5. Cooling rate was 2 deg./min. The thermogram, which was recorded during the actual XDDSC run, is shown in Fig. 5a. It features two exotherms, in agreement with the DSC-7 trace in Fig. 1b. Diffractograms in this run were recorded as 30 second time frames, i.e. every degree C. These are displayed in Fig. 5b, after coadding two by two adjacent frames; hence each curve in Fig 5b covers a temperature interval of 2 °C. The two bold thermograms correspond to arrowed positions, i.e. to exothermic peaks, in the DSC trace (Fig. 5a).

The main point to note in Fig. 5b is that the phase between the two exothermic transitions is indeed amorphous. Not only are there no wide angle reflections present, there are no low

angle peaks either. Thus the phase is neither crystalline nor smectic and, since it is birefringent, it can be unambiguously identified as nematic. This confirms previous tentative conclusions about the liquid crystal forming ability of this material [1-4]. More generally, it clearly illustrates that rigid moieties are not necessarily required to render a polymer nematogenic. It is evident that semiflexible units, like diphenylethane, are also capable of lending liquid crystal properties to a macromolecule, even where such units are themselves linked by fully flexible spacers. This conclusion will be further substantiated by additional examples below.

The lower temperature exotherm in Fig. 5a clearly represents crystallization. However, note that the crystal form in Fig. 5b is not the same as that in Fig. 4. The present form is metastable and will transform into that of Fig. 4 upon heat annealing. It may be mentioned that the diffraction patterns in Figs. 3 and 4 in fact represent superposed patterns of two similar forms present in the annealed sample [6]. As in other segmented mesogenic polymers [8,9] there is an abundance of crystal polymorphs in most homo- and copolymers studied [6].

MBPE-5,7 copolymer

Thermograms of MBPE-5,7, a typical representative of MBPE copolymers with odd-numbered spacers, are shown in Fig. 6. In this polymer $-O-(CH_2)_5-O-$ and $-O-(CH_2)_7-O-$ spacers, in 1:1 molar ratio, are randomly distributed along the chains, and crystallization is suppressed relative to either of the parent homopolymers [1,2]. A well annealed specimen gives only one melting endotherm on heating (curve a). On cooling two exotherms are seen (curve b) and on immediate reheating the two transitions reappear in reverse order (curve c). Such behaviour is also typical of most other copolymers with odd numbered spacers, such as MBPE-5,9, MBPE-7,11 and MBPE-9,11. Within the practicable range of cooling rates the two exotherms remain unchanged, unlike the situation in MBPE-9 (Fig. 1b and c). The lower temperature peak in the

copolymers is smaller in area than the higher one and it is always sharp. The enthalpies of the upper and lower exotherm in MBPE-5,7 are, respectively, 0.7 and 0.17 J/(mole repeat unit), while in MBPE-9 they are 1.1 and 2.5 J/mole.

The diffractogram in Fig. 7 confirms that the annealed copolymer is crystalline at room temperature. The XDDSC heating run performed with such a sample indeed shows that the crystals melt at 78 °C (cf. Fig. 6a).

It is an interesting finding, revealed by the present experiments on MBPE-5,7, that on cooling from the isotropic melt all three phases that appear are amorphous, i.e. neither of them displays any wide or small angle diffraction peaks, apart from the broad amorphous halo. The low temperature amorphous phase in MBPE-5,7, as well as in other copolymers such as MBPE-7,9 and MBPE-5,9, can be frozen at room temperature (glass transition temperature is around 15 °C). On reheating, such a non-equilibrium sample undergoes the reverse sequence of phase transitions. A reheating XDDSC scan is shown in Fig. 8 for MBPE-5,7. Immediately prior to the scan the specimen was cooled at 5 deg.C/min. As seen in Fig. 8b, there is no noticeable change in the powder diffractogram on going through the two first order transitions, apart from some change in position and width of the amorphous halo, which will be discussed further below. Optical studies have shown [1,2] that both low temperature phases are birefringent, displaying fine grain texture. Unfortunately, attempts to develop coarser textures by annealing failed due to incipient crystallization. In view of the fact that both low temperature phases show only amorphous scattering and that they are optically anisotropic, one would conclude that both phases are nematic. A more detailed study of this unusual phase behaviour is currently under way. It should be noted that the "nematic-nematic" transition is consistently occurring in most copolymers with odd spacers, as well as in some homopolymers (e.g. the middle exotherm in the fast cool thermogram of MBPE-9 -Fig. 1c).

As is clear from this example, the nematic phase in MBPE

copolymers with odd spacers can be easily made enantiotropic, i.e. to appear both on cooling and reheating, even though it is metastable (cf. discussion of metastable polymeric mesophases in ref. [10]).

MBPE-8,10 copolymer

MBPE polymers with even number of carbon atoms in their flexible spacers have a somewhat different phase behaviour than the odd MBPEs [3]. Both the crystal melting points and isotropisation temperatures, where a suspected N-I transition occurs, are higher than in the odd members. Most homopolymers do not actually show mesophases, while in a number of copolymers a thermodynamically stable nematic phase is suspected [3]. Here we show the example of MBPE-8,10, where two strong first order transitions are observed on both heating and cooling (Fig. 9a,b). The intermediate phase is birefringent and no amount of annealing will dispense of it, i.e. it is an equilibrium phase. A XDDSC heating scan is shown in Fig. 10. It confirms the previous tentative assignment [3] of the phases as crystalline, nematic and isotropic, in the order of ascending temperatures. No N-N transitions were observed with even-spacer polymers.

Degree of nematic order in polymers with even and odd spacers

In all polymers studied in this work there is a significant shift in the position of the amorphous peak upon the I-N transition towards smaller spacings (larger angles). This is accompanied by some decrease in peak width. The reverse happens on the N-I transition, where such transition is observed (see Fig. 8). This behaviour indicates that, with respect to the isotropic phase, improved intermolecular contact and correlation is found in the nematic phase. This is a general feature of the nematic state.

In order to illustrate these effects in a more quantitative way, the mean amorphous peak position, expressed as Bragg

spacing in Angstroms, was calculated as

$$\langle r \rangle = 1/\langle s \rangle \qquad (1)$$

where the mean wavevector <s> is given by

$$\langle s \rangle = \frac{\int_{s_1}^{s_2} s\, i\, ds}{\int_{s_1}^{s_2} i\, ds} \qquad (2)$$

i is the uncorrected scattered intensity and s_1 and s_2 are arbitrary integration limits. <r> can be viewed as an arbitrary empirical parameter of the radial distribution function which, in turn, is determined by molecular correlations in the liquid. The temperature dependence of <r> is shown in Fig. 11 for MBPE-9 (cooling), MBPE-5,7 (heating) and MBPE-8,10 (heating).

The jump in <r> upon the N-I transition is clearly seen in Fig. 11 for all three polymers. An additional small jump of about 0.02 A (marked by arrow) is observed in MBPE-5,7 at the "N-N" transition temperature. As would be expected, the <r> values for the isotropic phase of all three polymers fall on the same line (dotted line in Fig. 11), which is ascending with temperature due to thermal expansion. The isotropic melt can be taken as the reference state; its structure ought not to be significantly affected by the length of the flexible spacers as these should have a fairly random conformation anyway [11]. The notable distinction between the polymers in Fig. 11 is in the difference in <r> value between the isotropic and the nematic phase. This difference is significantly lower in MBPE-8,10 than in the two polymers with odd spacers, MBPE-9 and MBPE-5,7. The jump in <r> upon the N-I transition is 0.18 A for MBPE-8,10, and only 0.10 A for MBPE-9 and 0.8 A for polymers MBPE-5,7 and MBPE-7,9 (not shown). We interpret this difference as indicating that the nematic order parameter is roughly twice as high in the polymer with even spacers (MBPE-8,10), compared with that in polymers with odd spacers.

The latter conclusion is also supported by the measured values of the entropy of the N-I transition. A selection of these is listed in Table 1 for a number of MBPE polymers with even and odd spacers. The transition entropy for polymers with even spacers is seen to be consistently higher than those for odd spacer polymers, by a factor of 2.5 on average. The higher order in the nematic phase is also reflected by T_i, which is by about 40 °C higher for even spacer polymers than that for their odd spacer counterparts. As has been proposed previously [11], there is a rationale for a higher nematic order in polymers with even spacers: in such polymers the lowest energy all-anti conformation of the alkylene spacer will keep the attached mesogenic moieties parallel to each other, a favourable situation overall. On the other hand, for odd number of carbon atoms within the spacer, the adjacent mesogens attached to the terminal atoms will be at a considerable angle to each other. This is unfavourable for chain packing, so that a compromise will need to be established between the opposing tendencies for parallel alignment of mesogens and for the minimum energy conformation of the spacer.

CONCLUSION

The main results of the presently introduced XDDSC study on the newly available polymers with semiflexible mesogens and flexible spacers are:

1. It is conclusively proven that macromolecules as flexible as MBPE polyethers can exhibit the nematic phase, which is either monotropic or enantiotropic. Thus rigidly linear mesogens are not essential ingredients of a nematic polymer; even when interchange between extended and bent conformations is allowed in both the spacer and the "mesogen", nematic state is still possible. The simultaneous DSC and X-ray technique employed proved to be extremely useful in studies of this kind, especially where transient metastable phases, or phases occurring in a narrow temperature range, are

investigated.

2. The suggested existence of a metastable smectic phase in MBPE polymers [1,2] is not upheld by present experiments: neither crystalline nor smectic reflections are found below the sharp first order transition occurring in odd spacer copolymers below the I-N transition. The possibility of it being a nematic-nematic transition is currently being investigated.

3. It is shown that the nematic phase in polymers with even spacers is considerably more ordered than that in polymers with odd spacers.

ACKNOWLEDGEMENT

Financial support of the U. S. Army European Office, London, is gratefully acknowledged. One of the authors (JLF) wishes to acknowledge financial support from the Britannica Society (one year scholarship), the British Council (Venezuela) and the Simón Bolívar University.

REFERENCES

1. Percec, V.; Yourd, R. Macromolecules, in press.

2. Percec, V.; Yourd, R. Macromolecules, in press.

3. Percec, V.; Yourd, R. Macromolecules, in press.

4. Percec, V.; Tsuda, Y. Macromolecules, in press.

5. Ungar, G.; Feijoo, J.L.; Keller, A. Mol. Cryst. Liq. Cryst., in press.

6. Ungar, G.; Yourd, R.; Percec, V.; Keller, A., in preparation.

7. Russell, T.P.; Koberstein, J.T. J. Polym. Sci., Polym. Phys. Ed. 1985, 23, 1109.

8. Petraccone, V.; Roviello, A.; Sirigu, A.; Tuzi, A.; Martuscelli, E.; Pracella, M. Eur. Polymer J. 1980, 16, 261.

9. Ungar, G.; Keller, A. Mol. Cryst. Liq. Cryst., 1988, 155, 313.

10. Keller, A.; Ungar, G. Macromolecules, in press.

11. Yoon, D.Y.; Bruckner, S.; Volksen, W.; Scott, J.C. Faraday Discuss. Chem. Soc. 1985, 79, paper 4.

FIGURE CAPTIONS

Fig. 1 - DSC thermograms of MBPE-9: (a) heating scan of the polymer previously annealed at 87°C; (b) cooling scan, rate -20 deg./min.; (c) cooling scan, rate -2 deg./min.

Fig. 2 - Optical micrograph of MBPE-9, taken through crossed polars at 70°C immediately on cooling from the isotropic melt.

Fig. 3 - Room temperature X-ray diffractogram of homopolymer MBPE-9, which had been annealed at 85°C.

Fig. 4 - X-ray diffraction pattern of an annealed fibre of MBPE-9. Fibre axis vertical.

Fig. 5 - Simultaneous X-ray / DSC (XDDSC) cooling scan (-2 deg./min) for MBPE-9: (a) thermogram, b) diffractograms (one every 2 degrees C). Bold diffractograms correspond to arrowed positions in the thermogram. Cr = crystal, N = nematic, I = isotropic.

Fig. 6 - DSC thermograms of copolymer MBPE-5,7 (1:1 comonomer ratio): (a) heating scan of the sample previously annealed at 60°C; (b) cooling scan; (c) reheating scan after cooling. Rate of heating and cooling: 20 deg./min.

Fig. 7 - Room temperature X-ray diffractogram of copolymer MBPE-5,7, which had been annealed at 65°C.

Fig. 8 - XDDSC heating scan (5 deg./min) for MBPE-5,7 previously cooled from the isotropic phase at -5 deg./min.: (a) thermogram, b) diffractograms (one every 2 degrees C). Bold diffractograms correspond to arrowed positions in the thermogram.

Fig. 9 - DSC thermograms of copolymer MBPE-8,10 (1:1 comonomer ratio): (a) heating scan; (b) cooling scan. Scan rate: 20 deg./min.

Fig. 10 - XDDSC heating scan (5 deg./min) for MBPE-8,10

previously cooled from the isotropic phase at -5 deg./min.: (a) thermogram, b) diffractograms (one every 3 degrees C). Bold diffractograms correspond to arrowed positions in the thermogram.

Fig. 11 - Mean amorphous scattering peak position <r> (see eqs. 1 and 2) vs. temperature for homopolymer MBPE-9 (▲), and copolymers MBPE-5,7 (+) and MBPE-8,10 (□). The main jump in <r> corresponds to the N-I transition, and the small jump in MBPE-5,7, marked by arrow, to the "N-N" transition.

TABLE 1

TEMPERATURES (T_i) AND ENTROPIES (ΔS_i) OF N-I TRANSITION AND MEAN AMORPHOUS SCATTERING PEAK POSITION <r> FOR ODD AND EVEN SPACER MBPE POLYMERS

	T_i (°C)	ΔS_i (J/mole/K)	<r> (Å)
MBPE-8,10	120	27	0.18
MBPE-8,12	119	27	
MBPE-10,12	113	29	
average (even)	117	28	(0.18)
MBPE-5,7	70	8.5	0.08
MBPE-7,9	79	12	0.08
MBPE-9,11	81	13	
MBPE-9	74	13	0.10
average (odd)	76	11.6	0.09

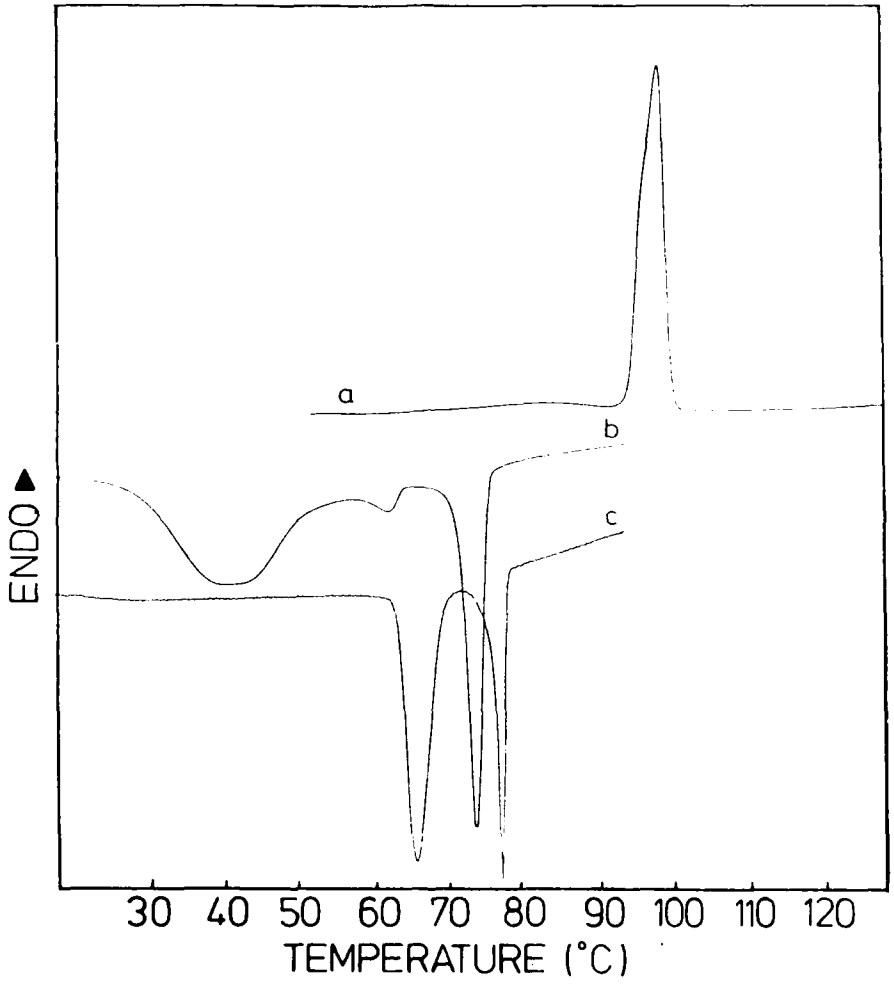
a
b
c
ENDO ▲
30 40 50 60 70 80 90 100 110 120
TEMPERATURE (°C)

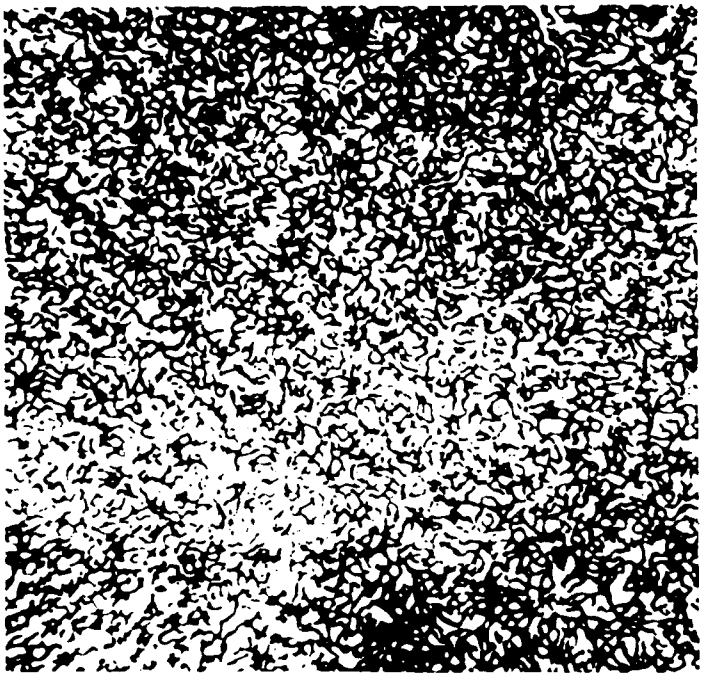

Fig 2

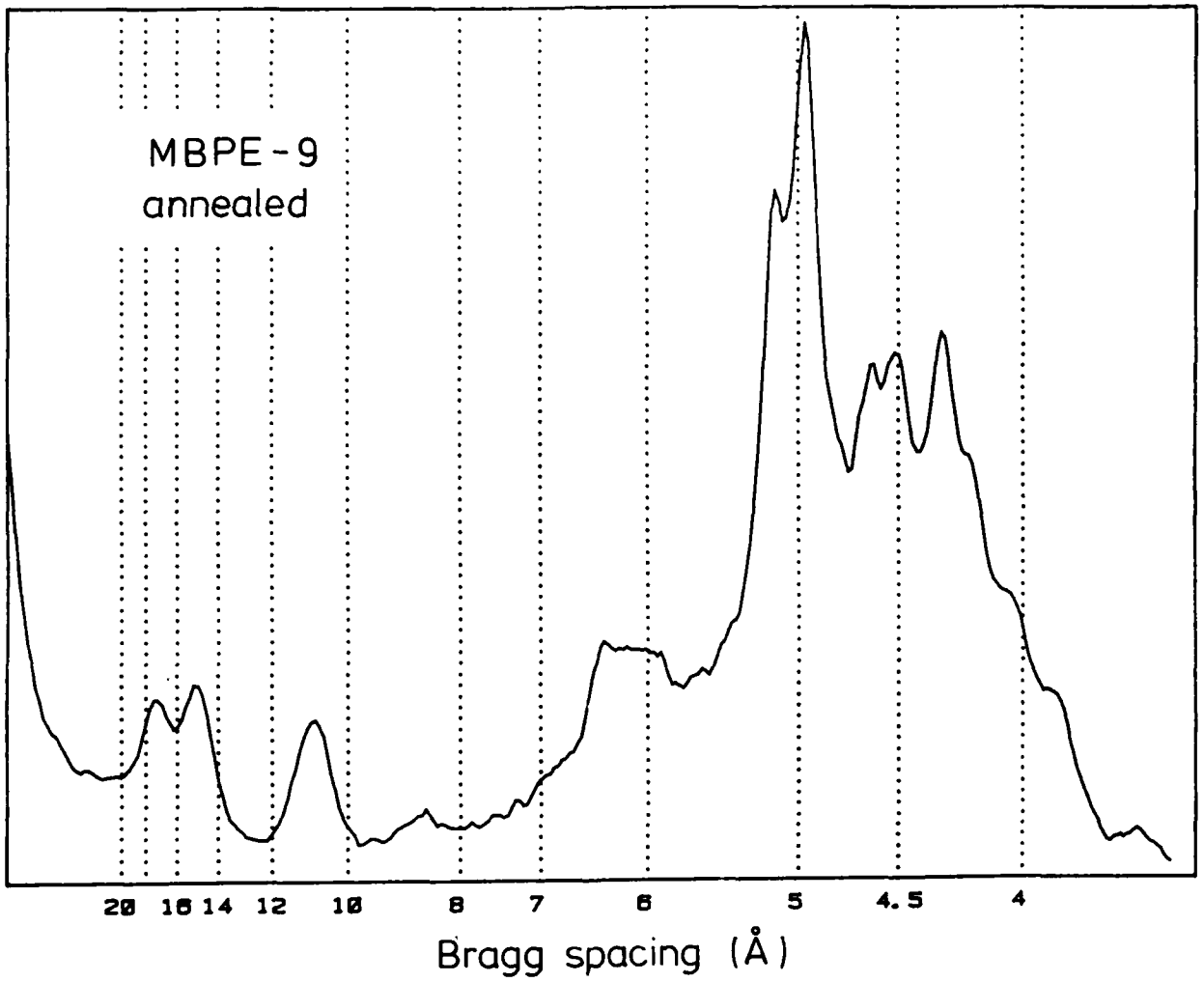
MBPE-9
annealed
20
16
14
12
10
8
7
6
5
4.5
4
Bragg spacing (Å)

FIG 4

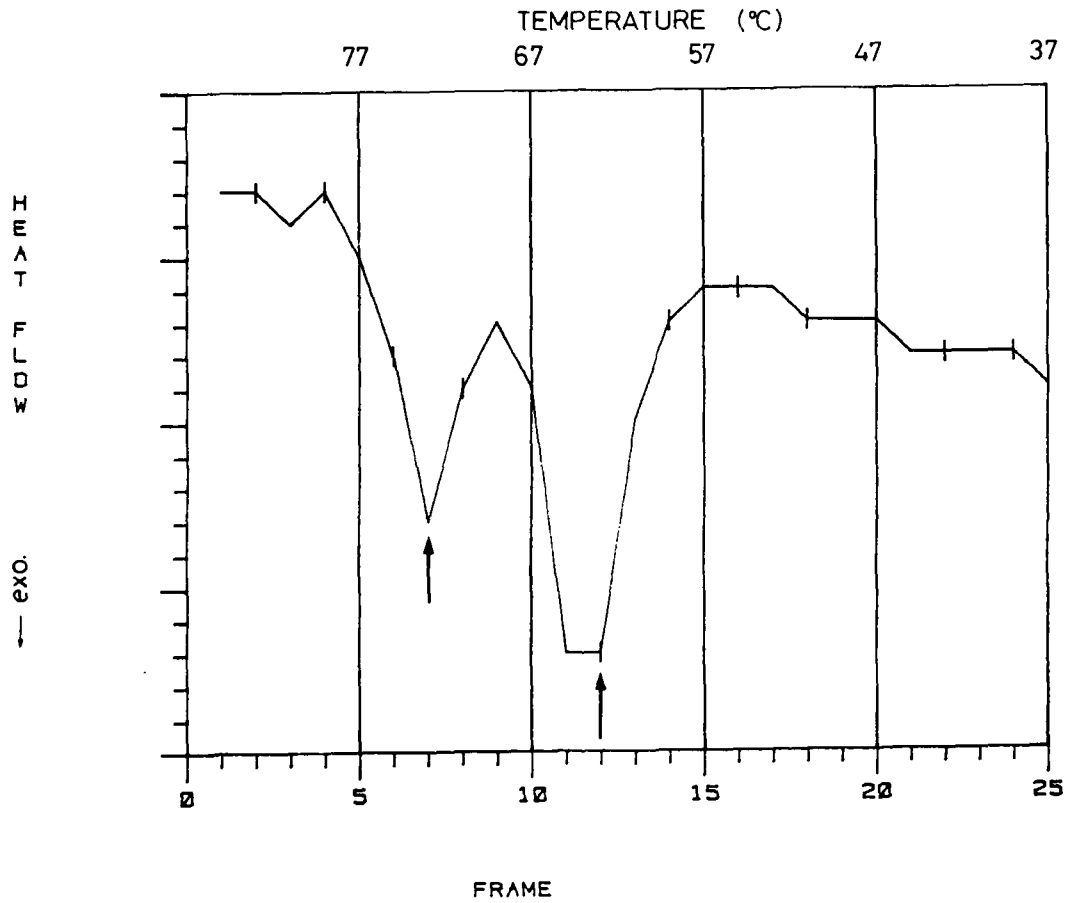
TEMPERATURE (℃)
77
67
57
47
37
HEAT FLOW
— exo.
0
5
10
15
20
25
FRAME

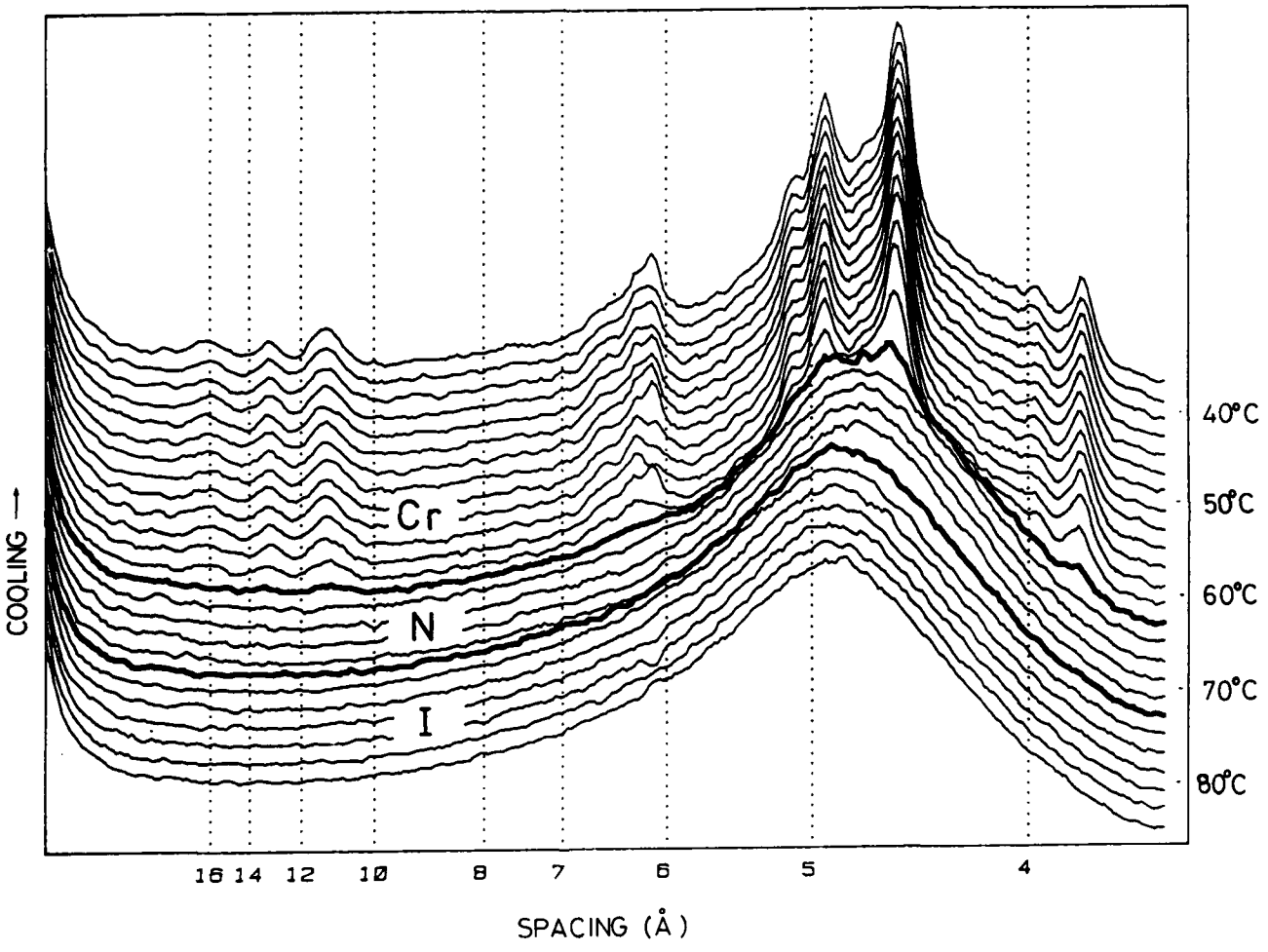

Fig 5c

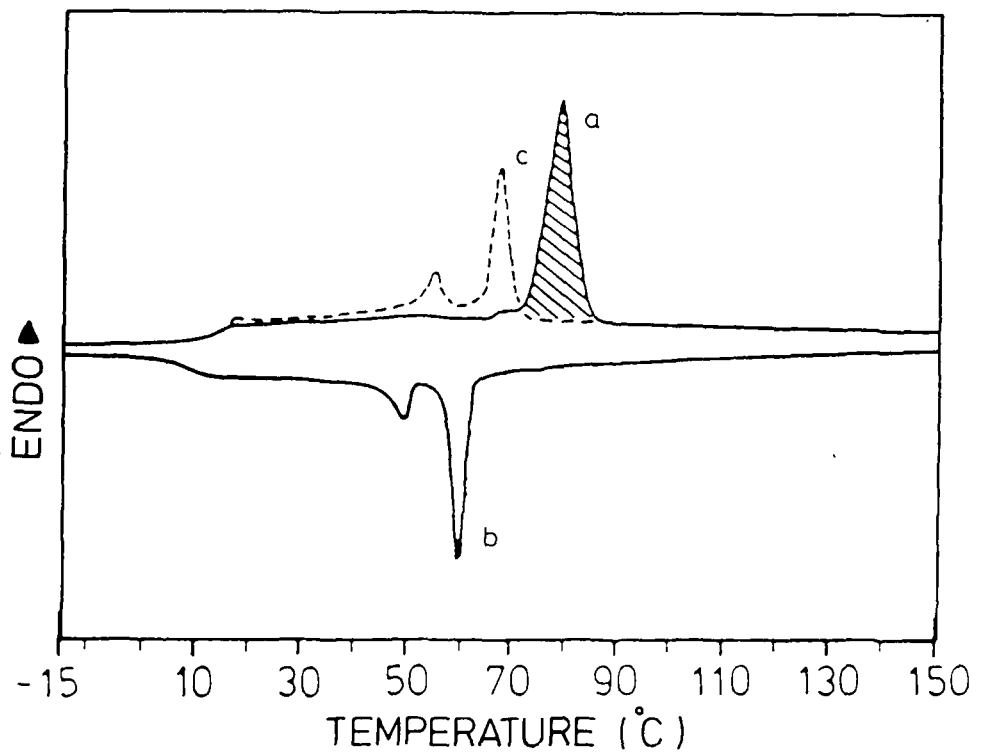
a
c
b
ENDO
-15
10
30
50
70
90
110
130
150
TEMPERATURE (°C)

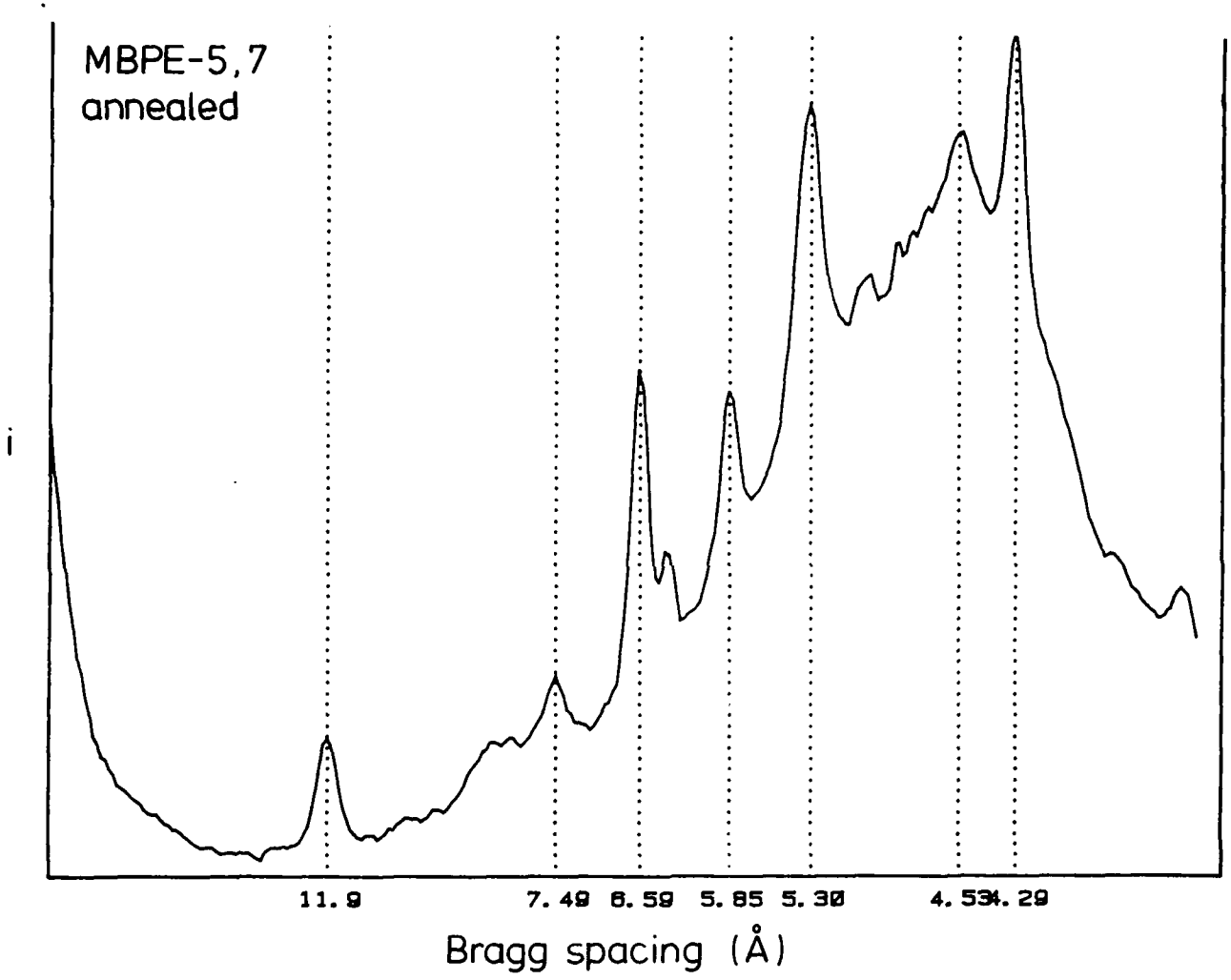

Fig 2

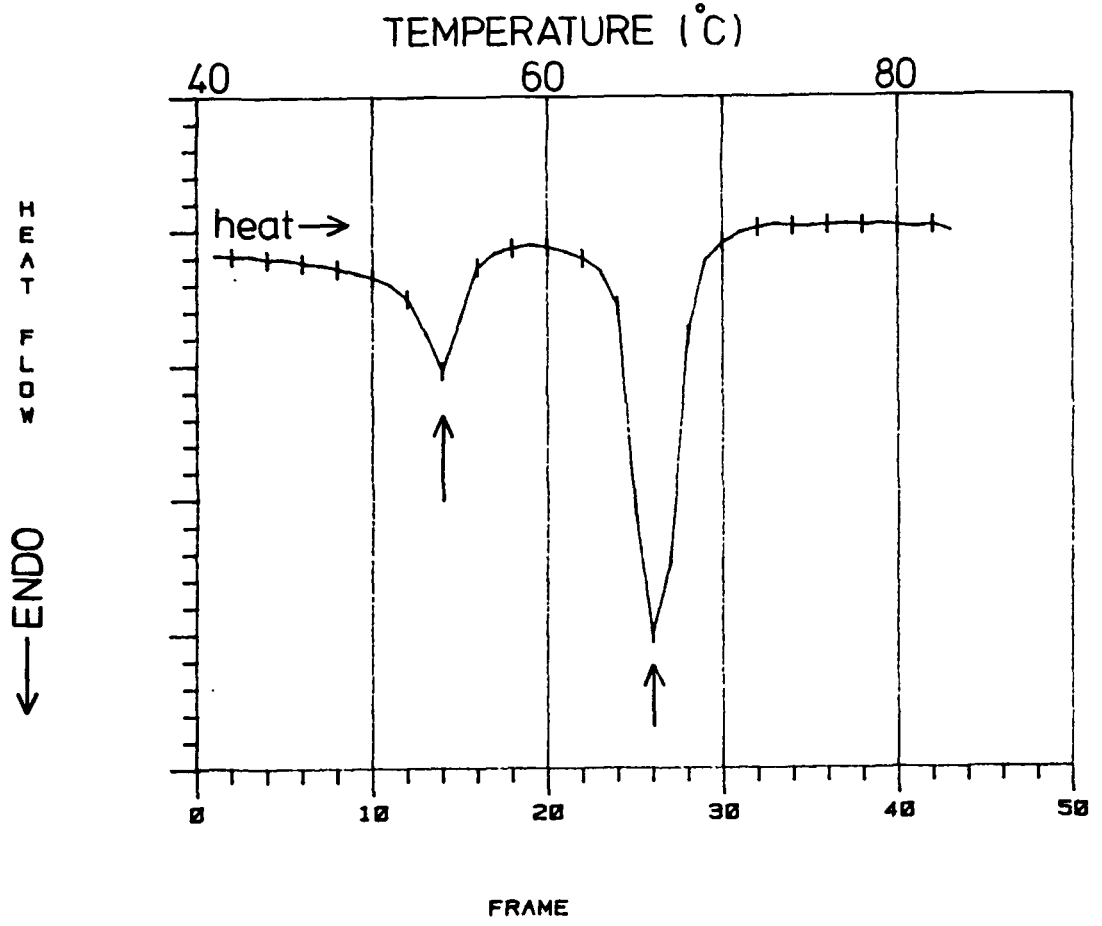
TEMPERATURE (°C)
40
60
80
heat
HEAT FLOW
ENDO
0
10
20
30
40
50
FRAME

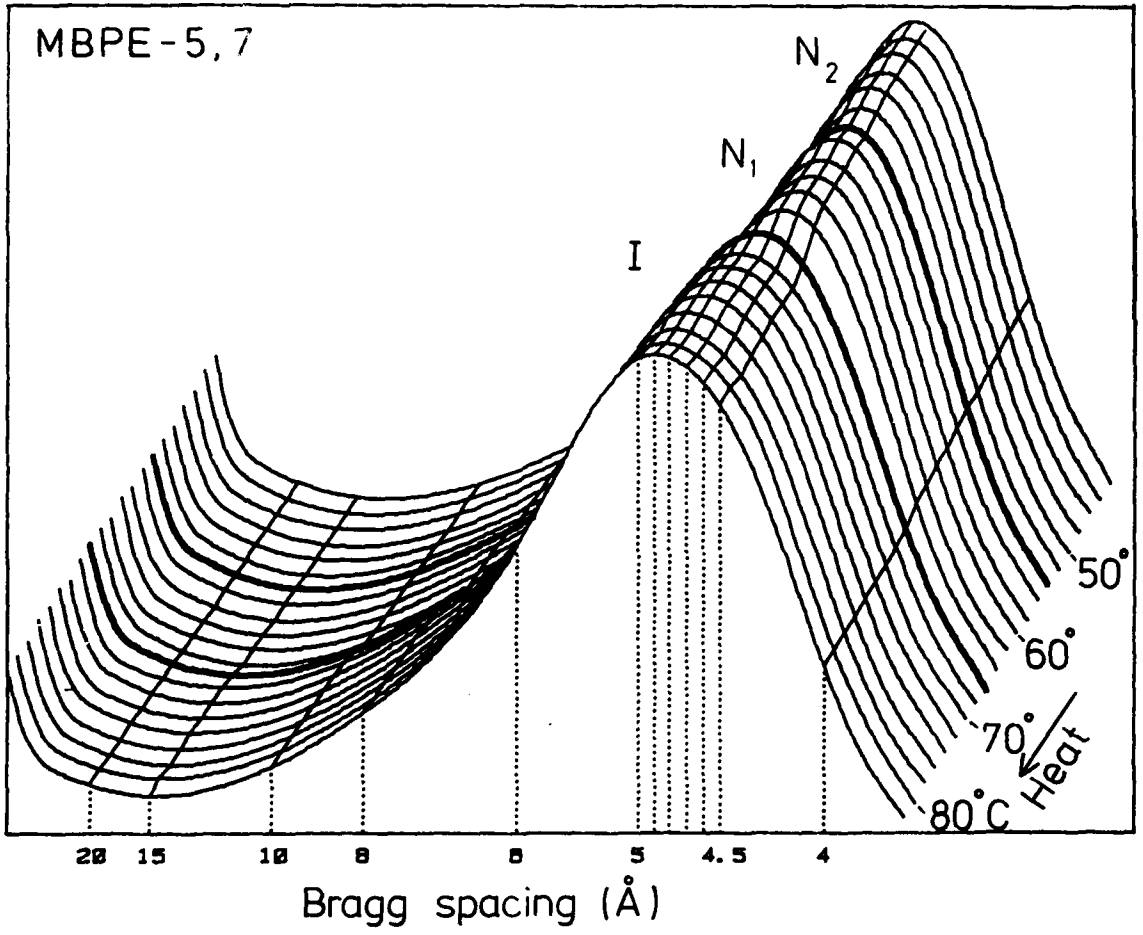

Fig 2b

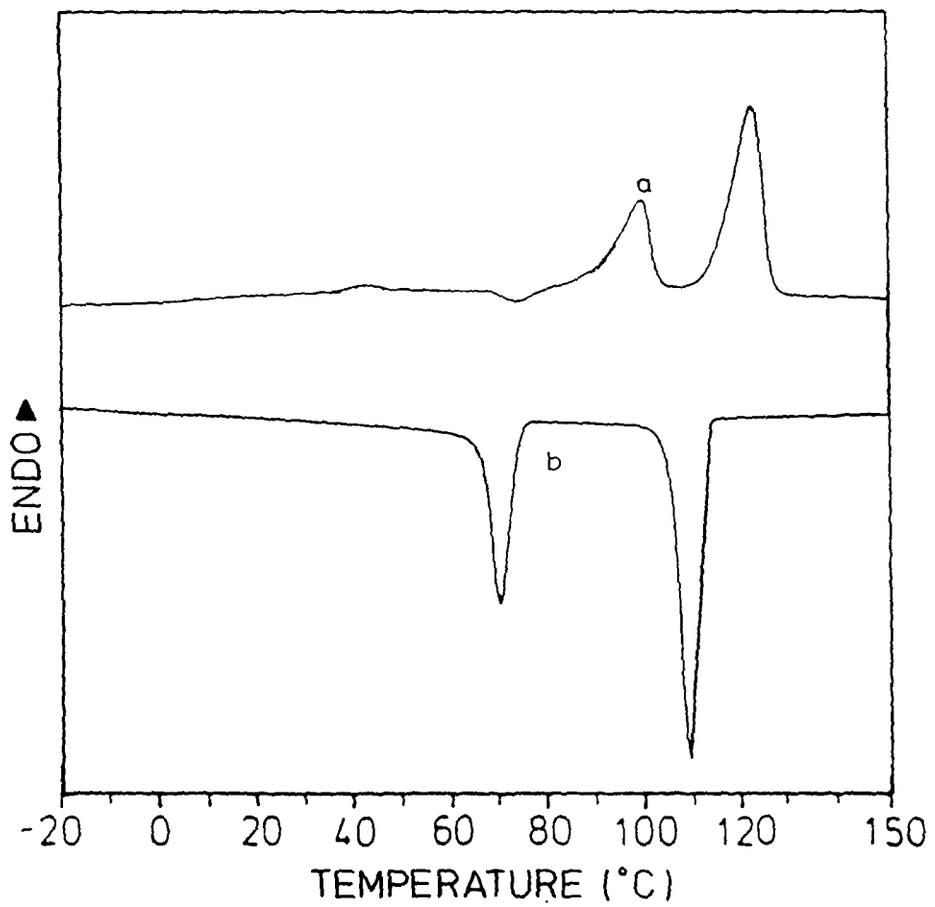

Fig 9

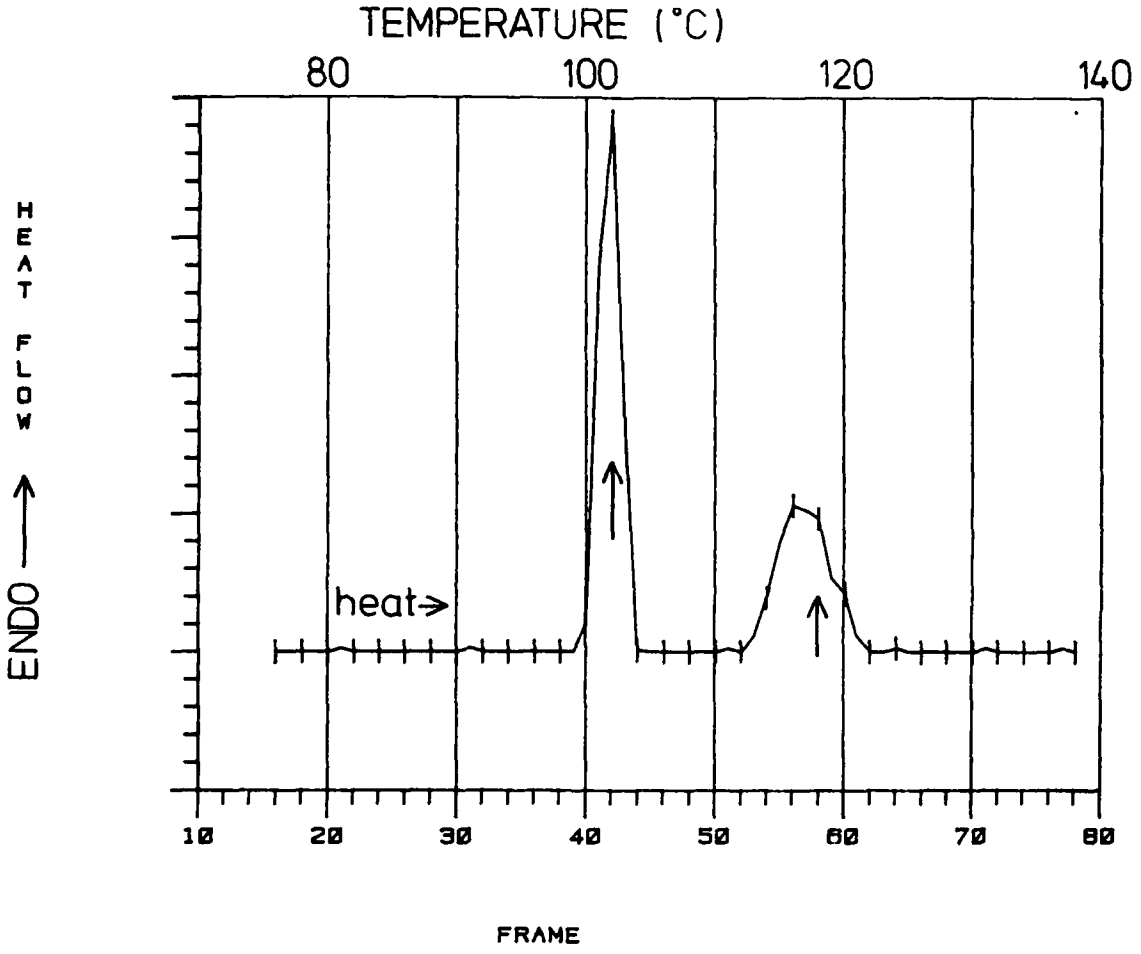
TEMPERATURE (°C)
80
100
120
140
HEAT FLOW
ENDO
heat→
10
20
30
40
50
60
70
80
FRAME

Fig 11

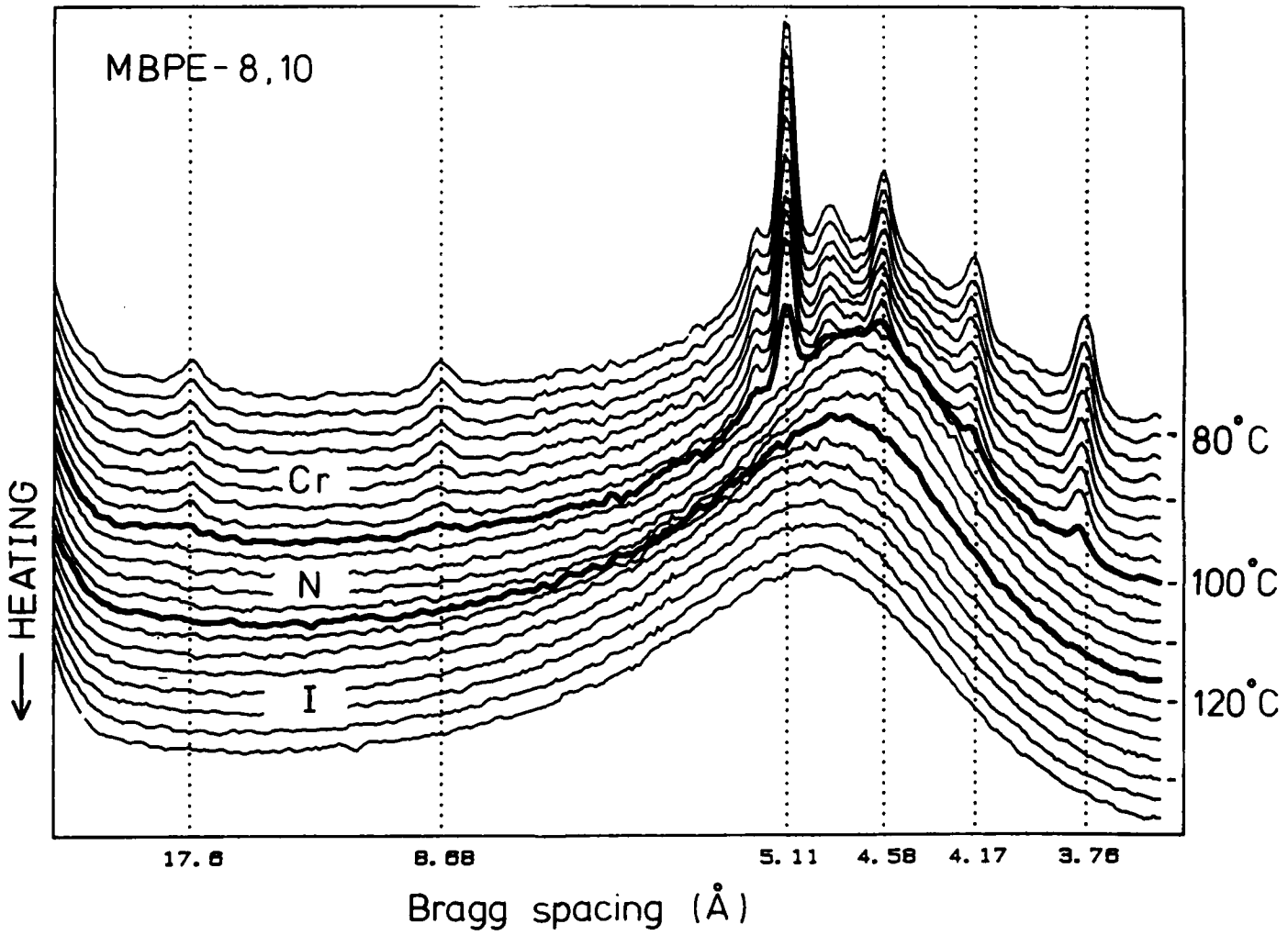
MBPE-8,10
Cr
N
I
HEATING
80°C
100°C
120°C
17.6
8.68
5.11
4.58
4.17
3.76
Bragg spacing (Å)

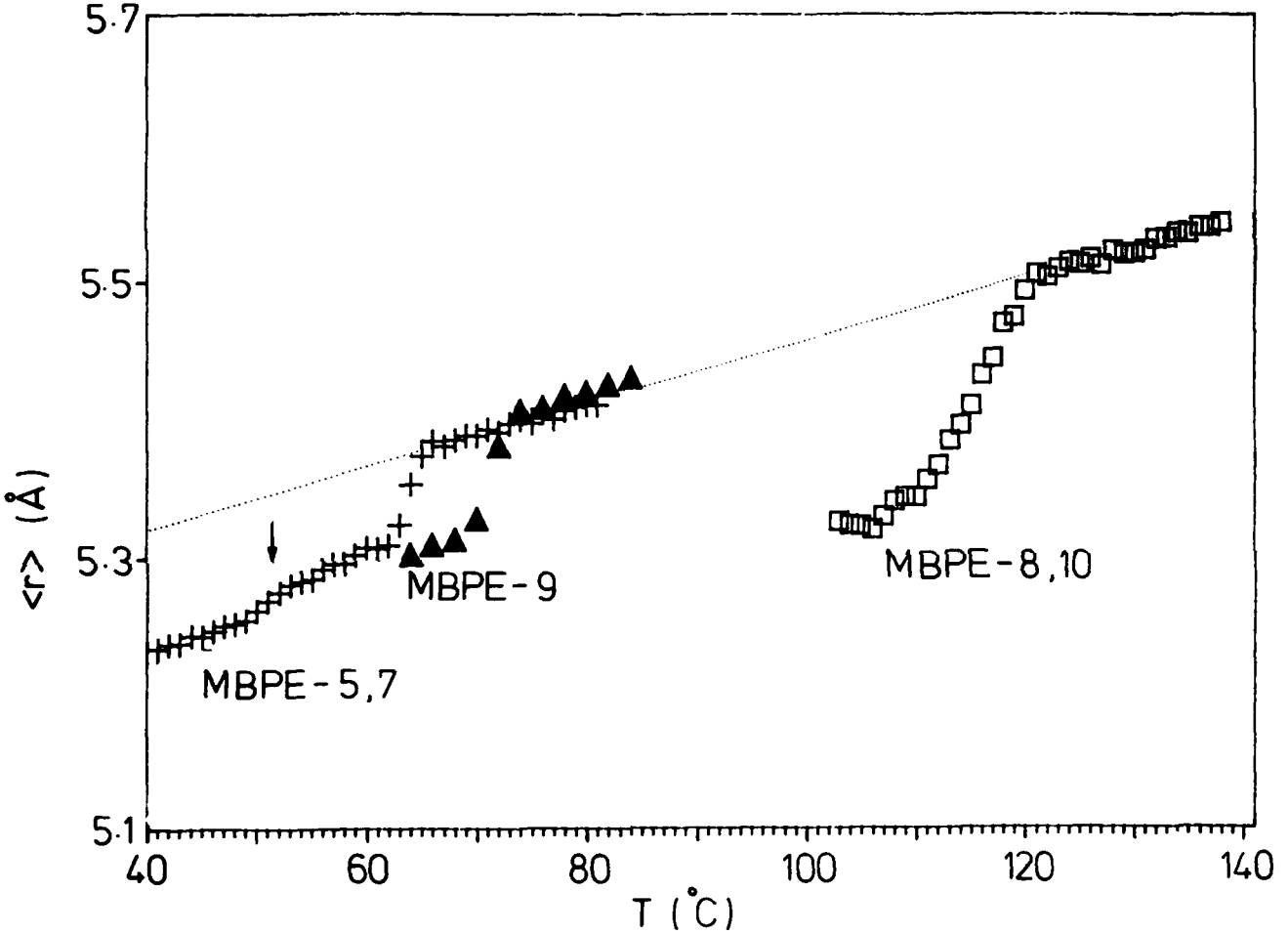

Fig 4

FEI/UN (1.2)

APPENDIX V

Mol. Cryst. and Liq. Cryst. (in the press)

Evidence for Disinclinations in the Isotropic State of Liquid Crystal Forming Polymers

J.L. Feijoo, G. Ungar, A. Keller, J.A. Odell, A.J. Owen
H.H. Wills Physics Laboratory, University of Bristol, U.K.

V. Percec
Case Western Reserve University, Cleveland, U.S.A.

The unexpected phenomenon expressed by the title has arisen at the junction of three lines of investigation on the light microscopic texture of the LC forming family of polymers, polyhydroxymethylstilbene with aliphatic spacers, the three being: i) the effect of molecular weight ii) the influence of prehistory iii) the effect of shear.

In common with most LCP-s these above polymers normally display only a grainy LC texture, increasingly finer with increasing molecular weight. However, after having been sheared and allowed to relax while in the isotropic state (realizable with these thermotropic polymers), and subsequently cooled below the isotropization temperature, rather strikingly, a large scale birefringent texture developed, such as normally observed in the nematic state of small molecular LC-s displaying disinclinations with extinction brushes extending to over distances of hundreds of μms. The same texture was seen irrespective whether cooled into the nematic or crystalline region of the phase diagram. Within this large scale texture a finer scale graininess was apparent which indicates that the orientation producing the effect is not directly due to a "liquid crystalline" arrangement of the molecular directors, but to the alignment of the same fine grain units as normally present in the nematic state without preceding shear in the isotropic state.

As yet we do not understand the role of shearing; it is obvious nevertheless that a skeleton of the disinclination - containing structure must have existed within the isotropic state itself and has developed to full visibility on cooling. We see further that we have a previously unsuspected multilevel hierarchy in the LCP texture. Implications for the whole LCP field include the molecular arrangement in isotropic melts, memory effects and flow behaviour also calling for retrospective reviewing of some past reports on LCP textures.

INTRODUCTION

The polarising optical image has always been the principal hall-mark of the liquid crystalline state by which it has been discovered and identified historically, and which ever since has been the basis of its classification providing the starting point for its more intimate, molecular characterization. While this has been unconditionally so for traditional small molecular weight liquid crystals (LC-s) the same light optical criteria were in general, not equally effectively transferable to liquid crystal polymers (LCP-s), at least to their thermotropic variety which are particularly topical at present as potential structural materials. The reason lies in the ever decreasing scale of the optically discernible structure features with increasing molecular weight (MW). For thermotropic main chain LCP-s of representative polymeric MW usually only a fine scale mottle is apparent (of say 1-3μ) (see e.g. Fig. 1) which, particularly as superposed on each other in film thicknesses normally used for polarising light optical (POL) examinations preclude their detailed study or even conclusive detection. At present state of knowledge the fine grains seen, are believed to correspond to regions of uniform orientation correlation within nematic structures, bounded by disclinations. Even,as e.g. our own work has shown [1], this texture can be developed (coarsened) by heat annealing in the nematic state (Fig. 2) the resulting increased size range still remains within only several microns and does not even approach the scale of texture in small molecular LC-s.

The latter (large scale POL textures) have occasionally appeared also in polymers (e.g. ref.2) but to our knowledge not sufficiently reproducibly to base any further work on them. We encountered this ourselves in the study of thermotropic polyethers. Inexplicably (at the time) the largest POL textures on the scale of hundreds of micrometers appeared in materials of the highest MW-s used, contradicting the general trend, otherwise observed also by ourselves, that the scale of the textures decreases with increasing MW. Fig. 3 (compare with Fig. 1) shows one example. However, at first, we could not reproduce these features, even ourselves, until the important part played by a new factor has been recognized. The purpose of this note is to

announce the recognition just indicated, in particular the observation of disinclinations in sheared isotropic melts and their frozen in versions in the nematic and crystalline states. We believe this could be significant even merely as an observational record, as it could influence preparative procedures and circumscribe the scope of what may be deduced from POL observations in this whole field. Additionally, however, we hope that the observations here to be reported point to new, so far unrecognized features of LCP-s which, when adequately interpreted, will contribute to their understanding and utilization.

Materials

Materials of experiments were polyethers constituted by a mesogenic α-methyl stylbene and flexible alkyl spacers linked through the ether oxygen of formula (3). Here n and m are variables determined by the synthesis. The case of n=m corresponds to a homopolymer , that of n≠m to random copolymer of two different flexible spacer lengths. The experimental material to be reported here will be on a copolymer with n=5 and m=7, but similar observations were made also on other members of the same family. It will be remarked that this type of polyether is less prone to chemical changes on heating than the more widely used, but otherwise analogous polyesters, enabling reversible passage between the isotropic, nematic and crystalline states. Also due to their particular route of synthesis the random copolymeric nature of the product is guaranteed, again in contrast to the usual polyethers (4). In brief, we have here both stable and well defined chemistry. While a range of MW-s was used throughout the work in the illustrations quoted M_n was 32000 with $M_n/M_w = 2$.

Experimental Procedure

The samples studied in the form of films cast from solvent on a microscopic slide. This method was adapted originally to ensure uniform film thickness which was in the range of 10-20μm in the different preparations. The observations were made in a hot stage mounted on a polarising microscope. The relevant transition temperatures were known from our previous calorimetric

works. These are in ascending order glass transition T_g = 35°C; crystal melting point (highest achievable) T_m^o = 110°C; isotropization temperature (highest achievable i.e. equilibrium - see ref. 1) T_i^o = 190°C.

In standard procedure the sample was heated above T_i^o i.e. to the isotropic state, then cooled into the nematic range (i.e. to between T_i^o and T_m^o or into the crystalline range (below T_m^o). POL observations were made in situ in all these ranges. The effects seen in the nematic or crystalline ranges were indistinguishable corresponding to the textures displayed in the nematic range. This is a reflection of the fact that the overall nematic texture is retained on crystallization, or conversely, that the crystalline texture remains indistinguishable from the nematic one on the scale of the POL observations, which in turn means, that the occurrence of crystallization cannot be detected by POL observations alone. It needs stressing that this is a characteristic of the present comparatively high MW material; in low MW LCP-s of the same family (e.g. MW = 1800), just as in small molecular LC-s, below T_m^o, the crystals are seen as distinct entities growing within a nematic background. The difference of behaviour with MW is clearly due to the decrease in chain mobility with increasing MW through which the memory of the preceding nematic texture is retained even in the crystalline state. While this is an important finding in itself, (possibly already noted in previous LCP works) it affects this note in as far that in what follows we need not distinguish between photographs taken in the nematic and crystalline states, as on the POL scale the images are the same for a given sample.

The actual observations to be reported here have been selected from a wide ranging experimental material, best seen or recorded on video) in service of the point announced in the Introduction.

Experimental Observations

As implied by the foregoings the new recognitions arose from the confluence of three lines of initially separate works involving the said polyethers: effects on the POL image of MW, of

prehistory (i.e. non equilibrium states [1]) and of shear. Combined, they led to the recognition that the large scale POL structure such as in Fig. 3 can be systematically obtained in the nematic state provided the MW is sufficiently high, and the sample has been subjected to shear while in the preceding isotropic state (Fig. 4). In the first stages the shear applied was unidirectional (cover glasses were slid with relation to each other) but by subsequent findings uniaxial compression (squeezing of the slides) against each other alone sufficed. Clearly in the latter case the shear produced by the compression must have been operative in bringing about the effect in question.

The procedure leading to a texture as in Fig. 4 was as follows: 1) heating cast film into the isotropic region to a temperature T where $T>T_i^o$. 2) Shearing at T (slide or squeeze cover glasses). At this stage overall birefringence appears while at T. 3) Holding at T, when the birefringence is seen to decay in a few seconds but not before displaying large scale extinction brushes before its final disappearance. 4) Cooling below T_i^o (as said before it makes no difference to the POL image whether cooling stops in the nematic or crystalline range) when the large scale extinction brushes such as has been seen transiently in the preceding isotropic state, reappear but this time are there to stay.

Images as in Fig. 4 clearly indicate nematic structures, with brushes as markers of disinclinations. The latter was tested by rotation of sample with relation to polariser/ analysis direction. In this way disclinations of s = 1 and of s = $^1/2$ (Fig. 5) were readily identified. Thus, by observing the POL images such as in Figs 3-5 on their own, there would be no reason to suppose that we are not viewing conventional nematic textures on the scale as usual in small molecular MW-s but in this case in (comparatively) high MW thermotropic polymeric materials.

Beyond the above, however, some further observations need noting from which it emerges that the large scale patterns as in Figs 3-5 are not the primary structure elements. Thus the higher magnification images reveal a grainy domain texture underlying

the large scale POL texture (fig. 6). This graininess, best visible within the dark brushes themselves, is on the scale of 1-3μ, hence on that of the usual dense disinclination texture [5] structure in LCP samples which have not been pretreated in the isotropic state (see Fig. 1). Its prominence can vary from sample to sample. Fig. 8 shows an example where the combination of large brush and fine grain is particularly evident. In particular, the prominance of the grains is a function of holding time (step 3 above) where this holding time itself is a function of molecular weight. For the highest MW sample (32,700) the holding time (within the limits permitted by thermal stability) had hardly any noticeable effect, while for the lower MW of 11000 the graininess became increasingly prominent on longer holding in the preceding isotropic state. This was increasingly at the expense of the large scale brushes until on protracted holding (e.g. over tens of seconds) the dense disclination texture structure alone remained. Thus, for low MW-s the large scale textures as resulting from the pretreatment in the isotropic state, may easily be missed, hence the MW dependence of the whole effect as already indicated.

The existence of grains clearly indicates that the large scale brush structure is not directly the consequence of the parallelisation of the molecular directors over the corresponding areas. Rather, these directors are in the first place organized over smaller scale domains, possibly defined by a correspondingly fine scale disclination network. These grains themselves have then common orientations on a larger dimensional level, giving rise to the large scale brush texture, the subject of our investigation. Thus, so it seems, we uncovered a two stage structure hierarchy in LCP-s: the primary grain texture, and a longer range organization of these grains, a kind of supertexture. The former seems to correspond to the previously described and commonly observed dense disclination texture, while the hitherto elusive super texture, seen only occasionally in the past, seems to arise through a further, longer range organization of these dense disclination texture as a kind of an overlay on the primary structure.

A further feature to note is the effect of bubbles present in profusion (e.g. Fig. 5). Bubbles are usually the centre points of extinction brushes, hence clearly can initiate such extinction patterns. Yet it is important to note that they are not a necessary condition for the existence of the latter. There are many clearly defined brushes without any visible bubbles at their centres which thus represent disclinations in the usual sense.

Discussion

Observational Consequences

As seen we succeeded in establishing the method of creating large scale nematic POL textures in high MW thermotropic polymers and simultaneously in tracking down the source of these textures where seen erratically before. Irrespective of the significance of such textures and their basic source of origin we hope the purely observational material as it stands should be helpful for LCP research. In the first place when and as required we are now in a position to provide a recipe for producing these textures. The scheme outlined here may well be general, except that for different compounds some of the parameters would need to be adjusted, e.g. the ratio of MW and holding time. Secondly, our findings may well invite rescrutinization of past reports and observations on such large scale textures when observed, as to how far they may have been dependent on pretreatment in the isotropic state, and further, how far they correspond to secondary structures resulting from organization of primary 'grains'. The latter point, i.e. the recognition of an (at least) two tier hierarchy is likely to have many further forward looking, and possibly retrospective consequences on which we refrain to speculate further at this stage.

Origin of large scale texture

The most surprising aspect of the present findings is that the structures in question originate from the treatment the samples have received in the isotropic state. This necessarily implies that the corresponding structures must have been created while in the isotropic melt. Indeed the birefringent pattern

fleetingly observed after compression does, before its disappearance, possess feature images such as are eventually displayed in a lasting manner by the nematic (or crystalline) state after cooling. The question clearly arises as to what are these textures and secondly why do they reappear on cooling and this only under certain circumstances?

The molecules in question are semi-rigid. This means in the first place that they always possess some localized orientation, and secondly and chiefly, that such short range orientational correlation can be readily extended over macroscopic volumes under externally imposed orienting influences. This is evidenced by the ready development of uniform birefringence on even slight shear or pressure, such as would hardly cause any visible effect in the case of the usual fully flexible polymers. This birefringence rapidly disappears after cessation of the flow,through stages which display large scale brush/disinclination textures. It is the vestiges of this latter, partially relaxed structure which must have remained in the isotropic state for them to reappear on cooling below T_i. At this point the effect of MW comes into play. Namely, the orientational relaxational of long molecules is expected to be much retarded which in general terms is responsible for increasingly pronounced memory effects in high molecular weight materials. In the present instance we may assume, that the longest species in the molecular weight distribution retain the long range orientational correlation created by the shear while the rest of the molecules disorient. The former being small in number will not produce a registrable effect in themselves, nevertheless retain an invisible skeleton of the original long range texture pattern. This skeleton then serves as a nucleus for the formation of the nematic state on subsequent cooling. More specifically, we suggest that it is the longest molecules which determine the director orientation of the nematic domains developing on cooling below T_i. In support of this suggestion we recall the well established fact that T_i of a high MW polymer is higher than that of a low MW polymer. Thus nematic self-ordering is expected to be nucleated by the highest MW molecules upon cooling through the T_i range. Hence the average domain orientation in a given area will be pre-determined by the remaining preferential orientation of the high MW component. Accordingly the

role of the nematic state would be to 'develop' a latent 'texture' present to begin with, to full visibility. The scheme just outlined would account for the sequence of events observed including the requirement of high molecular weight (which would thus serve to retain the memory in the isotropic state).

It is evident that shear induced orientation is the factor responsible for the long range order under discussion. It seems to matter little as to whether this shear is unidirectional or multidirectional as would arise by compression. The overall final textures seem to bear no obvious relation to the orientation caused by the shear initially. It seems that it reflects not the initial but a relaxed texture as indeed seen transiently within the isotropic melt while the shear induced birefringence decays. Beyond stating the above we are not in a position to be more specific at this stage.

An important outcome of this work, we believe, is the realization that the changes in orientation in any continuous phase made up of reasonably rigid anisotropic objects imply the existence of disclinations. This must be true irrespective of whether we have a nematic liquid crystal, i.e. a self-ordered system, or an intrinsically isotropic melt which has attained preferential molecular orientation through the action of an external field such as flow field. The combined effects of such a field and slow overall relaxation due to high molecular length may lead to unusual transient non-equilibrium states of which the present coarse texture 'isotropic' state appears to be an example. While the current observations raise a number of unanswered questions, they seem to illustrate a wider generality of the curvature elasticity theory [6,7]; the principle of the latter, i.e. the minimization of the splay, bend and twist elastic energies through disclinations, as usually seen in the self-ordered nematics, ought to also apply to systems which have been oriented through external action. The necessity of disclinations will arise as long as some directionality is associated with a given position in sample space in an orientationally non-uniform but otherwise continuous structure. In this sense the features identified e.g. in Figs 4,5 are true disclinations. We consider the extension of the disclination

concept to, what is thermodynamically an isotropic phase, as one of the notable outcomes of this work. Even if self evident from abstract geometric considerations this may not be so from the point of view of material science where the existence of line singularities in materials otherwise believed to be homogeneous could be of tangible consequence. The above contention is not at all confined to presently described large scale texture. The disclinations could be present on any scale. In this respect the large scale of the features as in Figs 3,4 merely serves to make the effects in question conspicuously apparent.

To end with we remark that the shear or pressing treatment when applied in the nematic state did not produce the above effects. Unidirectional shear of course produces strong unidirectional orientation which relaxes via the conspicuous but familiar regular cross-banding effect into the initial fine grained texture. Neither did compression have any lasting effect on the final relaxed nematic texture. It appears that the long range orientation effect in question can only be attained from the initially isotropic true melt.

ACKNOWLEDGEMENTS

Sponsorship by US Army European Office, London, is gratefully acknowledged. One of the authors (J.L.F.) wishes to acknowledge financial support from Britannic Society (1 year scholarship), the British Council (Venezuela) and Simón Bolívar University.

References

1. J.L. Feijoo, G. Ungar, A.J. Owen, A. Keller and V. Percec, Mol.Cryst. Liq. Cryst., 155, 487 (1988).

2. M.R. Mackley, F. Pinaud and G. Siekmann, Polymer, 1981, 22, 437-446.

3. T. Shaffer and V. Percec, Makromol. Chem. Rapid Commun. 6, 97 (1985).

4. G. Chen and R.W. Lenz, Polymer, 26, 1307 (1985).

5. N.J. Alderman and M.R. Mackley, Faraday Discuss. Chem. Soc., 1985, 79, 149-160.

6. Oseen, Trans. Faraday Soc., 1933, 29, 883.

7. F.C.Frank, Discuss. Faraday Soc., 1958, 25, 19.

Figure Captions

Fig. 1 Dense disclination texture in copolymer PHMS-517 (1:1), M_n = 32,700, as seen under the polarizing microscope.

Fig. 2 Same as in Fig. 1, but after annealing in the nematic state.

Fig. 3 Large scale texture in copolymer PHMS-517, as seen under the polarizing microscope.

Fig. 4 Typical optical micrograph viewed between crossed polaroids, of a PHMS - 5,7 sample heated to the isotropic state (220°C), pressed while in the isotropic state and cooled down to room temperature.

Fig. 5 Large scale structures (brushes) showing disclinations of strength s=1 (full arrow) and s=1/2 (half arrow).

Fig. 6 Dense disclination texture underlying large POL texture in Fig. 5, revealed at increasing magnification.

Fig. 7 Combination of large POL texture and dense disclination texture in PHMS-5/7.

10 µm

FIG 1

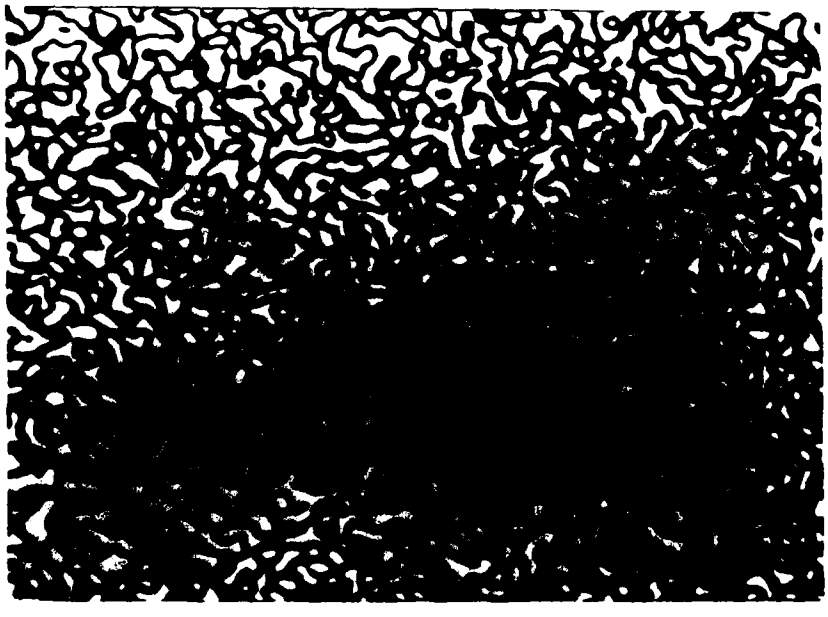

10 µm

FIG 2

100 µm

FIG 3

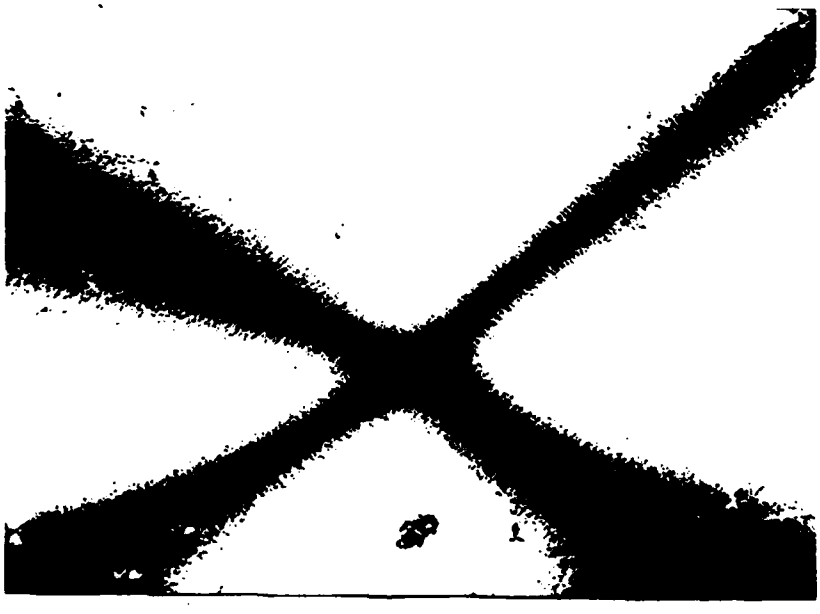

50µm

FIG 4

100 µm

FIG 5

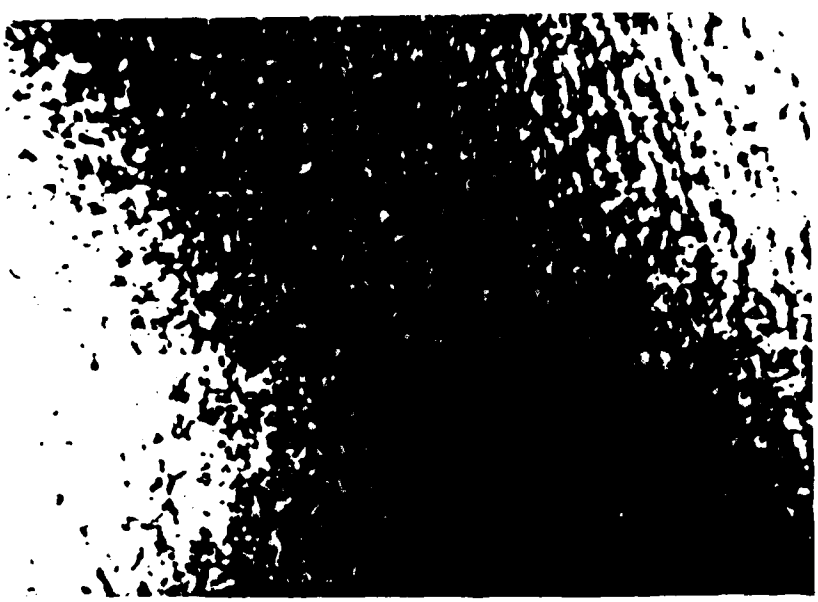

10 µm

FIG 6

FIG 7

10 µm

A. VI 1.

APPENDIX VI

Mol. Cryst. Liq. Cryst., 1988, Vol. 155, pp. 313-325
Photocopying permitted by license only

Printed in the United States of America

CRYSTAL AND PSEUDO-CRYSTAL PHASES IN MAIN CHAIN MESOGENIC HOMO- AND COPOLYMERS WITH FLEXIBLE SPACERS

GORAN UNGAR and ANDREW KELLER
H.H. Wills Physics Laboratory, Tyndall Avenue, Bristol BS8 1TL, U.K.

Abstract Some packing principles of polymers containing rigid and flexible segments are presented, as revealed by X-ray diffraction of crystal phases. Two types of conformationally disordered crystal states are recognized: (a) with "layered" disorder (quasi-2-dimensional) and (b) with "occluded" disorder (3-dimensional). In both cases the flexible spacer is non-crystalline, which is ascribed to the mismatch in cross-sectional areas of the spacer and the mesogen. The relative ease of crystallization of random copolymers containing spacers of varying length is attributed to their miscibility in the disordered layers.

INTRODUCTION

While the nature of long range order in crystal phases of mesogenic compounds can provide clues about molecular short range ordering in the mesophases, studying crystalline phases may be of considerable interest in its own right. It is felt that neither the conformational disorder associated with the flexible parts of the molecule, nor the question of the true dimensionality of such crystals, have received adequate attention. In this paper we report on some novel features of molecular arrangement and disorder in crystals of main chain mesogenic polyethers with flexible alkylene spacers.

A. VI

EXPERIMENTAL

Polyethers of α,ω-dibromoalkanes and 4,4'-dihydroxy- α -methylstilbene, with the structural formula:

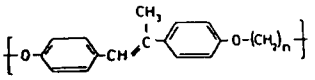

were prepared by V. Percec and T.D. Shaffer of Case Western Reserve University. The polymers (polyhydroxymethylstilbenes) are denoted PHMS-n, where n is the number of CH groups in the alkylene spacers. Homopolymers with n=5, 7, 9 and 11 were studied, as well as a random copolymer containing spacers 5 and 7 in 1:1 molar ratio (denoted PHMS-5/7). All polymers, except for some very low molecular weight ones, display the nematic phase above the crystal melting point [1,2].

Fibres for X-ray diffraction were prepared by, first, extruding the nematic melt and quenching it as a moderately well oriented glass at room temperature. This was then followed by drawing somewhat above the glass transition temperature (T_g), which is in the range 10 - 30°C, to obtain a well oriented stress crystallized sample.

X-ray diffraction patterns were recorded in vacuo with a high-temperature flat plate camera.

Experimental [3,4] and calculated [5] values for bond parameters of compounds closely related to the PHMS polymers were employed for molecular modelling.

RESULTS AND DISCUSSION

Models of two lowest energy extended conformations of the isolated PHMS-5 molecule (three monomer units) are shown in Figure 1. The two-monomer repeat distances for the most extended conformation of PHMS homopolymers, assuming an all-trans spacer conformation, are listed in Table 1 (second column).

A. VI.3.

FIGURE 1. Extended conformation of the isolated PHMS-5 chain

A number of polymorphic forms are observed below the melting temperature of all homopolymers. Fig. 2 shows a typical sequence of X-ray fibre patterns with increasing temperature for the homopolymer PHMS-7. The polymorphic transitions are irreversible, i.e. Forms III and II do not convert into Forms II and I, respectively, upon cooling. The behaviour of PHMS-5 is essentially the same. In PHMS-9 Forms I and II are not observed and Form III appears to be stable at all temperatures below the melting point. The polymer with the longest spacer, PHMS-11, displays an altogether different phase behaviour, all modifications having layer normals highly inclined to the fibre axis. Metastable tilted forms are also observed with PHMS-9. Only one crystal form (Form III) was ever observed with the copolymer PHMS-5/7.

A VI

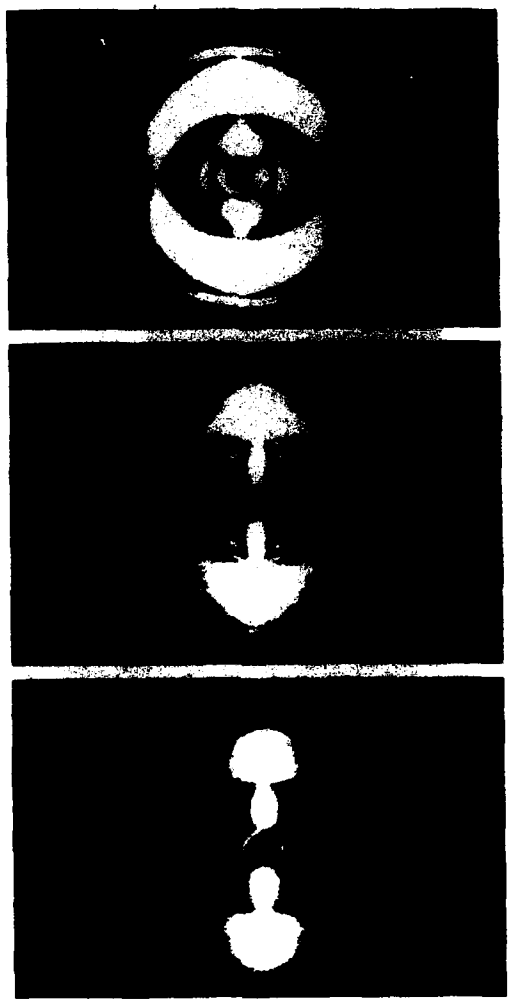

a) Form I b) Form II c) Form III

FIGURE 2. X-ray diffraction patterns of the three crystal forms of PHMS - 7 (fibre axis vertical)

A.VI.5.

TABLE 1. 2-Monomer repeat distance and density of the Layered form III

Spacer length (C-atoms)	5	7	9
calc. extended conformation (nm)	3.79	4.30	4.81
observed (nm)	3.78	3.78	4.20
contraction w.r. extd. conform. (nm)	0.01	0.52	0.61
spacer conformation (extended, contracted)	extd.	contr.	contr.
overal unit cell density (g/cm^3) increases by spacer contraction from:	(1.07)	1.03	1.01
to:	(1.07)	1.17	1.16

In the case of PHMS-5 and PHMS-7 the nematic glass first crystallizes into Form I whose diffraction pattern is characterised by comparatively broad and scarce equatorial and off-equatorial hkl reflections and horizontally streaked meridional reflections which are sharp in the meridional direction. This structure will not be discussed here further, except for noting the close resemblance of the diffraction pattern to that of Form II into which it transforms on heating. It is believed that Form I is unstable but is favoured by crystallization kinetics. The periodicity of meridional reflections corresponds approximately to the length of one monomer unit.

A.VI.

FORM II - "INTERMESHED"

Form II appears through an exothermic solid state transformation of Form I at approx. 100°C in both PHMS-5 and PHMS-7. It is distinguished by a large number of sharp hkl reflections extending to large angles, both equatorially and meridionally. Unlike in Form I, layer lines are not well defined (cf. Fig. 2). This indicates that the fibre axis does not coincide with any of the principal axes of the real lattice. The characteristic texture of Form II is impaired by the particular mechanism of the Form I - Form II transition.

The most conspicuous feature of the diffraction pattern of Form II, when compared with Forms I and III, is the absence of odd-numbered meridional reflections. The periodicity of meridional reflections in Form II is $1/c^* = 1.04$ nm and is identical for both polymers where it is observed, i.e. PHMS-5 and PHMS-7. It corresponds closely to half the calculated extended monomer length for PHMS-5 with the alkylene group in the all-trans conformation.

The molecular packing in Form II, consistent with the halving of the fibre period, is schematically presented in Fig. 3a. The principal feature is the "intermeshing" of mesogen and spacer moieties. The fact that the fibre periodicity is independent of spacer length (1.04 nm in both PHMS-5 and PHMS-7) suggests that the structure is essentially determined by the intermolecular contact between mesogen units, while the spacers only fill the voids between them. In order to account for the observed fibre repeat distance it must be assumed that the spacer in PHMS-5 is nearly fully extended to span the gap between two consecutive mesogens. On the contrary, in PHMS-7 the spacers appears to adopt a contracted form, most likely involving dynamic conformational disorder.

In PHMS-9 Form II is not observed, suggesting that the $-(CH_2)_9-$ spacer is too large to fit into the interstices between the mesogens.

A. VI. 7.

FORM III - "LAYERED"

Around 130°C the "Intermeshed" form in PHMS-5 and PHMS-7 undergoes an endothermic transition into Form III (see Fig. 2). This modification is also found in PHMS-9 and the copolymer PHMS-5/7, in both cases apparently being the only stable crystal form. Its unit cell is orthorhombic, with the lateral dimensions a = 0.761±0.002 nm and b = 0.637±0.005 nm. The fibre periodicities c are listed in Table 1 (3rd column). The space group was determined as Pnam. There are four monomer units in the cell, situated on two nonequivalent polymer chains.

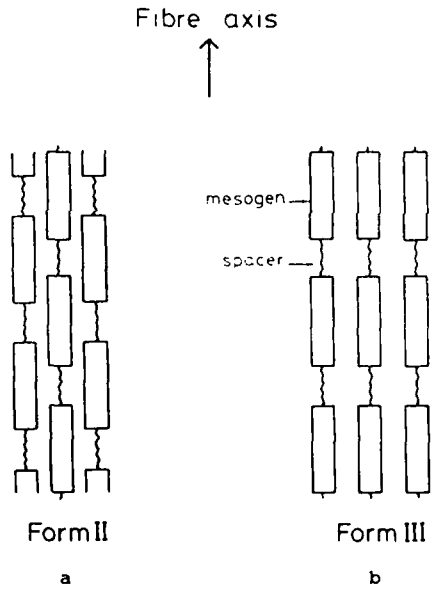

FIGURE 3. Mesogen - spacer packing in (a) Form II (Intermeshed) and (b) Form III (Layered)

A. VI. 8

The essential packing arrangement in Form III is schematically shown in Fig. 3b. The mesogens and the spacers are located in alternating layers which are normal to the chain axis.

It is interesting that the copolymer PHMS-5/7, which contains equal amounts of randomly distributed $-(CH_2)_5-$ and $-(CH_2)_7-$ spacers, is capable of crystallizing in Form III to a considerable extent (up to ca. 40% crystallinity). Since both spacer types cannot be accommodated in the ordered extended conformation at the same time, at least the longer spacer $-(CH_2)_7-$ must adopt a non-planar contracted form. This implies that the spacer layers are by themselves not crystalline, but rather conformationally disordered. Nevertheless, they are constituents of what would normally be considered a crystalline structure. Note that the diffraction pattern of Form III (Fig. 2) contains a number of hkl reflections (up to l=7), in addition to hk0 and 001 ones. Otherwise, the sharp and numerous hk0 reflections indicate good lateral crystalline order due to the high regularity within the mesogen layers.

As it is isomorphous with the copolymer PHMS-5/7 crystals, the "Layered" form (Form III) in homopolymers must also contain non-crystalline spacer layers.

Note that the alternating ordered-disordered layers in Form III make up an equilibrium structure. The fact that even in the homopolymers the spacer layers are non-crystalline is thought to be due to the large cross-sectional area of the mesogen compared to that of the spacer, which precludes close packing of the spacers. The measured cross-sectional area per chain in Form III is 0.242 nm^2, which results from mesogen packing. This value is considerably higher than the area in close packed alkane crystals or even in the more disordered alkane mesophases, the corresponding values being as follows [6,7]:

- ordered orthorhombic or triclinic crystal (paraffins and polyethylene): 0.186 nm^2
- "rotator" phase in n-paraffins: 0.19-0.205 nm^2
- hexagonal phase in polyethylene (1 bar): 0.21-0.225 nm^2

All these cross-sections are less than that of the mesogen in PHMS. Thus alkane spacers on adjacent

A. VI 9.

PHMS chains are held too far apart and cannot crystallize.

SPACER CONFORMATION IN FORM III

An indication of spacer conformation in the "Layered" form is obtained by comparing the measured 2-monomer repeat distance (cell parameter c) with that calculated for the extended chain (see Table 1). As seen from the Table, while the $-(CH_2)_5-$ spacer in PHMS-5 is practically fully extended, the measured c-parameter for PHMS-7 and PHMS-9 is significantly shorter than the values calculated for extended spacer. It follows that the spacer in PHMS-7 and PHMS-9 is contracted.

A possible explanation for the different conformation of spacers of different length may be sought in the optimal balance between the following three tendencies: (i) that for high density of the spacer layer, (ii) that for low intramolecular (conformational) energy and (iii) that for high conformational entropy. The first two tendencies could be satisfied simultaneously only if the spacers were allowed to crystallize, as in n-alkanes. Short of this, comparatively high density (point i) can only be achieved by abandoning the all-trans extended conformation and thereby increasing the effective spacer cross-section to match that of the mesogen. Such disordering of the spacer would also lead to favourable increase in entropy (point iii). Simple calculation shows that the density of the alkylene layer in Form III is only 0.77 g/cm^3 if the spacers are extended, as in PHMS-5. This is even less than the density of liquid n-alkanes (0.86 g/cm^3). However, in order that density be increased and the intermolecular energy lowered, unfavourable conformations must be introduced which raise the intramolecular energy (point ii above).

As seen in Table 1, the polymers with longer spacers PHMS-7 and PHMS-9 opt for higher density and entropy at the expense of increased conformational energy; the reverse is true when the spacer is shorter (PHMS-5). Such trend can be rationalized qualitatively on the account of both density and entropy effects:

A.VI

(a) The introduction of conformational defects is not compensated for by the concomitant, rather small, overall increase in density when the spacer is short - note that the overall unit cell density in PHMS-5 is not too low (1.07 g/cm^3) even when the spacer is extended (Table 1, 6th column). Thus the spacer in PHMS-5 remains extended. On the other hand, extended spacers in PHMS-7 and PHMS-9 would lead to a too low overall density (1.03 and 1.01 g/cm^3, respectively). Thus the spacers in PHMS-7 and PHMS-9 contract, the overall density increasing to 1.16-1.17 g/cm^3 as the result.

(b) Introduction of a defect into a long alkylene spacer increases the entropy as the defect can be located at different sites. However, if the spacer is short as in PHMS-5 this positional freedom is limited and the favourable effect of increased entropy is small.

The above concept of spacer conformation in Form III is summarized in Table 2.

TABLE 2.
Two options for minimizing spacer free energy realized in the Layered structures of PHMS

Spacer length (C-atoms)	SPACER *EXTENDED* + low intramolecular (conformational) energy	SPACER *CONTRACTED* + high density + high conform. entropy
5	o	
7		o
9		o
copol. 5/7		o

A.VI.11.

DIMENSIONALITY OF FORMS II AND III

The crystal in the "Intermeshed" form (Form II) has high long range order in all three dimensions, which is manifested in the appearance of sharp X-ray reflections with high values of all three Miller indices. The existence of high translational order, in spite of the inclusion of conformationally disordered spacers (cf. PHMS-7) is attributed to the existence of direct contact between rigid mesogen units bearing the three-dimensional structure.

A different situation can be expected in the "Layered" form (Form III), where the interaction between mesogen layers, i.e. along the fibre direction, is solely via the conformationally disordered spacers. The coupling force between the layers is therefore partially entropic and the minimum in the inter-mesogen potential in the chain direction is broad compared to that in Form II. This should lead to comparatively large fluctuations in the c repeat distance in the "Layered" form. The X-ray pattern of this form indeed reveals much fewer layer lines than that of Form II (Fig. 2). This is true in spite of the fact that Form III crystals are obtained and annealed at a higher temperature than Form II ones and, *everything else being equal*, the former would be expected to be larger and more perfect.

OTHER FEATURES OF THE "LAYERED" AND THE "INTERMESHED" FORM

Both forms II and III can be classified as "condis" (conformationally disordered) crystals [8]. The type in Form II is, to our knowledge, new and can be described as having "occluded" disorder. The type in Form III has "layered" disorder and is similar in nature to that observed in alkylated perovskites [9] and phospholipids [10] and, possibly, in some other segmented mesogenic polymers [11].

A potentially important consequence of the different spacer-mesogen arrangement in the two crystal forms concerns the mechanical properties. In the "Layered" structure stiff and flexible segments are coupled in series, while in the

"Intermeshed" structure, as presently envisaged, they are coupled in parallel. The former should give a low crystal modulus, elastic up to high strains, while the latter the converse, i.e. high crystal stiffness but low elastic limit. The potential for utilising these features through appropriate design of lattices for macroscopic mechanical properties will be apparent.

CONCLUSIONS

- Two crystal types with conformational disorder are recognised: (a) the "Intermeshed" and (b) the "Layered" type, the former representing a novel mode of mesogen-spacer packing and a new condis phase, with "occluded" disorder and truly 3-dimensional.
- The orthorhombic "Layered" form is an example of a stable structure with alternating crystalline and non-crystalline layers, an arrangement arising from the mismatch in mesogen - spacer cross-section. Random copolymers containing different spacer lengths can also crystallize with this crystal type.
- Depending on spacer length, balancing of the conflicting requirements for high packing density and low conformational energy of the spacer layer is achieved either (a) by tolerating a low density layer, (b) by increasing its density through the introduction of unfavourable conformations.
- Viewing the crystals as molecular composites, the stiff (mesogen) and soft segments (spacer) are coupled in parallel in Form II ("Intermeshed") and in series in Form III ("Layered"). Dynamic mechanical studies on these systems are currently in progress.

ACKNOWLEDGEMENT

The authors gratefully acknowledge the support by the U.S. Army European Office (London) making this work possible.

A. VI, 13.

REFERENCES

1. T.D. Shaffer and V. Percec, Makromol. Chem., Rapid Commun., 6, 97 (1985).

2. J.L. Feijoo, G. Ungar, A.J. Owen, A.Keller and V. Percec, Mol. Cryst. - Liq. Cryst., this volume.

3. C.M. Weeks, A. Cooper and D.A. Norton, Acta Crystallogr., B26, 429 (1970).

4. J. Shashidhara Prasad, ibid., B35, 1404 (1979).

5. A. Bromberg and K.A. Muszkat, Tetrahedron, 28, 1265 (1972).

6. G. Ungar, J. Phys. Chem., 87, 689 (1983).

7. U. Leute and W. Dollhopf, Colloid Polymer Sci., 258, 353 (1980).

8. B. Wunderlich and J. Grebowicz, Adv. Polym. Sci., 60-61, 1 (1984).

9. R. Blinc, M. Kozelj, V. Rutar, I. Zupancic, B. Zeks, H. Arend, R. Kind and G. Chapius, Faraday Disc. Chem. Soc., 69, 58 (1980).

10. D. Chapman, Adv. Liq. Cryst., 5, 1 (1982).

11. A. Roviello and A. Sirigu, Makromol. Chem., 183, 409 (1982).

APPENDIX VII

Mol. Cryst. Liq. Cryst., in the press

SIMULTANEOUS X-RAY DIFFRACTION AND DIFFERENTIAL SCANNING CALORIMETRY (XDDSC) *IN STUDIES OF MOLECULAR AND LIQUID CRYSTALS*

G. Ungar, J.L. Feijoo and A. Keller

H.H. Wills Physics Laboratory, Tyndall Avenue,
Bristol BS8 1TL, U.K.

INTRODUCTION

An attractive proposition for studies of molecular and liquid crystals is to combine thermal analysis and X-ray diffraction techniques, whereby time-resolved X-ray diffractograms could be rapidly recorded simultaneously with the heat flow into or out of the specimen during a heating, cooling or isothermal cycle. Thus structural transformations as revealed by changes in the diffraction pattern could be unambiguously correlated with thermal events such as endo- or exotherms or changes in heat capacity. Combination of differential scanning calorimetry (DSC) and small angle X-ray scattering (SAXS) has in fact recently been applied in studies of polymers by Russell and Koberstein [1,2], using a synchrotron source of X-rays. We have improved their technique by selecting a more X-ray transparent material for specimen cells and have applied the method successfully to studies of phase behaviour in a number of molecular and liquid crystal systems, both polymeric and non-polymeric. Small as well as wide angle diffraction ranges were covered.

Experimental arrange ent will be described in the first part of the paper. This will be followed by selected examples of application. Further examples are or will be reported in separate publications on specific studies on polymeric liquid crystals [3,4], metallo liquid crystals [5], cyanoterphenyls [6] and hexagonal columnar polymeric phases [7].

EXPERIMENTAL SETUP

To achieve the high X-ray flux necessary to perform time-resolved experiments synchrotron radiation is used. Our experiments are carried out using the Daresbury SRS facility. A modified Mettler hot stage DSC system FP 84 is employed, originally designed to enable simultaneous DSC and optical microscopy experiments. An important prerequisite for

obtaining optimum results with this technique was finding a material for sample containers that would fulfill the following requirements: (a) be highly transparent for X-rays, (b) would not give intense diffuse scattering or a multitude of Bragg reflections, (c) have good thermal conductivity, (d) would resist high temperatures and would not undergo phase changes itself, and (e) be easily machineable. Two materials were found to satisfy most of these requirements: graphite and boron nitride. Both are commercially available in highly pure form. They have very similar crystal structures: the materials are isoelectronic, both forming hexagonal layers. Their high crystal symmetry means a small number of crystalline reflections. The higher cost of boron nitride is offset by its somewhat superior mechanical properties.

X-ray diffraction / DSC arrangement

The experimental arrangement is drawn schematically in Fig. 1. The incident X-ray beam emanating from the storage ring is first focussed horizontally by a bent mirror and then vertically by a bent crystal monochromator to produce an image of the source in the detector plane. The size of the beam at the sample is approx. 1.5 x 0.3 mm. The beam is passed first through an ionizing chamber which monitors any fluctuations in beam intensity so that all recorded counts can be normalized to the same incident intensity. The beam then passes through the container (pan or cuvette) with the specimen. The container is held in the sample compartment of the DSC stage, with an identical empty container placed in the reference compartment. Viton O-rings are used to press the containers against the heaters and temperature sensors at the base, and a mica holder keeps the containers centered. A small hole in the base allows unhindered passage of the X-ray beam. The specimen environment is purged with helium both to avoid oxidative degradation of the specimen and to eliminate air scatter within the sample compartment. For low temperature experiments helium is pre-cooled. The DSC stage is aligned by remotely controlled stepper motors. An evacuated chamber of

variable length is placed between the specimen stage and the detector.

The detector used in this work is a linear delay-line position sensitive counter capable of operating at high count rates. In the current experiments wide to intermediate angular range was investigated, covering Bragg spacings between 3 and 60 Å. By shifting the detector further away from the specimen and refocussing, either the low angular range can be investigated (up to approx. 1000 Å) or, alternatively, by additionally moving the detector away from the primary beam, high resolution measurements can be made in a limited range of wide angles.

The data aquisition system is equipped with a time frame generator and front processor memory capable of storing several hundred diffractograms of 512 pixels each. Individual diffractograms collected during intervals as short as 2 seconds were found to have an acceptable signal to noise ratio, although usually somewhat longer collection times are used. The analogue DSC output, proportional to the flow of heat into or out of the specimen, is fed both to a chart recorder and to a voltage-to-frequency converter whose count was recorder in a separate calibration channel of each timeframe containing the scattering data. In this way any ambiguity in correlating the diffractograms with particular points on the thermogram was eliminated. The ionizing chamber count was stored in an additional calibration channel.

Sample containers and specimen preparation

Two basic types of sample containers were used: pans with lids, and cuvettes (Fig. 2a and b). Pans (Fig. 2a) can be used in all cases where the XDDSC run does not involve melting into a low viscosity liquid. Since the lids are either simply pushed into the pan or glued lightly by an inorganic cement, the low viscosity fluid would leak out of the pan which is

held upright in an XDDSC experiment. Pans were found adequate for polymeric samples and for crystal and ordered smectic phases of low molar mass compounds. The thickness of pan walls and lids was around 0.2 mm, i.e. twice that of the conventional aluminium DSC pans. However, due to the lower density of boron nitride (2.25 g/cm^3 as opposed to 2.7 g/cm^3 for aluminium) and much lower mass absorption coefficient (μ/ρ =4.96 cm^2/g for BN, 50.2 cm^2/g for Al, 1.54 Å radiation), a standard BN pan with lid of 0.5 mm combined thickness transmits as much as 57% of the incident X-ray radiation, while an Al pan (0.2 mm combined thickness) transmits only 5.8%. Transmission of graphite is very similar to that of BN. Thus a tenfold improvement in intensity is achieved using BN or graphite pans compared with aluminium pans, with no noticeable loss in thermal conductivity.

For samples which will at some point during the XDDSC experiment become liquids of low viscosity, such as isotropic, nematic or smectic A and C phases of low molar mass compounds, we use BN or graphite cuvettes shown in Fig. 2b. These can be conveniently machined using ultrasonic techniques, and 0.2 mm thin walls can be easily achieved by subsequent sanding. In order to fill the 0.5-0.8 mm thick cavity without leaving air gaps, we first press the powdery specimen in a micropress to obtain pellets 5 mm in diameter and of desired thickness. With the sample in place, the cuvette is then heated above the melting point of the sample, preferably in a vacuum oven. Usually replenishing is required in order to fill the cuvette completely. For most experiments the sample weight was of the order of 10 mg.

EXAMPLES OF APPLICATION

Thermotropic transitions in HEPTOBPD

HEPTOBPD, or N,N'-bis(4-n-heptyloxybenzal)-1,4-phenylenediamine, is an appropriate compound for illustrating the technique's potential as it undergoes a series of transitions between different crystal and smectic phases. A heating XDDSC scan is presented in Fig. 3. The thermogram recorded during the scan is shown in Fig. 3a, and the corresponding diffractograms, recorded at 1°C intervals, are shown in Fig, 3b. Heating rate was 5 deg.C/min. The bold diffractograms refer to arrowed positions in the thermogram, i.e. to the temperatures of endothermic peaks. Layer reflections are seen on the left, and the "outer" peaks on the right in Fig. 3b. On heating between 120 and 190°C the sample passes through two conventional crystal phases (denoted Cr1 and Cr2), and several fluid phases: crystal K and J and smectic I and C. The phases have been identified previously [8] and the present transition data correlate fairly well with those reported. An additional minor transition within the Sm-C range is observed around 184 °C. Current experiment reveals some further novel details of the phase behaviour of HEPTOBPD, which will be reported separately.

Multiple melting in PEK oligomer

Poly(aryl ether ketone) (PEK) and poly(aryl ether ether ketone) (PEEK) are thermoplastics of considerable commercial importance. Scientifically they show certain interesting properties, such as multiple melting, which are not yet fully understood [9,10]. We have been investigating monodisperse oligomers of PEK as model compounds. PEK-6, the oligomer with six phenylene rings

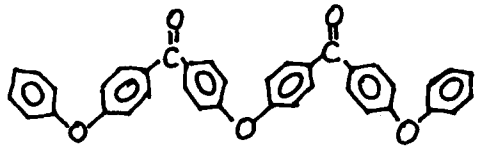

shows a particularly complex melting behaviour, with four closely spaced endotherms for a sample crystallized from the melt at a moderate rate. The lower melting phases are metastable, since annealing can reduce the number of endotherms to only two or possibly even one.

The melting thermogram of PEK-6 oligomer recorded during an XDDSC heating scan is shown in Fig. 4a, and the corresponding diffractograms in Fig. 4b. There are no major changes in the diffraction pattern associated with the individual endotherms, apart from an overall stepwise reduction in diffracted intensity. Thus the crystalline subcell, i.e. local arrangement of phenylene groups, remains unchanged. However, associated with each endotherm is a small discontinuous change in position of the layer reflections. Fig. 4b shows the change in the second order layer reflection: simultaneously with each of the endothermic transitions seen in Fig. 4a there is a reduction in intensity and a shift to lower spacings (marked in Fig. 4b in Angstroms). There are other subtle but distinct changes in the diffraction pattern, and their analysis is still in progress. It should be noted that the layer thickness in the highest melting form, which is found between 221 and 222°C, closely corresponds to that calculated for orthogonal layers of extended molecules.

Hexagonal columnar phase in gel-drawn polyethylene

The final example refers to metastable short-lived phases whose temperature range and lifetime greatly depend on particular specimen geometry and other experimental conditions; thus reliable correlation between separate X-ray and thermal analysis experiments is difficult or indeed impossible. A good example is the hexagonal phase of polyethylene which has been observed, amongst other circumstances, when a highly oriented high molecular weight polyethylene fibre or tape is constrained to inhibit retraction and then heated to above the normal melting point

of orthorhombic polyethylene, i.e. above ca. 140°C [11,12]. Rather than melt, the polymer will undergo a transition into a hexagonal columnar phase, where the chains are still largely extended, although with a considerable number of conformational defects and no longitudinal long range order. This phase is the simplest example of an important class of columnar phases which have been observed in a whole range of flexible and rigid polymers [13], but have not been recognized as such. In fact they have, often ambiguously, been termed "rotator" [14], "liquid crystal" [15], "smectic" [16,17], "condis crystal" [13], "thermotropic" [18], or simply "mesophases" [19]. A general discussion of these columnar phases is given in [20].

The ultra-highly oriented tape has been obtained by hot drawing a mat of dried polyethylene gel. The tape was embedded in epoxy resin in a BN pan and the XDDSC experiment performed. The detector was oriented normal to the draw direction and equatorial reflections were monitored. The sample was heated at 5 deg./min to 152 °C, and then cooled at the same rate. The thermogram thus recorded is shown in Fig. 5a and the series of diffractograms in Fig. 5b. As a rule multiple endotherms are observed with constrained highly oriented polyethylene [11,12], and usually it has not been possible to assign the DSC peaks with certainty. Here we see that the first endotherm (centered at frame 32, 142 C) is related to direct melting of a portion of orthorhombic crystals, presumably those which were not fully constrained. The second endotherm at 148-149 °C is clearly related to the transition of the remaining crystals into the hexagonal phase, as indicated by the appearance of the characteristic single hexagonal 100_h reflection, with a spacing of 4.35 Å, in place of the two orthorhombic peaks 110_o and 200_o. Had the sample been left at or above this temperature it would have melted completely within minutes, as the hexagonal phase is in a superheated state. However, we started the cooling cycle immediately on reaching 152 °C and a portion of the material was preserved in the hexagonal phase. Thus, for the first

time in the case of oriented polyethylene, we could observe the reverse hexagonal-orthorhombic transition, or the three dimensional crystallization from the columnar phase (frame 55-56, 139-138 °C). Moreover, we could unambiguously relate this transition to a DSC exotherm. The larger exotherm at a lower temperature is attributable to direct crystallization of the orthorhombic form from the isotropic melt.

DISCUSSION AND CONCLUSION

The examples described, as well as others that we studied, show that simultaneous X-ray diffraction and thermal analysis can be a very useful, sometimes indispensable, technique in studies of liquid and molecular crystals. This is particularly true in the following circumstances:

1. where absolute certainty in temperature cross-calibration between the diffraction and thermal experiment is essential; e.g.:

    1. where transitions are poorly resolved, i.e. when they occur at only slightly different temperatures;

    2. where continuous, e.g. lambda-type, transitions occur, in which case the DSC maximum is not as easily correlated with structural changes as in the case of first order transitions;

2. where metastable forms appear which are short lived and cannot be detected by conventional diffraction experiments;

3. where there is a possibility that the surface of the specimen container might affect phase changes so that direct comparison of independent thermal and diffraction experiments performed using different containers is doubtful (e.g. heterogeneous nucleation, liquid crystal alignment on surfaces etc.); and

4. where non-equilibrium conditions exist whose reproducibility is difficult to maintain (e.g. phase transitions in mechanically constrained fibres).

The question we will be investigating shortly is whether a rotating anode or even a sealed tube X-ray generator may provide a sufficiently intense beam for the XDDSC experiments. It is likely that individual intense diffraction peaks, such as fundamental smectic layer reflections often are, could possibly be monitored without the use of the synchrotron. Oriented specimens may also be amenable to such experiments, if only selected reflections are of interest. It should be noted, however, that the minimum practicable heating / cooling rate, and thus the maximum collection time for a diffractogram, is governed by the finite sensitivity of the calorimeter, since its output is proportional to the heat flow. A manyfold improvement in collection efficiency could, of course, be achieved by using a two dimensional detector. Thus the reduction in primary beam intensity on substituting the storage ring by a conventional X-ray source could, for powder diffraction, be largely offset by the greater collection efficiency of the 2-D detector. However, extensive memory capacity is required for immediate storage of the large number of 2-D patterns recorded during a scan.

In conclusion, considering its demonstrated potential, the XDDSC technique is expected to find important applications in the field of molecular and liquid crystals.

ACKNOWLEDGEMENTS

We are indebted to Professor G.W. Gray of Hull University for supplying the sample of HEPTOBPD, to Drs. D.J. Blundell of ICI and A. Waddon of Bristol University for supplying the PEK oligomer, and to K.J. Dunn, F.G. Porter and D. Milsom for building the mechanical components and producing specimen containers. Financial support of the U. S. Army European Office, London, is gratefully acknowledged. One of the authors (JLF) also wishes to acknowledge financial support from the Britannica Society, the British Council (Venezuela) and the Simon Bolivar University.

REFERENCES

1. T.P. Russell and J.T. Koberstein J. Polym. Sci., Polym. Phys. Ed. 1985, 23, 1109.

2. T.P. Russell, Adv. Polymer Sci. (1989) in press.

3. G. Ungar, J.L. Feijoo, A. Keller, R. Yourd and V.Percec, Macromolecules, submitted.

4. E.D.T. Atkins, J.L. Feijoo, G. Ungar and R.W. Lenz, in preparation.

5. A.S. Cherodian, J.L. Feijoo, R.M. Richardson, G. Ungar and P.M. Unitt, presented at the Annual Conference of the British Liquid Crystal Society, Sheffield, 10-12 April 1989.

6. A.S. Cherodian, R.M. Richardson, G. Ungar, J.L. Feijoo and G.W. Gray, in preparation.

7. J.L. Feijoo and G. Ungar, in preparation.

8. P.A.C. Gane, A.J. Leadbetter and P.G. Wrighton, Mol. Cryst. Liq. Cryst. 66, 567 (1981).

9. D.J. Blundell, Polymer 28, 2248 (1987).

10. D.C. Bassett, R.H. Olley and I.A.M. Al Raheil, Polymer 29, 1745 (1988).

11. A.J. Pennings and A. Zwijnenburg, J. Polym. Sci., Polym. Phys. Ed. 17, 1011 (1979).

12. N.A.J.M. van Aerle and P.J. Lemstra, Polymer J. 20, 131 (1988).

13. S. Isoda, A. Kawaguchi and K. Katayama, J. Polym. Sci., Polym. Phys. Ed. 22, 669 (1984).

14. M. Yasuniwa and T. Takemura, Polymer 15, 661 (1974).

15. H.W. Starkweather, Jr., J. Polym. Sci., Polym. Phys. Ed. 17, 73 (1979).

16. D.C. Bassett, in "Development in Crystalline Polymers" Vol. 1, D.C. Bassett ed., Applied Science Publishers, London, 1982.

17. B. Wunderlich, M. Moeller, J. Grebowicz and H. Baur, Adv. Polym. Sci. 87, 1 (1988).

18. M. Kojima and J.H. Magill, Polymer 30, 579 (1989).

19. Yu.K. Godovsky and V.S. Papkov, Adv. Polym. Sci. 88, 129 (1989).

20. G. Ungar, Polymer, submitted.

FIGURE CAPTIONS

Fig. 1 - Block diagram of the experimental setup for XDDSC. S = sample, R = reference, 1-D PSD = one-dimensional position sensitive detector. Δq = differential heating current, ΔT = differential temperature. Ion chamber is positioned before the specimen stage. For small angle diffraction experiments an additional ion chamber is placed between the specimen and the detector.

Fig. 2 - (a) Sample pan and lid made of boron nitride or graphite. (b) Cuvette for low viscosity liquids made of the same materials.

Fig. 3 - Heating XDDSC scan of HEPTOBPD. Heating rate 5 deg./min. (a) Thermogram, (b) diffractograms recorded at 12 seconds (1 °C) intervals. Lorentz, polarization and geometrical corrections were applied. Bold curves correspond to arrowed positions in the thermogram. The range of d-spacings covered is from 3.5 Å (right) to 65 Å (left).

Fig. 4 - Heating XDDSC scan of PEK-6 oligomer in the melting range. Heating rate 0.5 deg./min. (a) Thermogram, (b) diffractograms showing the 2nd order layer reflection (002). Two adjacent frames, each recorded for 40 seconds, were coadded, hence each curve in Fig. 4b covers a temperature interval of 2/3°C. Bold curves, designated by roman numerals, correspond to arrowed positions in the thermogram. A stepwise decrease in intensity and shift to smaller d-spacings occurs at each melting endotherm.

Fig. 5 - Heating and cooling XDDSC cycle for high-strength high-modulus polyethylene tape drawn from dry gel and embedded in epoxy resin to inhibit contraction on melting. (a) Thermogram, (b) diffractograms showing the most intense equatorial reflections: orthorhombic 110 and 200 and hexagonal 100. Two adjacent frames were coadded in Fig. 5a

to give one curve for every two degrees C. Heating (5 deg./min.) was stopped and cooling started (-5 deg./min.) at the end of frame 42, i.e. at 152°C. Bold curves refer to the arrowed positions in the thermogram. Orthorhombic - hexagonal (o-h) and hexagonal - orthorhombic (h-o) transitions are seen, as well as direct melting (o-m) into the isotropic liquid and direct crystallization from it (m-o).

XDDSC
Block Diagram

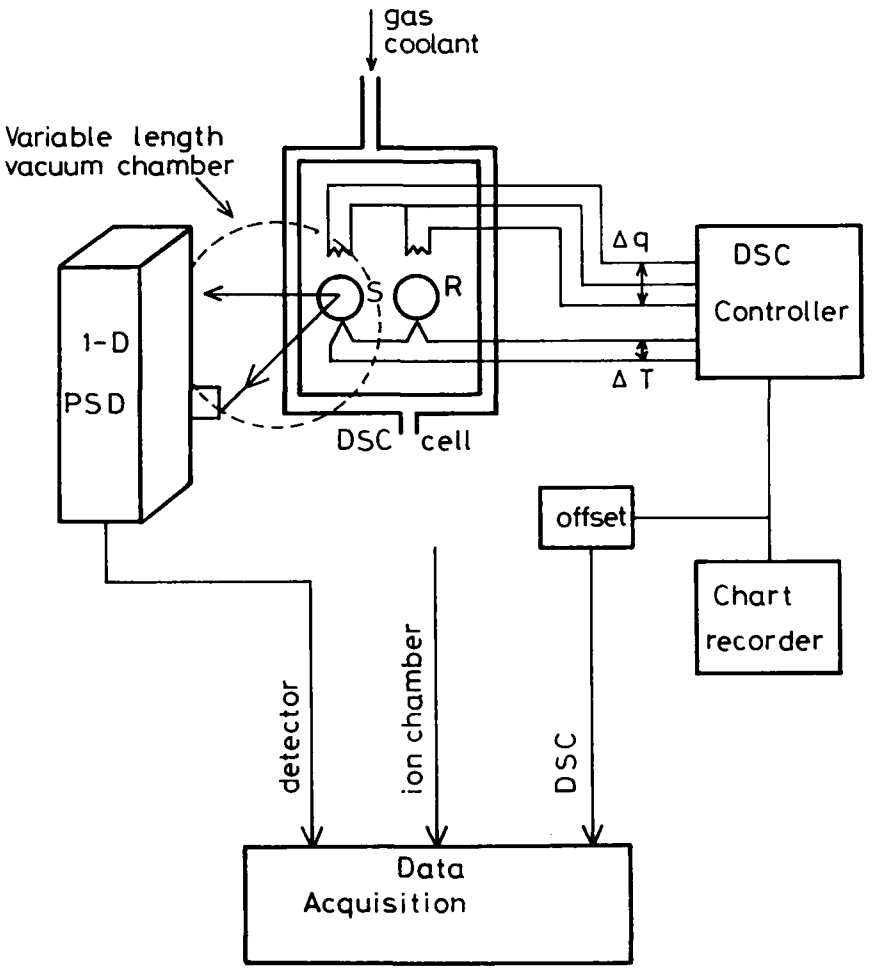

Fig.

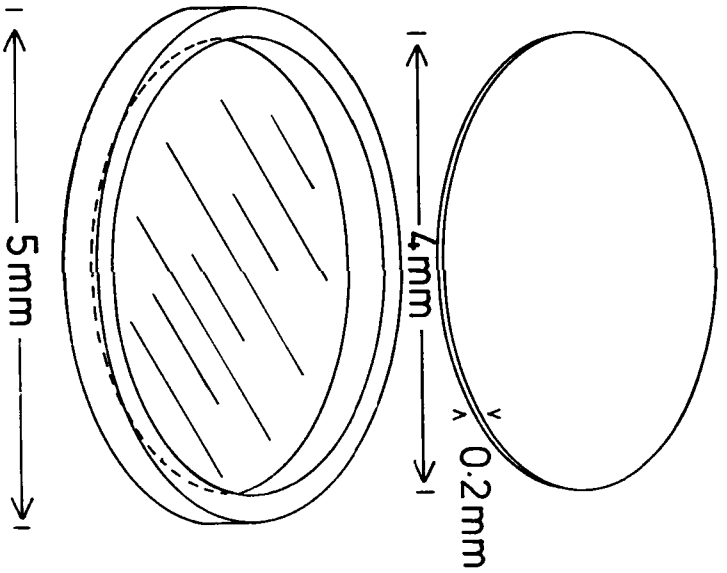

Fig. 2

Fig

CUVETTE

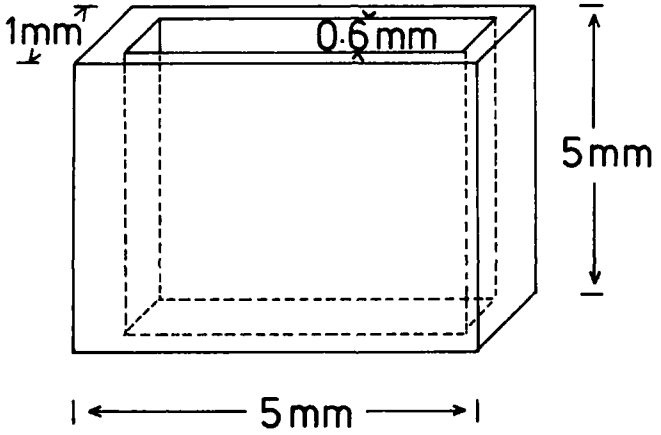

Fig. 3a

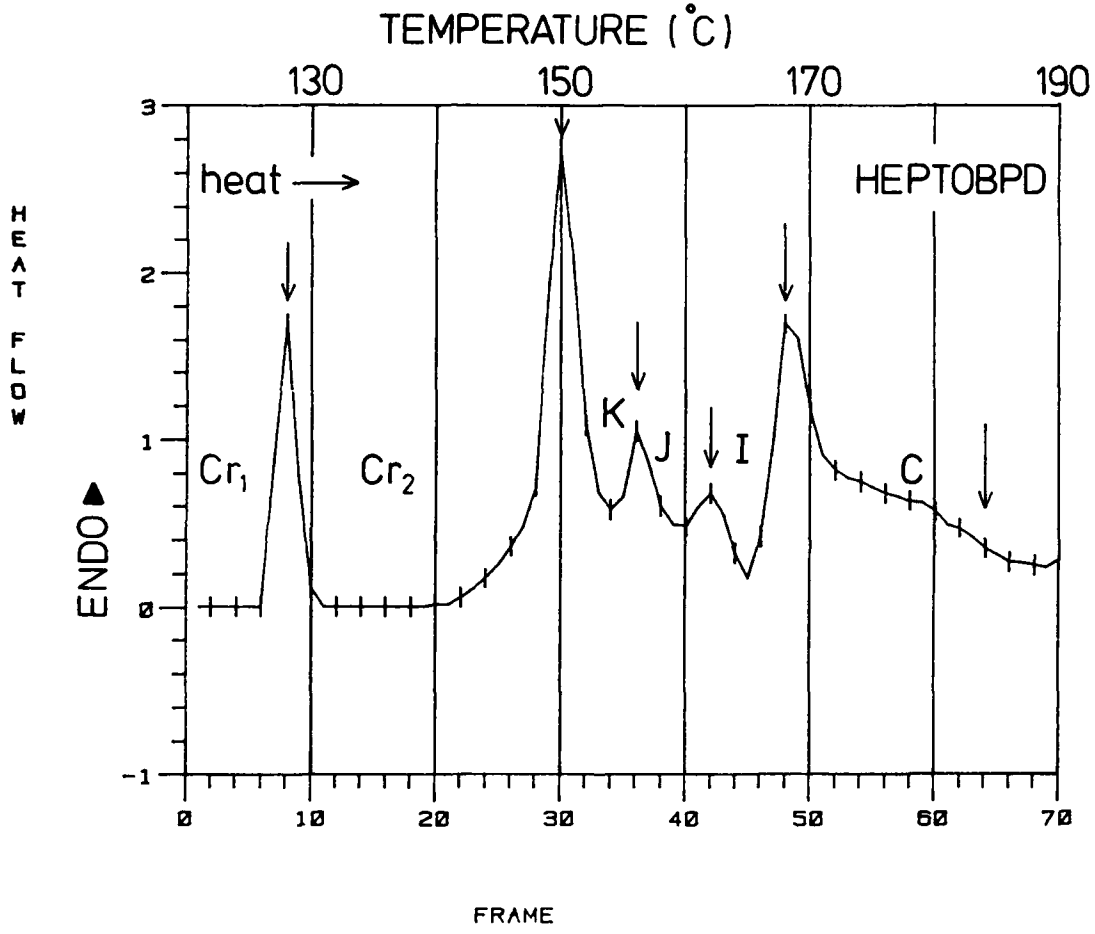
TEMPERATURE (°C)
130
150
170
190
heat
HEPTOBPD
Cr1
Cr2
K
J
I
C
ENDO
HEAT FLOW
3
2
1
0
-1
0
10
20
30
40
50
60
70
FRAME

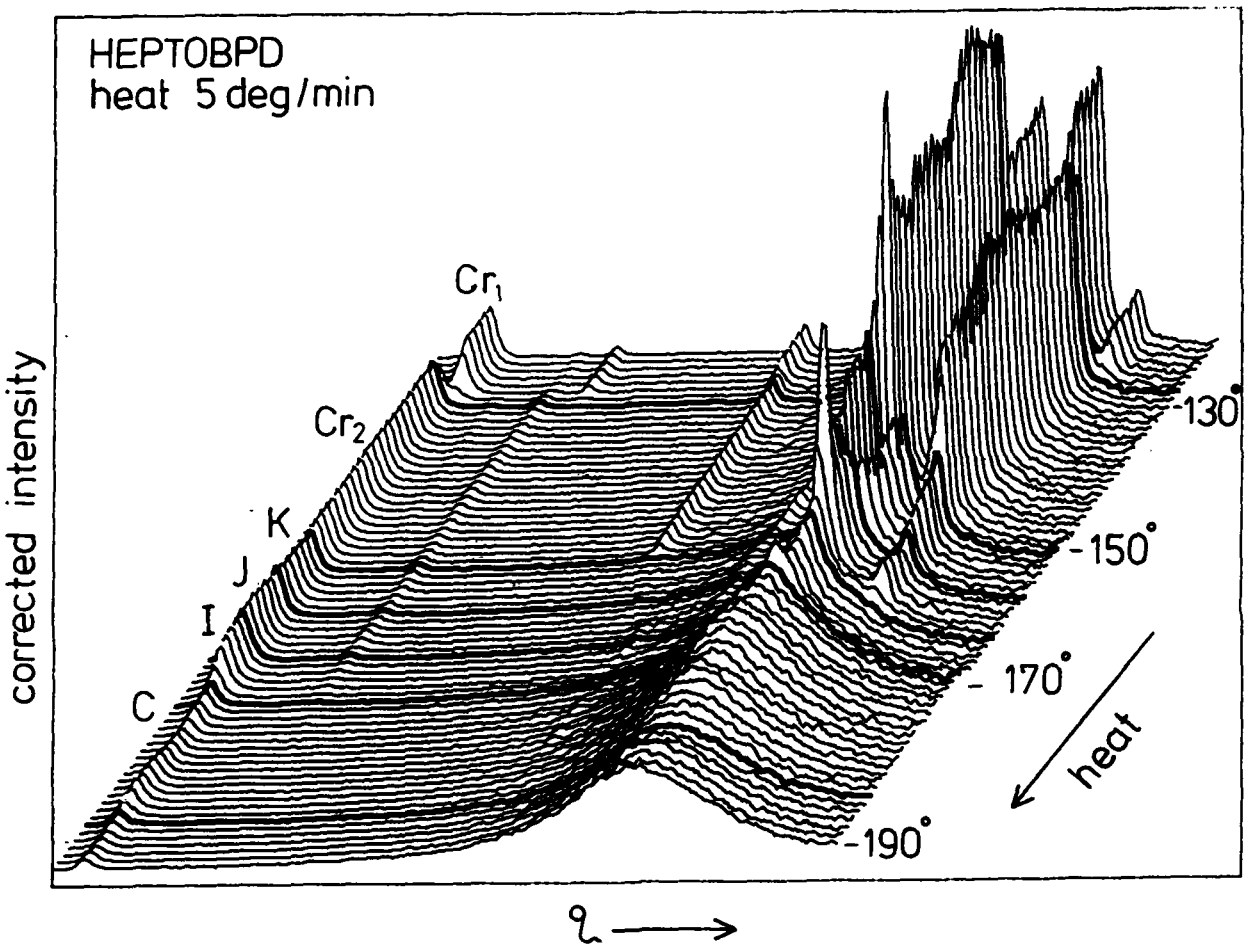
HEPTOBPD
heat 5 deg/min
corrected intensity
Cr1
Cr2
K
J
I
C
-130°
-150°
-170°
-190°
heat
q

Fig.

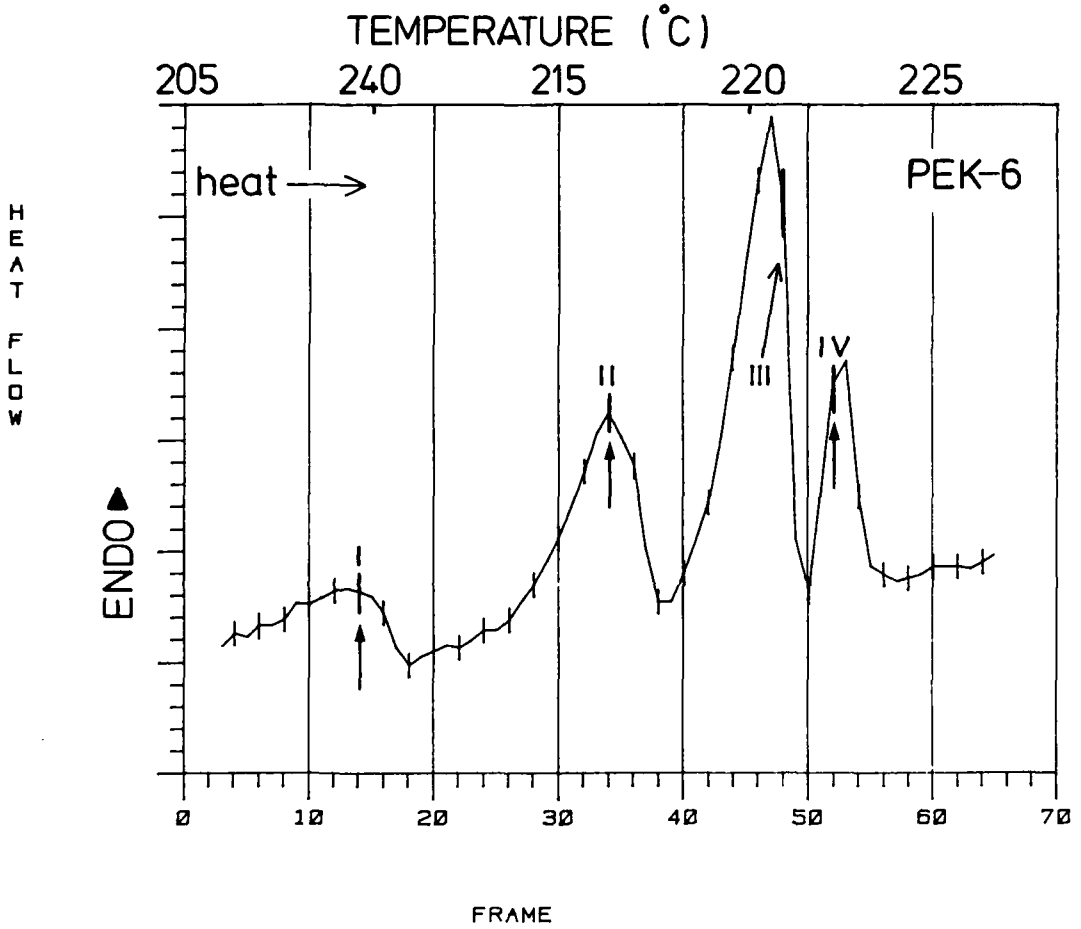
TEMPERATURE (°C)
205
240
215
220
225
heat
PEK-6
I
II
III
IV
ENDO
HEAT FLOW
0
10
20
30
40
50
60
70
FRAME

Fig. 4a

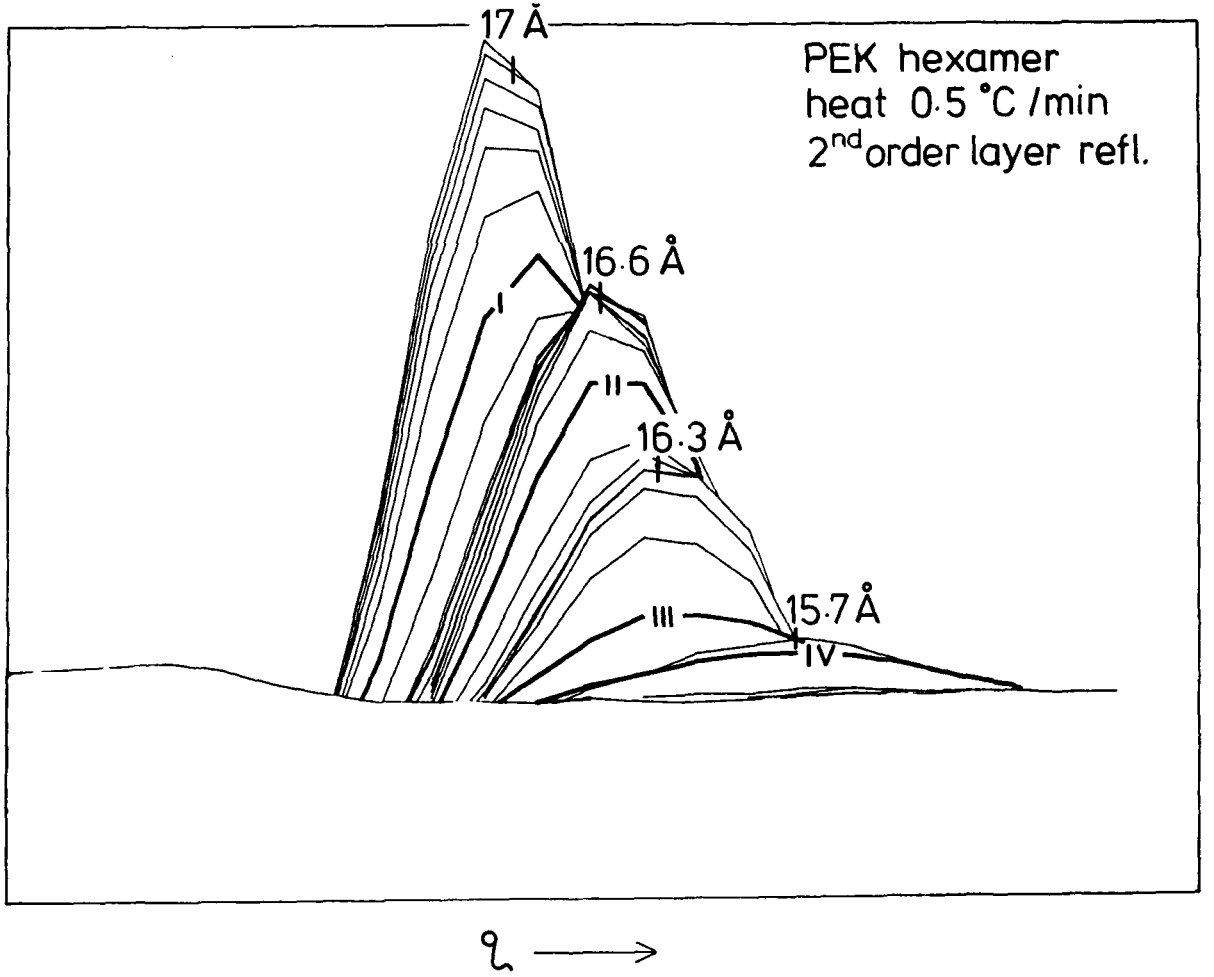
17 Å
PEK hexamer
heat 0·5 °C /min
2nd order layer refl.
16·6 Å
I
II
16·3 Å
III
15·7 Å
IV
q ⟶

Fig

Fig.5a

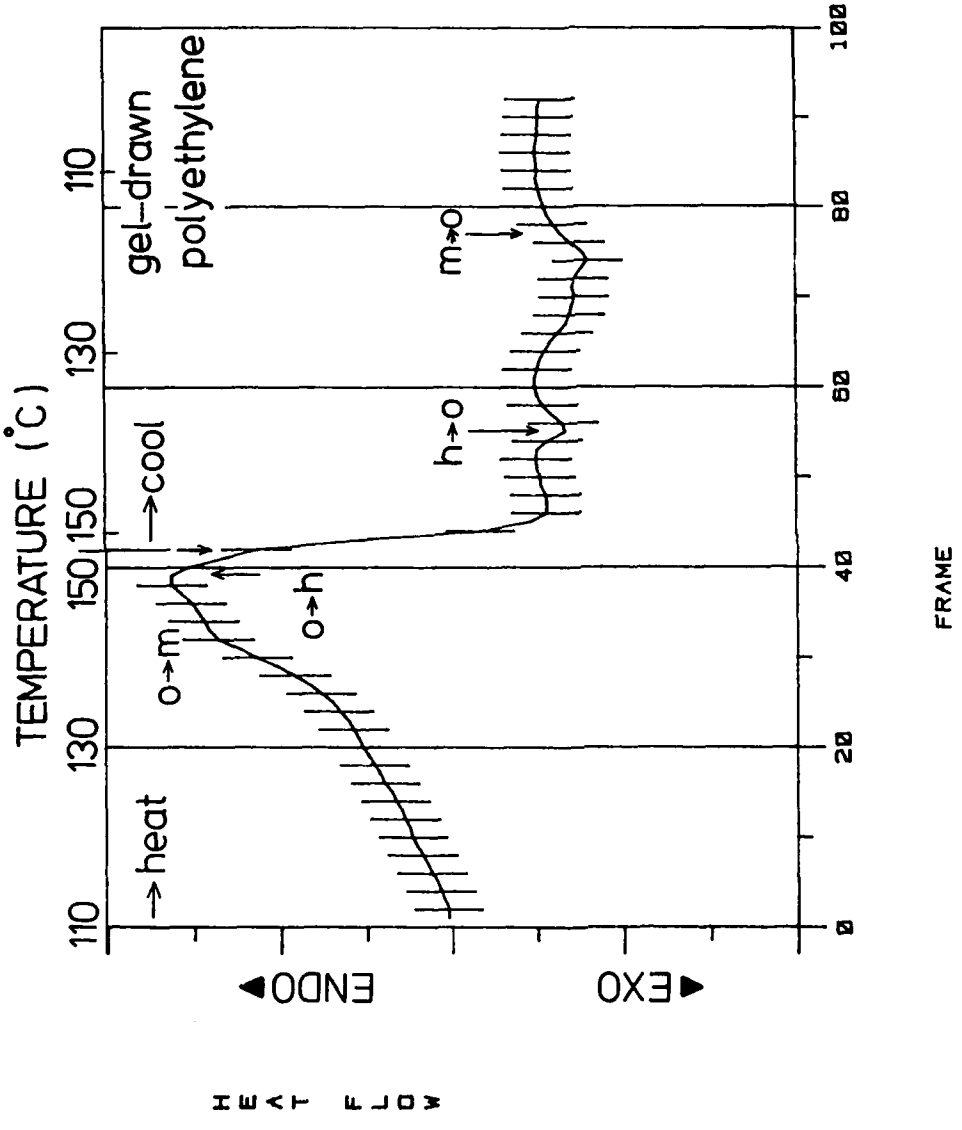
gel-drawn polyethylene
TEMPERATURE (°C)
110
130
150
150
130
110
→heat
→cool
o→m
o→h
h→o
m→o
ENDO▶
◀EXO
HEAT FLOW
0
20
40
60
80
100
FRAME

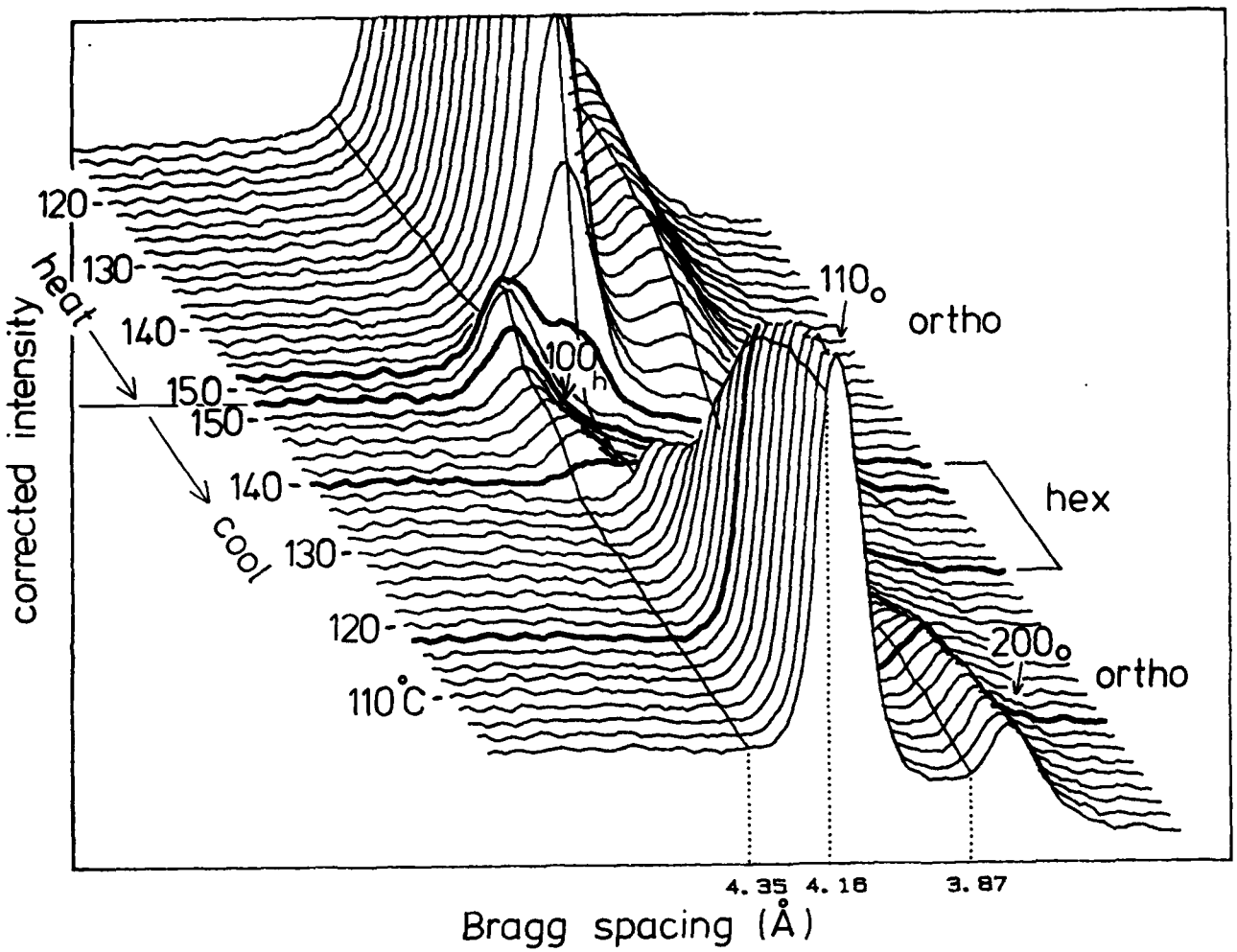
corrected intensity
heat
120-
130-
140-
150-
150-
140-
cool
130-
120-
110°C-
100h
110o
ortho
hex
200o
ortho
4.35
4.16
3.87
Bragg spacing (Å)

APPENDIX VIII

Extract from paper in: Materials Research Society Preprints "Rigid Rod Polymers", presented November 1988, Boston (in the press).

through a single rotational jump, there will still be certain directions where it can momentarily do so (the spikes which extend to the large circle periphery). Clearly, the rod will not take much note of such an artificially imposed mean constraint but will avail itself of the opportunity to escape from its 'cage' in whichever direction there is an opportunity to do so at any particular instance. While we have no theory of our own to propose, we can probably state, based on numerous simulation diagrams such as Figure 4, that mean barriers far over-constrain the rods, and that theoretical approaches relying on them are likely to be inappropriate. This, to say the least, is in line with our experimental findings.

III. Disorientation of rigid rod molecules (PBT) from the highly oriented state in solution

In a way this represents an extension of method iii) in the previous section with the difference that here the emphasis lies exclusively on the relaxation process from a state of as high an orientation as is possible to achieve. The work has been pursued in two stages along two, so far separate lines [5,6].

At the first, earlier stage a dope of PBT in methane sulphonic acid, was oriented in the form of a thin layer sheared between two slides to its maximum orientation, as assessed by birefringence. The orientation was then allowed to decay and followed as a function of time, again as diagnosed by birefringence. It will be apparent from the example of Figure 5 that the disorientation cannot be described by a single process. The initial process is very rapid giving way to a much slower one later. It is this

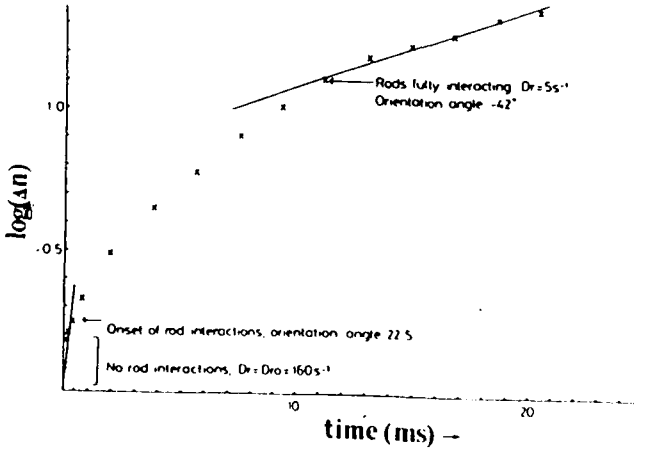

Figure 5. The relaxation process of an entangled rigid rod solution (below the concentration giving rise to liquid crystalline order) from almost perfect orientation (time=0) to the isotropic state. The process of decay of orientation is characterised by the loss of birefringence [Δn (t)] of poly-p-phenylene-benzbisthiazole in methane sulphonic acid)[5]

later, slower process which corresponds to the one assessed by the elongational flow method in the preceding section corresponding to the appropriate value of D_r. The first, faster process is specially noteworthy. It corresponds to a mean disorientation angle of 22.5°. This agrees well with the tilt angle of a rod abutting in its parallel aligned nearest neighbour for the concentration involved (calculated to be 23°). Thus we seemed to have identified the mean elementary free rotational "jump" before the entanglement barrier due to the surrounding chains is reached, a jump which in existing theories has been considered instanteous, hence in practice unrecordable.

The present, second stage of the disorientation work, taken up recently, relies on in situ recording of orientation by X-rays. For this the process needed to be slowed down which was facilitated by turning to the much more viscous solvent system of polyphosphoric acid. This shifts the time scale from milliseconds to minutes. Even so, the high intensity of a synchrotron X-ray source was needed for the time resolution required. An appropriate shearing cell was constructed for the purpose. This enables the realization of controlled shear at required constant temperatures. The prime source of diffraction information is that from the isolated molecule itself, in particular the meridional reflexion, present in 2 orders (Fig. 6). This corresponds to the intrinsic periodicity within the molecule, which as a rigid rod in a fully extended state, produces its own diffraction pattern. When all chains are parallel this should correspond to the calculated Fourier transform. (Fig. 1). Features of

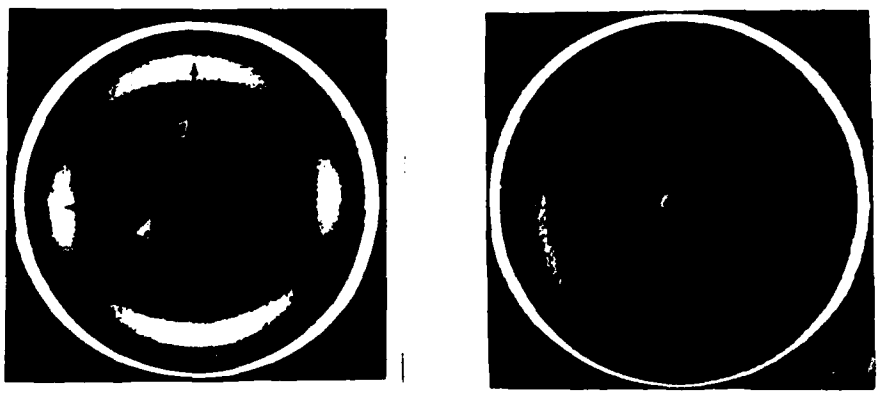

a) b)

Fig. 6. X-ray diffraction patterns (synchrotron source) from a 10% PBT solution in polyphosphoric acid (PPA). a) during shearing at $3s^{-1}$ at 23°C. Arrowed (white): sharp reflections on the meridian corresponding to monomer periodicity along the rod-like molecule and broad reflections along the equator corresponding to "nematic" packing of the rods. Black arrows point to the liquid halo of PPA. b) same system as a) but 7.5 min. after cessation of flow [6].

Fig. 1 are indeed recognizable in the highly oriented solutions. However, as we find, there are noticeable effects due to the solvent such as the altered intensity ratio of the meridional polymer reflections. In addition, a diffuse equatorial reflection is also apparent. (Fig. 6); this we associate with the inter-rod separation in what we presume is the nematic state. Indeed, the nematic "spacing" is in agreement with expectations from the given concentration. They are in fact the correspondingly expanded versions of the broad equatorial diffraction maxima seen in the condensed state (Fig. 1), where they are attributable to close packing of uncorrelated cylinders.

Preliminary results are very encouraging. Figs 6a and b provide two stages from a relaxation sequence. The radial densitometer scans of the pattern in Fig. 6a are shown in Fig. 7 and the azimuthal distribution of the PBT peak intensity in Fig. 8. Attention is being drawn to the fact that, in addition to the orientation in the polymer, a complex orientation pattern (meridional and equatorial arcs) is also observed in the halo due to the solvent suggesting specific polymer-solvent interaction (see 4.2A peak in Fig. 7 and maxima in solvent halo in Fig. 6a). Evaluation of all these effects is in progress, and tying up with the earlier birefringence results (Fig. 5) is hopefully expected with the added information power of X-ray patterns which provide full distributions in addition to the averages given by the birefringence.

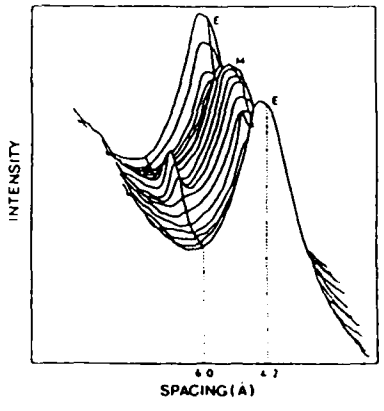

Figure 7. Radial densitometer series of the pattern Figure 6a) over an azimuthal angular range of 180°. M meridional, E equatorial scan. The peaks at 6A and 4.2A are due to PBT and the solvent respectively.

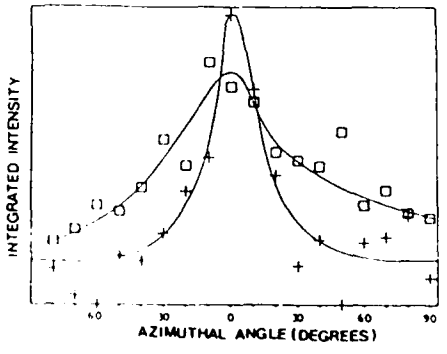

Figure 8. Azimuthal distribution of the intregrated intensity of the 6A peak of PBT during shear (+) and 92.5 mins after cessation of flow (□)

APPENDIX IX

'Polymer Communications'

in the press.

SYNCHROTRON X-RAY ANALYSIS OF DISORIENTATION IN NEMATIC SOLUTIONS OF PBZT

J.L.Feijoo, J.A.Odell and A.Keller

H.H.Wills Physics Laboratory
University of Bristol
Tyndall Avenue
Bristol BS8 1TL, U.K.

Abstract

We describe a shear cell enabling high orientations to be obtained in liquid crystalline polymers, whilst detecting the X-ray Scattering Pattern. Used in conjunction with the Daresbury Synchroton X-ray Source, this enables orientation and disorientation to be followed dynamically. Initial results are presented on nematic solution of poly (1,4 - phenylene - 2,6 benzobisthiazole) (PBZT) in polyphosphoric acid, at room temperature, 80°C and 100°C.

Keywords: Orientation, flow, liquid-crystalline, nematic solution, Rodlike Polymer, poly(1,4 - phenylene - 2,6 benzobisthiazole), X-ray.

INTRODUCTION

The achievement of high ordering in polymeric systems is an absolute prerequisite for obtaining the ultimate strength and stiffness of which a material is capable. This is made easier in the case of mesogenic molecules by the inherent rigidity of the molecule minimizing the required reduction in entropy to achieve a perfectly aligned state.

In practice this often means that materials are processed from the liquid crystalline state, so that reordering becomes a cooperative process. The order is usually imposed by a shearing or stretching flow-field, which serves to align the molecules closely around a single ('stiff') direction. The achievement of this highly ordered orientational state from an initial random domain-like liquid-crystal state is little investigated, but might be likened to achieving a 'single crystal' from a polycrystalline material. Few processed materials, however, match this perfect orientation - disorientation by Brownian Motion is constantly at work.

The ultimate properties of any wet spun product (lyotropic or otherwise) are limited by the disorientation which takes place during the time that elapses between the dope leaving the spineret and solidifying, say, in a coagulation bath. Understanding and ultimately controlling this reorientation is therefore crucial. It is a common finding that products from solidified oriented mesophases possess a sharply banded transverse structure[1-4] as revealed by the polarizing microscope, which in general is detrimental to ultimate properties. While its origin is totally unclarified, we believe that it is a consequence of a cooperative relaxation of previously aligned rigid molecules. Analogous polarizing

optically banded structures can also occur in natural structural materials such as collagen[5] with explicit mechanical purpose.

In this short communication we report initial results from our program of research, following dynamically by X-ray scattering the development of flow orientation, and subsequent disorientation on cessation of flow.

The orienting shear field is provided by a parallel plate shear-cell. Normally following of orientation/disorientation processes is achievable only by "fast" techniques (principally measurement of birefringence). Such techniques give only an average orientation which masks the mechanisms involved, also the high opacity of such materials often precludes optical techniques. We use X-ray scattering during flow to investigate the full orientational distribution. This is not normally possible due to the long required sampling times compared to the rate of the relaxation process. We have used the powerful X-ray fluxes of the Daresbury Synchrotron Radiation Source (DSRS) to enable the dynamic relaxation processes to be followed. Our method enables the determination of the orientational distribution even from weak and poorly resolved scattering maxima, such as are obtained from solutions.

The polymer system we have examined here is a nematic solution poly (1,4 - phenylene - 2,6 benzobisthiazole) (PBZT) dissolved in polyphosphoric acid (PPA). Not only is this a solvent of potential interest for this system but also its very high viscosity lengthens the time-scale of the orientation - disorientation processes, which is of great help to in situ studies of these phenomena. PBZT with which we have had previous experience is amongst the most rigid organic macromolecules[6], and serves as a good model for other materials in its class (eg Kevlar).

Two types of X-ray information may be anticipated. The first corresponds to diffraction from a one-dimensional periodic system, such as represented by the chemical repetition along a perfectly straight rod. Such an X-ray signal has in fact been found by us in the form of sharp reflections (001) in the highly oriented nematic liquid crystalline state. This provides the most direct possible information on the rigid chain orientation, irrespective of whether the chain is in a liquid crystalline state or not. The second type of diffraction information is expected from diffraction due to lateral packing of rods: this arises in the liquid crystalline state in the form of broad haloes.

EXPERIMENTAL

From analysis of such reflections X-ray measurements were made with a parallel plate cell. The front plate (window) is stationary while the back plate is rotated with an angular velocity Ω . With this arrangement we have the shear rate varying linearly with the distance (from the centre) and inversely with the separation t of the plate

$$\dot{\gamma} = \left(\frac{r\Omega}{t}\right)$$

r = radius

t = thickness (separation of the plates)

Boron Nitride windows, with built-in or external reinforcement to provide mechanical stability are used to ensure transparency for X-rays. The shear cell includes a DC servomotor drive system and a temperature control system precise to 1°C. The PBZT/PPA dope (concentration 10% PBZT, $[\eta] = 31 dl/g$) was injected into the cell using a positive pressure of dry nitrogen. To avoid contact of moisture with the dope all operations are carried out using a dry box.

RESULTS

For this system experiments were conducted at room temperature to follow orientation and relaxation processes in the well-defined shear cell and extended to higher temperatures of 80°C and 100°C, which are of technological importance since the PBZT dope is heated during jet wet spinning.

Room Temperature

Fig.1 illustrates the X-ray diffraction pattern during steady-shear at 23°C and $3s^{-1}$ shear rate. Shear direction vertical. The main features of this pattern are:

a) Meridional 1st and 2nd order reflections of the 12.25Å chemical repeat unit of PBZT. These reflections are highly oriented at even very low shear rates. Note that the second order reflection is strongly present in the case of the nematic *10% solution, but absent in the* solid fibre[6]. This reflects the different structure factors of PBZT in PPA and as a single phase.

b) Equatorial nematic reflection, highly oriented at a spacing of ~13Å. This spacing is in line with expectation for the solution. The orientation distribution parameter (P_2) was determined from this reflection as 0.963.

c) A strong PPA solvent peak at 4.2Å. This ring is quite strongly biaxially oriented when the nematic diffraction shows high orientation; as disorientation proceeds the ring rapidly becomes isotropic. This solvent orientation was noticed by ourselves previously[8,9]. We believe this has an important message to convey on polymer solvent interaction, of significance also for processing.

Disorientation is extremely slow at room temperature reflecting a very long relaxation time, consistent with high orientations being

produced by the lowest shear-rates. This is attributable to the extremely high value of the viscosity of PPA at room temperature, almost immobilizing the PBZT mesogens. This high viscosity is responsible for the relative lack of tractability of the material, such that processing requires heating of the dope. To this end, we have examined disorientation at 80°C and 100°C.

80°C

High steady state orientations are still attainable at modest shear rates. Fig.2a) illustrates orientation at 80°C,3s^{-1}. The orientation is almost as perfect as at room temperature (P_2 = 0.925). Initial disorientation is, however, much faster. After only 3·5 minutes, a significant reduction in orientation is observed Fig.2b (P_2 = 0.844).

Only in the highly oriented steady state patterns could P_2 be determined from the equatorial nematic reflection. Otherwise P_2 was determined from the second order meridional reflection. These values have not been corrected for smearing of the meridional reflection.

This disorientation increases up to 80 minutes, beyond which time the disorientation process becomes much slower - Fig 2(c)(P_2 = 0.650).This we are attempting to correlate with visual observations of the disorientation process. The first (fast) stage of disorientation is of great significance, both theoretically and practically. Although the degree of disorientation may be modest, its effect upon the realizable modulus is expected to be profound.

100°C

The 100°C results show a similar, though even faster, relaxation at short times - Figs 3(a) (P_2 = 0.9) and 3(b) (P_2 = 0.695). At longer times, however, the system slowly approaches complete disorientation - Fig 3(c) (P_2 = 0.536). The system PBZT/PPA still appears to be nematic at 100°C, again correlation with visual observations is proceeding.

CONCLUSION AND PROSPECTS

We are working towards a theoretical understanding of disorientation in both nematic and isotropic states. On a practical level,however, it appears that the preservation of high orientation in wet spun PBZT/PPA may be pursued by a temperature quench followed by coagulation.

A programme that is still under development will calculate the polar distribution and the orientational order parameter. By observing the time dependence of the latter we shall be able to extract the relaxation times both of the polymer and of the solvent. Even more importantly, the change in the shape of the orientation distribution function could be followed, providing a critical experimental test for the theoretical predictions on the rotational diffusion in rigid chain systems.

ACKNOWLEDGMENTS

We are indebted for financial support to the U.S.Army European Office (London), one of the authors (J.L.F.) wishes to to acknowledge partial financial support from the British Council (Venezuela). Finally, our thanks go to Mr.Richard Exley, who helped to design and constructed the shearing cell.

A.12.9

REFERENCES

1) Kiss G. and Porter R. S., *Mol. Cryst .Liq. Cryst* . 1980, **60**, 267

2) Simmens, S C., and Hearle, J.W.S., J.*Polym.Sci., Polym.Phys. Ed.*, 1980,**18**,871.

3) Graziano D., Mackley,M.R., *Mol.Cryst.Liq.Cryst.* 1984,**106**,73.

4) Viney C., Donald A.H., Windle,A.H., *J.Mat.Sci.*, 1983, **18**,1136.

5) Diamond J., Keller A., Baer E., Litt M. and Arridge R.G.C. *Proc. Roy. Soc. Lond. B.* , 1972, **180**, 293.

6) Odell J.A., Keller A., Atkins E.D.T., and Miles M.J., *J.Mat.Sci.*, 1983, **16**, 3309.

7) Odell J.A., Keller A., and Atkins E.D.T., *Macromolecules*, 1985,**18**, 1443.

8) U.S.Army ERO report, DAJA45-85-C-004 April 1988

9) Odell J.A., Keller,A., Atkins,E.D.T., Feijoo, J.L., Nagy, M., and Ungar,G., *Material Research Society Preprints, presented* Nov. 1988, Boston.

FIGURE CAPTIONS

Fig.1 X-ray diffraction pattern from a 10% PBZT solution in polyphosphoric acid (PPA), during shear at $3S^{-1}$ at 23°C. Arrowed white; sharp reflection on the meridian (2nd order) corresponding to monomer periodicity along the rod-like molecule and broad reflections along the equator corresponding to "nematic" packing of the rod molecules. ($P_2 = 0.963$).

Fig.2 X-ray diffraction patterns of 10% PBZT solution in PPA sheared at 80°C:

a) during shear at rate of $3s^{-1}$ ($P_2 = 0.925$)

b) and c) after cessation of flow, time elapsed; 3.5 min ($P_2 = 0.844$) and 80 min ($P_2 = 0.65$) respectively.

Fig.3 X-ray diffraction patterns of 10% PBZT solution in PPA sheared at 100°C:

a) during shear rate at $3s^{-1}$ ($P_2 = 0.9$)

b) and c) after cessation of flow

time elapsed; 1.5 min ($P_2 = 0.695$) and 92 min ($P_2 = 0.536$) respectively.

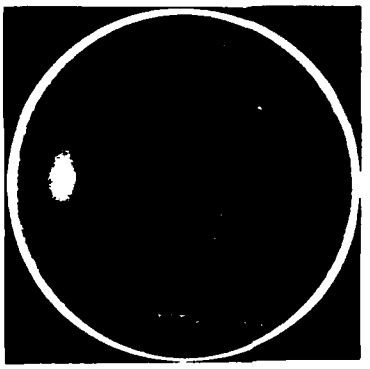

FIG 1

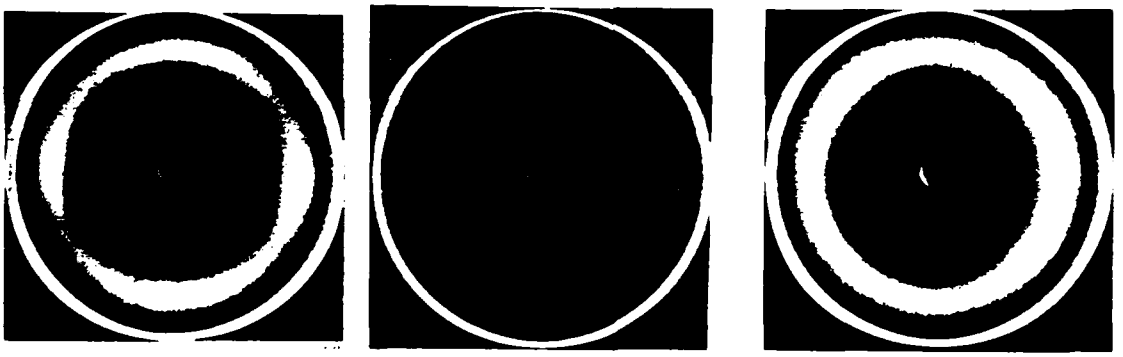

A B C

FIG 2

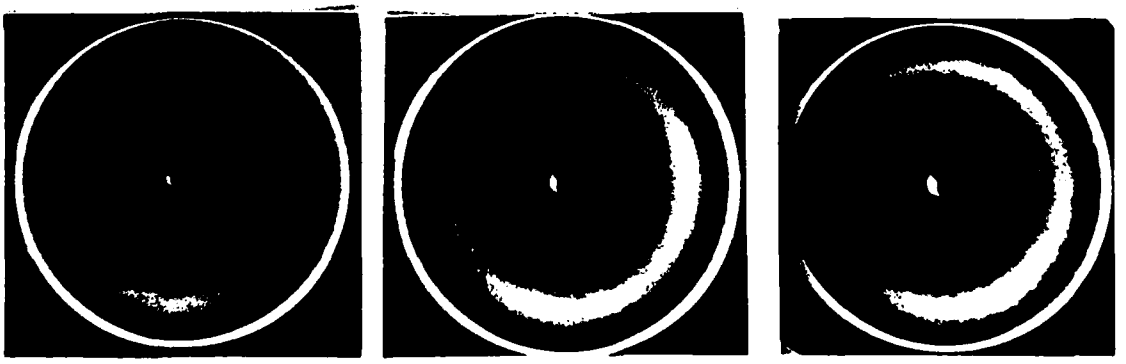

A B C

FIG 3